

# **OPTICAL DESIGN for VISUAL SYSTEMS**

**Bruce H. Walker**

Tutorial Texts in Optical Engineering  
Volume TT45

**Arthur R. Weeks, Jr.,** Series Editor  
Invivo Research Inc. and University of Central Florida



**SPIE PRESS**

A Publication of SPIE—The International Society for Optical Engineering  
Bellingham, Washington USA

Library of Congress Cataloging-in-Publication Data

Walker, Bruce H.

Optical design for visual systems / Bruce H. Walker

p. cm. — (Tutorial texts in optical engineering; TT45)

Includes bibliographical references and index.

ISBN 0-8194-3886-3 (softcover)

I. Optical instruments—Design and construction. I. Title. II. Series.

QC372.2.D4 W35 2000

681'.4—dc21

00-059488

CIP

Published by

SPIE—The International Society for Optical Engineering

P.O. Box 10

Bellingham, Washington 98227-0010

Phone: 360/676-3290

Fax: 360/647-1445

Email: [spie@spie.org](mailto:spie@spie.org)

WWW: [www.spie.org](http://www.spie.org)

Copyright © 2000 The Society of Photo-Optical Instrumentation Engineers

All rights reserved. No part of this publication may be reproduced or distributed in any form or by any means without written permission of the publisher.

Printed in the United States of America.

## Introduction to the Series

---

The Tutorial Texts series was initiated in 1989 as a way to make the material presented in SPIE short courses available to those who couldn't attend and to provide a reference book for those who could. Typically, short course notes are developed with the thought in mind that supporting material will be presented verbally to complement the notes, which are generally written in summary form, highlight key technical topics, and are not intended as stand-alone documents. Additionally, the figures, tables, and other graphically formatted information included with the notes require further explanation given in the instructor's lecture. As stand-alone documents, short course notes do not generally serve the student or reader well.

Many of the Tutorial Texts have thus started as short course notes subsequently expanded into books. The goal of the series is to provide readers with books that cover focused technical interest areas in a tutorial fashion. What separates the books in this series from other technical monographs and textbooks is the way in which the material is presented. Keeping in mind the tutorial nature of the series, many of the topics presented in these texts are followed by detailed examples that further explain the concepts presented. Many pictures and illustrations are included with each text, and where appropriate tabular reference data are also included.

To date, the texts published in this series have encompassed a wide range of topics, from geometrical optics to optical detectors to image processing. Each proposal is evaluated to determine the relevance of the proposed topic. This initial reviewing process has been very helpful to authors in identifying, early in the writing process, the need for additional material or other changes in approach that serve to strengthen the text. Once a manuscript is completed, it is peer reviewed to ensure that chapters communicate accurately the essential ingredients of the processes and technologies under discussion.

During the past nine years, my predecessor, Donald C. O'Shea, has done an excellent job in building the Tutorial Texts series, which now numbers over forty books. It has expanded to include not only texts developed by short course instructors but also those written by other topic experts. It is my goal to maintain the style and quality of books in the series, and to further expand the topic areas to include emerging as well as mature subjects in optics, photonics, and imaging.

*Arthur R. Weeks, Jr.  
Invivo Research Inc. and University of Central Florida*

## Preface

---

In the field of optical engineering there exists a complete genre of instruments that are intended to be used with the human eye as the final system sensor. The optical design of such instruments involves a unique approach, dealing with a special set of requirements and design methods. This book will provide the reader with a basic understanding of these methods and the reasons behind them.

Initial chapters will deal with the human eye, its unique design characteristics and its function. A mathematical model of the eye, closely simulating the dimensions and performance of the *typical* eye, and suitable for computer analysis, will be generated. Computer simulation and analysis will be used to establish a baseline of performance for this eye model. This analysis of the visual system includes the use of an Aerial Image Modulation (AIM) curve, which describes the performance of the visual sensor, i.e., the eye's retina. While generation of this AIM curve has involved some assumptions, it has been based on known characteristics of the retina. Results found when combining the Modulation Transfer Function (MTF) of the model eye with this AIM curve are consistent with the resolving capability of the *typical* visual system. This will permit performance comparisons in later chapters to determine the effectiveness of a variety of designs. Some time will be spent on describing the various reasons for the introduction of optical instruments that are intended to enhance the performance of the *naked* eye.

The simple magnifier (loupe), the eyepiece, and the microscope represent the most basic tier of optical designs for visual applications where near objects are being viewed. When viewing objects at great distances, the eyepiece is combined with an objective lens to form a telescope design. Several telescope designs will be developed and described in some detail. Design procedures will illustrate how these telescope designs are modified to make them suitable for a variety of applications.

In a number of unusual applications, it is required that a relatively large distance exist between the objective and the eyepiece of a telescope design. The basic submarine periscope and the field of industrial and medical borescope design will be discussed in order to demonstrate the interesting and unique aspects of these instruments.

Finally, the topic of biocular lens designs will be touched upon. In a biocular design the optics must be configured such that a common object

can be viewed by both eyes simultaneously. This leads to a lens system that is quite large physically, and has a small  $f$ -number (often around  $f/1.0$ ). The design of a biocular lens is complicated by the fact that the relatively small pupil of the eye is sampling the output of this large lens. Several designs in this category will be presented.

Each design that is to be presented here (including the model eye) has been generated using the OSLO optical design software package from Sinclair Optics. Optical design methods and procedures will be discussed in some detail, with emphasis on the *real world* reasons behind them. While the typical reader may not use this information to make him or her self into a *bonafide* optical designer, a familiarity with this category of instruments and the design methods involved in creating them will permit an intelligent exchange of concepts and ideas with the Optical Designer on the program.

The level of mathematics and physics involved in the preparation of this book has been limited to fundamental algebra and trigonometry, along with the basic principles of optics that will be found in all basic optics textbooks. In this age, the lens design software package and the modern personal computer have assumed much of the *heavy lifting* (in a mathematical sense).

It is hoped that this book will successfully convey to the reader an understanding and appreciation of the basic human visual system, its function, and its rather remarkable performance capabilities. Second, the reader should come away with an understanding of the many unique considerations involved in the optical design of a system to be used in conjunction with the visual system. As is often the case, while the flexibility and responsiveness of the visual system tends to simplify the actual design process, the design is simultaneously made more difficult by the optical and physical limitations of that same visual system.

It is recognized that in most engineering fields (and optics is not an exception), the most effective engineering solutions involve the serious balancing of numerous design considerations, i.e., *trade-offs*. This book will be useful to the optical designer, as well as others peripherally involved, in helping to decide on the most effective way of incorporating those many compromises into a successful final design.

Readers are invited to visit the author's web site at [www.waoptics.com](http://www.waoptics.com), and to submit any questions or comments dealing with the content of this book via the e-mail link that will be found at that site.

Bruce H. Walker  
July 2000

# Contents

---

Foreword / xi

Preface / xiii

Acknowledgements / xv

## Chapter 1 Introduction / 1

## Chapter 2 The Eye / 3

- 2.1 General / 3
- 2.2 Eye Model / 3
- 2.3 Spot-Size Analysis / 6
- 2.4 The Retina / 7
- 2.5 Image Quality / 8
- 2.6 *Normal* Vision / 8
- 2.7 Peripheral Vision / 11
- 2.8 Review and Summary / 11

## Chapter 3 Magnification and Vision / 15

- 3.1 Introduction / 15
- 3.2 Near Object Standard / 15
- 3.3 Loupe Magnification / 16
- 3.4 Microscope Magnification / 19
- 3.5 Distant Object Magnification / 21
- 3.6 Photographic Systems / 24
- 3.7 Video Systems / 26
- 3.8 Review and Summary / 28

## Chapter 4 The Magnifier–Design / 29

- 4.1 Introduction / 29
- 4.2 The Biconvex Magnifier / 29
- 4.3 The Doublet Magnifier / 31
- 4.4 The Triplet Magnifier / 39
- 4.5 The Symmetrical Two-Doublet Magnifier / 43
- 4.6 Resolution / 43
- 4.7 Review and Summary / 45

**Chapter 5 The Eyepiece—Design / 47**

- 5.1 Introduction / 47
- 5.2 The Generic Eyepiece / 47
- 5.3 The Huygenian Eyepiece / 49
- 5.4 The Ramsden Eyepiece / 49
- 5.5 The Kellner Eyepiece / 52
- 5.6 The RKE Eyepiece / 52
- 5.7 The Orthoscopic Eyepiece / 52
- 5.8 The Symmetrical Eyepiece / 56
- 5.9 The Erfle Eyepiece / 56
- 5.10 The Scidmore Eyepiece / 56
- 5.11 The RKE Wide-Angle Eyepiece / 60
- 5.12 Eyepiece Focus / 60
- 5.13 Eyepiece with the Eye / 62
- 5.14 Review and Summary / 67

**Chapter 6 The Microscope—Design / 69**

- 6.1 Introduction / 69
- 6.2 Basic System Specifications / 69
- 6.3 Resolution Goals and Limits / 70
- 6.4 10× Objective, Starting Lens Form / 71
- 6.5 New 10× Objective Design / 74
- 6.6 Adding the Eyepiece / 74
- 6.7 Performance Evaluation / 77
- 6.8 Review and Summary / 81

**Chapter 7 The Telescope—Design / 83**

- 7.1 Introduction / 83
- 7.2 The Astronomical Telescope / 83
- 7.3 Resolution Goals and Limits / 84
- 7.4 The Terrestrial Telescope / 93
- 7.5 Resolution Goals and Limits / 94
- 7.6 Review and Summary / 95

**Chapter 8 The Borescope—Design / 101**

- 8.1 Introduction / 101
- 8.2 General Optical Configuration / 101
- 8.3 Objective Lens Design / 103

- 8.4 Common Relay Lens Design / 106
- 8.5 Final Relay Lens Design / 109
- 8.6 Eyepiece Selection / 109
- 8.7 Magnification Evaluation / 114
- 8.8 Review and Summary / 115

## **Chapter 9 The Submarine Periscope—Design / 117**

- 9.1 Introduction / 117
- 9.2 General Optical Configuration / 117
- 9.3 Objective Lens Design / 119
- 9.4 Relay Lens Pair Design / 126
- 9.5 Visual Performance Analysis / 129
- 9.6 True Resolution Gain / 134
- 9.7 Review and Summary / 137

## **Chapter 10 Biocular Design / 139**

- 10.1 Introduction / 139
- 10.2 Biocular Eyepiece / 139
- 10.3 Head-Up Display (HUD) / 147
- 10.4 Review and Summary / 148

## **Chapter 11 Review and Summary of Design Concepts / 151**

- 11.1 Introduction / 151
- 11.2 The Model Eye / 151
- 11.3 Model Eye Resolution / 151
- 11.4 Visual Magnification / 152
- 11.5 Other Visual Instruments / 153
- 11.6 Conclusion / 153

References / 155

Index / 157



## 1

# Introduction

---

As demonstrated by our ability to read this printed page, the human visual system is really quite marvelous. The key optical device contained within that system is the eye. Often referred to as the camera that allows us to take pictures for processing by the brain, it is worth noting that our eye is the original, while all cameras represent attempts (usually in vain) to copy the function and performance of that original instrument.

This book will deal with the basic principles that are involved in the design of an optical system to be used in conjunction with the eye. Such systems are often thought of as improving upon the performance of the eye. In reality, while eyeglasses, contact lenses, and surgery can improve vision, the introduction of an optical system is generally intended to permit the designer to trade off certain performance characteristics of the eye, such as field of view vs. resolution, spectral bandwidth vs. sensitivity, or depth of field vs. image brightness. In each case it is the optical designer's responsibility to produce a system design that will function well with the eye, taking advantage of its unique characteristics, while maximizing overall performance in those areas that are critical to the particular application. In order to do this the designer needs to have a basic understanding of the eye, its structure, function, and performance characteristics. In the next chapter we will present a simplified model of a *typical* eye that is suitable for computer analysis. By establishing the performance of this model (primarily image quality), it may then be combined with designs of various optical systems to demonstrate the impact that they will have upon the performance of the eye.

One of the unique aspects of optical design for visual applications is the condition of the final system output, i.e., the light as it emerges from the optical system. In most other cases, it is the optical designer's task to generate a system that will produce a *real* image that is compatible with the ultimate system sensor, such as film or a video CCD chip. This type of optical system (one that forms a real image) has come to be referred to as a *focal* system. In the case of a system to be used with the eye, it is required that the light emerging from the optics project a *virtual* image that appears at some substantial distance from the eye (usually between 10 inches and infinity). The optics of the eye will then take this output

and form the final image on the eye's retina. The optical system that projects a final virtual image at infinity has come to be referred to as an *afocal* system. It is extremely important that the optical design of a system to be used with the eye assures that the output from the afocal optical system can be collected and imaged by the optics of the eye. Thus, the interface between the optical system and the eye must be carefully defined and controlled.

The unusual aspect of the eye as an optical device is that it is dynamic. At any point in time the iris will assume a diameter that is consistent with the ambient light level. Also, the distance at which the eye is focused will be variable. Finally, characteristics and optical properties of the eye will vary between individuals. The eye model to be presented in Chapter 2 will represent a *typical* eye, one that is capable of normal vision under normal conditions. It is reasonable to assume that the results generated using this model will represent a close approximation of actual performance and image quality to be found in the eye of the typical viewer.

Most often the purpose of a visual instrument will be to collect light from an object and to increase the size of that object's image which is formed on the eye's retina. This subject of image magnification will be reviewed and presented in Chapter 3 in a manner that is easily understood and can be applied to the various optical systems that are to be subsequently presented.

Following the early chapters dealing with the eye and its function, a complete range of optical instrument designs will be described and details of the optical design procedures involved in generating each of these designs will be presented. The general philosophy will involve understanding of the fundamental principles of the instrument in order to better understand the optical design procedures to be used, and the criteria for acceptance of final design performance.

All of the computer design and analysis for examples contained in this book have been executed using the OSLO optical design software package from Sinclair Optics. Complete lens data are presented for each example. These data can be easily converted for use with other popular software packages.

# 2

## The Eye

---

### 2.1 General

The (human) eye is a natural optical instrument that has developed and evolved over the years. The adult eye can be described physically as a white, spongy, water-filled sphere, approximately 25 mm (one inch) in diameter (Fig. 2.1). On the front surface of this sphere there is a circular transparent spot about 10 mm in diameter. The surface of the sphere bulges outward slightly in this area, forming what is known as the *cornea*. Because the eye is filled with a water-like fluid, it is the first surface of the cornea that produces most of the optical lens power of the eye. In terms of diopters, the typical unaccommodated eye (viewing an object at infinity) has about 57 diopters of total power. Of this, approximately 43 diopters are provided by the cornea. Typically, as shown in Fig. 2.1, the cornea is 0.6 mm thick, and it is followed by an approximately 3-mm-thick layer of a water-like fluid called the *aqueous*. Light passing through the cornea and aqueous then encounters the *eyelens*, which is suspended within a muscular structure that is capable of changing the lens shape to provide focus on near objects, a process called *accommodation*. The *iris* of the eye, which gives it its color, is located just in front of the eyelens. The circular opening in the iris is adjustable over a useful range of from 1- to 7-mm diameter. The black spot that we see at the center of the iris is actually the front surface of the eyelens.

### 2.2 Eye Model

For purposes of analysis in the sections and chapters to follow, we have assigned fixed values to the variable features of the eye. For most examples it will be assumed that the eye is not accommodated, that is, its focus is set to view objects at infinity. For a few special cases, which will be noted, we will assume that the eye is fully accommodated to view objects at a distance of 254 mm (10 inches), the accepted near point of vision for the typical eye. Note in Fig. 2.1 that the eyelens assumes a nearly symmetrical shape when the eye is focused on objects at the near point.

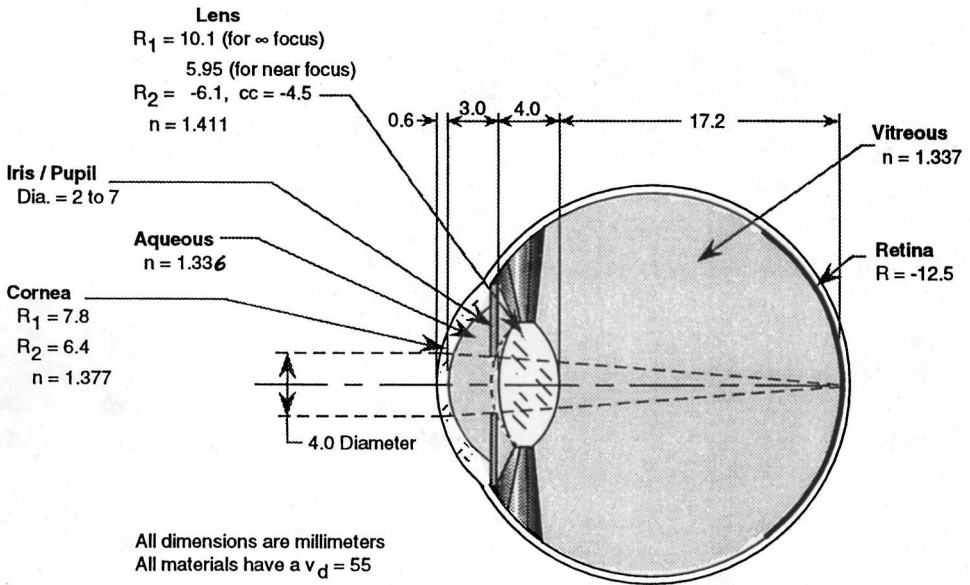


**Figure 2.1** The final component in any visual system is the eye. The model shown here is a simplified version of a *typical* eye, suitable for computer analysis of on-axis performance (image quality).

While the eye's pupil diameter will vary depending on the ambient light level, we have assumed a fixed pupil diameter of 4 mm for this analysis. A conic constant of  $-4.5$  has been assigned to the second surface of the eyelens. This conic constant simulates the performance of the eye due to several aspheric surfaces along with variations in the index of refraction within the eyelens. This results in a final model with about 1 wave of residual spherical aberration.

Also note that all optical material within the eye model has a  $v_d$  (dispersion constant) of 55, similar to that of water. While the standard  $d$ ,  $F$  and  $C$  spectral lines (wavelengths) are often used for analysis of visual systems, these wavelengths must be weighted in an appropriate manner. This author prefers to determine and use the three wavelengths that can be equally weighted. In Fig. 2.2 the spectral sensitivity of the eye has been

plotted. Following elimination of the tails of the curve ( $<0.10$ ), the area under the curve has been divided into three equal areas. A representative wavelength for each of these areas is then assigned which divides that area into two equal parts. The end result is a central wavelength of 0.56 microns (yellow-green), a short wavelength of 0.51 microns (blue) and a long wavelength of 0.61 microns (red). These are the wavelengths that will be used, with equal weights, for analysis throughout this book. This has been a decision of convenience as much as scientific precision. Experimentation will show that computer analysis results do not vary significantly with minor variations in the wavelengths and weights used. Using the wavelengths from Fig. 2.2, the model of the eye is found to have about  $\pm 0.75$  waves of residual chromatic aberration. While residual aberrations in the eye may be more complex than those of this model, the ultimate image quality of both is essentially the same.

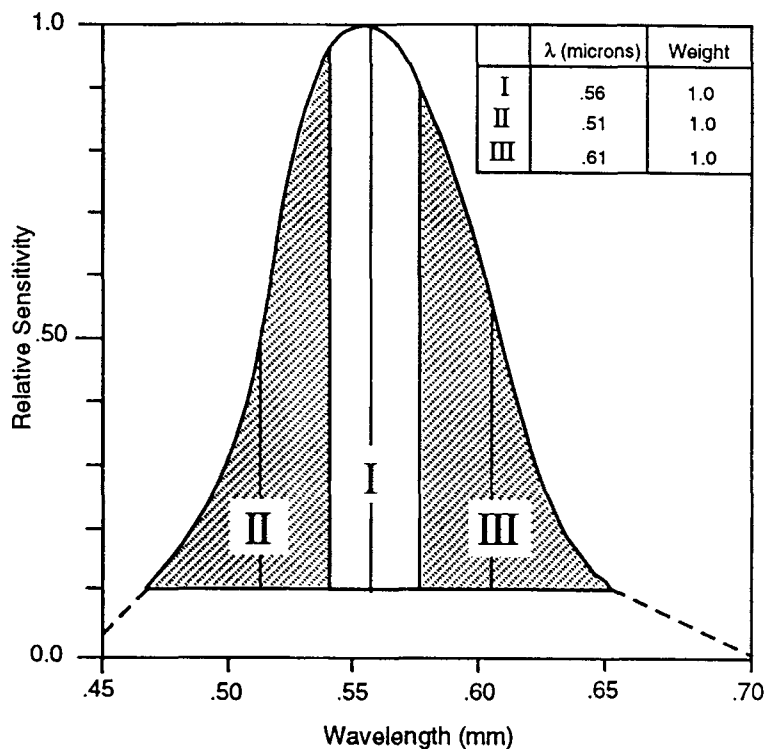


Figure 2.2 Spectral response for visual system analysis. Wavelengths have been chosen to have equal spectral weighting.

### 2.3 Spot-Size Analysis

When white light from a distant point source object is imaged onto the retina, residual aberrations of the eye's optics will create a finite spot image. Figure 2.3 shows the variation of this spot diameter as a function of pupil diameter. For a pupil diameter of 4 mm, the spot diameter formed by the optics of the model eye—for 80% of the incident light—will be about 14 microns. This is just a bit more than the minimum value of 12 microns, which occurs when the eye pupil diameter is reduced to 3 mm.

Figure 2.3 also shows a plot of the resolution of the eye as a function of pupil diameter, for targets located at the near point (254 mm). From that curve it is seen that the maximum resolution of 7.8 cycles/mm occurs when the pupil is from 2 to 3 mm in diameter. For very small pupil diameters (<1 mm), diffraction effects reduce the resolution to the 4–5 cycle/mm range. Likewise, when the pupil is increased beyond 4 mm in diameter, the resolution value falls gradually to about 5.5 cycles/mm due to increased aberrations.

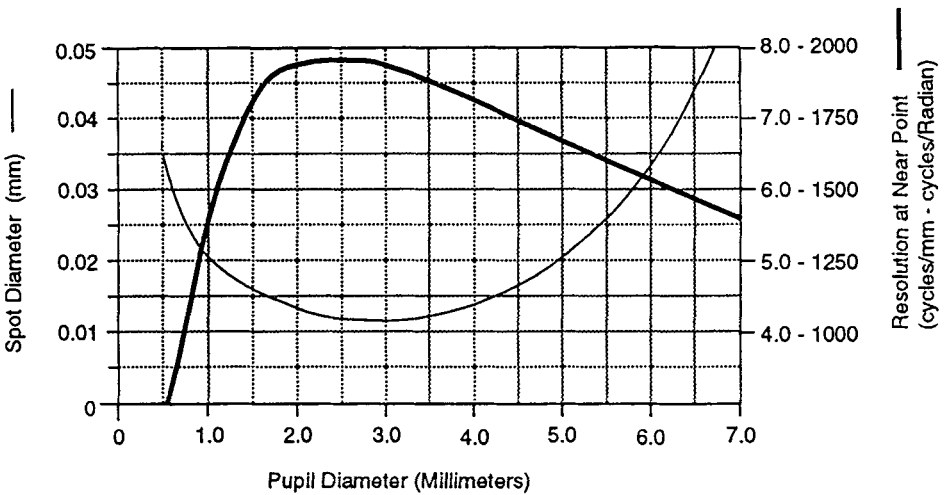


Figure 2.3 Spot diameter and near point resolution as a function of pupil diameter for the model eye shown in Fig. 2.1. Spot diameter plotted is for 80% of the polychromatic energy collected by the eye. Resolution for a target at a distance of 254 mm is given in both cycles/mm and cycles/radian.

It may be concluded that, for the model (typical) eye shown in Fig. 2.1, with a pupil diameter of 4 mm, spherical and chromatic aberrations will result in an 80% spot diameter of 14 microns. For the same model, the resolution when viewing a target at the eye's near point will be 7.3 cycles/mm. This level of image quality is due to approximately 1 wave of spherical aberration and 1.5 waves of chromatic aberration. As stated earlier, wavelengths used for spot size and MTF calculations have been 0.56, 0.51, and 0.61 microns, equally weighted.

## 2.4 The Retina

The volume between the eyelens and the back of the eye is filled with a water-like fluid called the *vitreous*. The final image gathering surface of the eye, the *retina*, is located on the inside of the back surface of the eye. The retina contains light sensitive elements called rods and cones. There are about 120 million rods and about 6 million cones. The rods, which are more sensitive to light and less sensitive to color, and provide lower resolution than the cones, basically provide our peripheral vision. There is a spot located on the horizontal center of the eye, about 2 mm to the temporal side, called the *fovea*. The fovea is about 0.3 mm in diameter and contains all cones, no rods. There are approximately 15,000 cones within the fovea, with an average center to center spacing of about 2.5 microns. Once again, this description deals with a *typical* eye, while actual numbers will vary slightly from individual to individual.

Anything that is to be viewed critically must have its image brought to the fovea in order to be resolved. For example, it will be found that in viewing a printed page (such as this one) at a distance of about 10 inches, two printed letters will essentially fill the fovea. Thus, as we view those two letters, the letters next to them will not be resolved unless their image is brought to the fovea, replacing the previous letters. Fortunately, this scanning function is performed by our visual system naturally and very effectively, so that letters, words, sentences, and paragraphs are easily consumed without conscious effort.

While the fovea is some 5 deg off the optical axis of the eye, computer analysis of the eye model indicates that the off-axis aberrations of the eye, at that field angle, are not of such a magnitude as to significantly degrade the image quality found for the on-axis case. As a result, all of the image quality analysis performed on the eye model of Fig. 2.1 will be done for the on-axis case.

## 2.5 Image Quality

If we assume perfect alignment of the cones within the fovea, and ideal orientation of the image of a high contrast target consisting of equally spaced black and white bars and spaces, the ultimate possible resolution at the fovea will be  $1/(2 \times .0025) = 200$  cycles per mm. Owing to the random nature of cone alignment and target orientation, it is appropriate to apply a degradation factor (similar to the *Kell Factor* in TV systems) of about 70%, resulting in a maximum resolution capability at the fovea of about 140 cycles per mm.

It will be found that this 140 cycle per mm resolution limit is never actually realized by the typical viewer. Residual aberrations of the eye's optics (with a 4-mm pupil) will limit the resolution capability at the fovea to about 110 cycles per mm. Figure 2.4 contains the Modulation Transfer Function (MTF) of the image at the fovea, for the optics of the model eye. While not precisely correct, for purposes of this discussion MTF, modulation, and contrast may be thought of as interchangeable terms. The MTF data in Fig. 2.4 has been calculated assuming a sine wave target, a pupil diameter of 4 mm, and equal spectral weighting at wavelengths of 0.56, 0.51, and 0.61 microns. Superimposed on the MTF curve is an Aerial Image Modulation (AIM) curve for the fovea. This AIM curve is based on the cone size and spacing described earlier, along with known performance characteristics of the eye. While this curve is not an exact representation of actual visual performance, it does represent a very close approximation. This AIM curve will be used throughout this book, primarily for the purpose of generating comparative performance values between designs. At the point of intersection of the two curves in Fig. 2.4 (110 cycles per mm), it can be seen that the optics of the eye model will deliver an MTF value of 0.30 which, according to the AIM curve, is the minimum MTF required at the fovea to resolve that frequency. At any frequency greater than 110 cycles per mm, the MTF of the optics will be less than what is required per the AIM curve, thus these higher frequencies will not be resolved. Resolution of 110 cycles/mm at the fovea corresponds to a frequency of 7.4 cycles/mm at a target located at the eye's near point, 254 mm from the eye. This MTF calculation was repeated for other pupil diameters, with the resulting resolution values plotted in Fig. 2.3.

## 2.6 Normal/Vision

The designation for *normal* visual resolution is 20/20. This means that our naked eye, or the eye provided with corrective lenses, is able to resolve



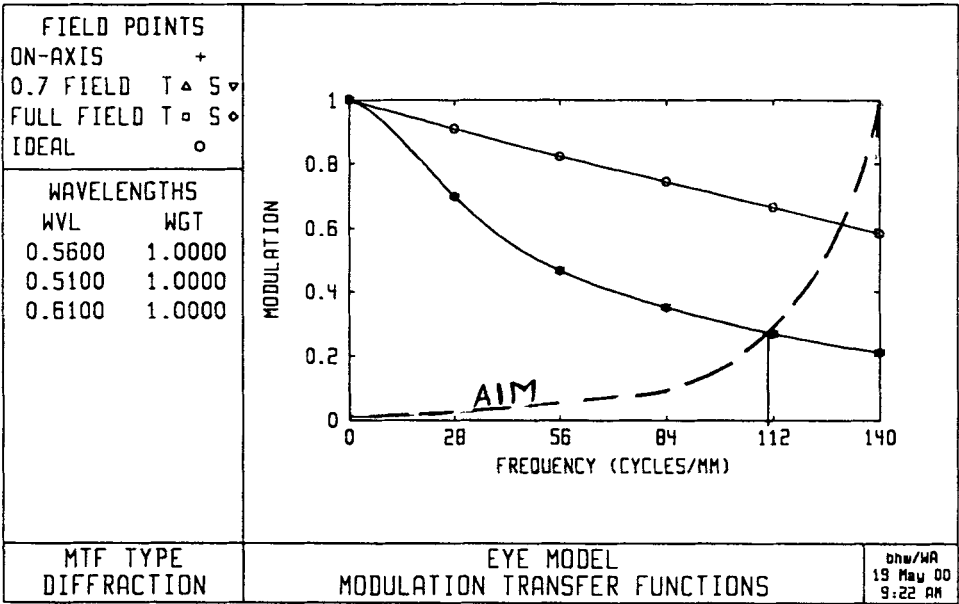


Figure 2.4 Modulation transfer function (MTF) for the optics of the eye model with a 4-mm-diameter pupil, as shown in Fig. 2.1. Also shown is the estimated Aerial Image Modulation (AIM) curve for the retina at the fovea.

detail at a distance of 20 feet that is equal to the level of detail that can be resolved by the standard (average) eye at that same distance. One common test target for evaluating vision is made up of a series of high-contrast block letters. The letter **E** for example, will be made with its horizontal and vertical lines equal in width to the space between them (see Fig. 2.5). The established criteria for normal vision is that the viewer should be able to resolve these letters when each component (line or space) subtends an angle of 1 arc minute to the eye. Therefore, for a test target at a distance of 20 feet (6096 mm), the block letter with 3 lines and 2 spaces, which subtends an angle of 5 arc minutes, would result in a letter height of 8.9 mm. From the geometry of Fig. 2.5, we can calculate the height of the image formed on our retina. That image will be approximately .025-mm (.001 inch) high. The enlarged illustration showing that image relative to the cone spacing at the retina indicates that the letter will be resolved. The shaded area around the image approximates the blurring that will take place due to the residual spherical and chromatic aberrations of the eye's optics.

From Fig. 2.5 it is seen that the image of the block letter **E** is .025-mm high and it contains 3 bars and 2 spaces, or 2.5 cycles. This converts quite simply to a frequency of  $2.5 \text{ cycles} / .025 \text{ mm} = 100 \text{ cycles/mm}$ . Looking back at the MTF data shown in Fig. 2.4, it is possible to determine that the image MTF of the eye's optics at 100 cycles/mm will be about 0.33, while the AIM curve indicates that an MTF of just 0.22 is required at the retina in order to resolve that frequency. Since the image MTF exceeds the required MTF, it can be concluded that this frequency (100 cycles/mm) will be resolved by the visual system.

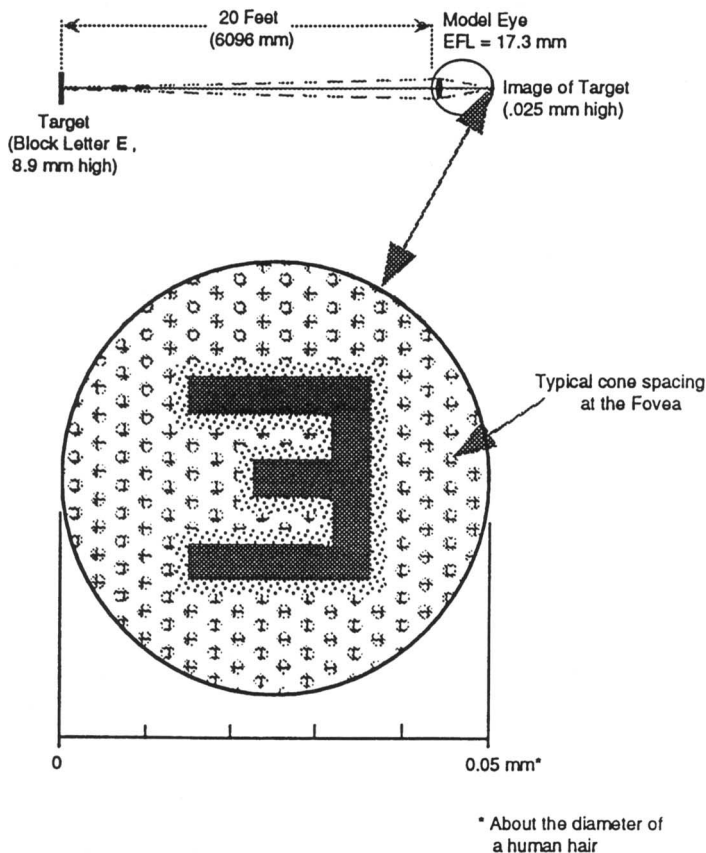


Figure 2.5 Illustrating the standard eye test used to determine normal (20/20) visual resolution. Also shown is an enlarged view of the image formed at the fovea.

## 2.7 Peripheral Vision

Figure 2.6 illustrates the field of view for each eye and for both eyes combined. When viewing an object at some distance, the axes of both eyes will converge so that the object is imaged on the fovea of both eyes. This degree of convergence between the left and right eyes is one of the major cues to our depth perception.

The region of vision defined by the fovea represents a visual field of view of about one deg. Within this region the normal eye will achieve a visual acuity (resolution) of 1 arc minute. Outside this central one-deg field, the acuity of the eye falls quite rapidly. Figure 2.7 shows the rate at which visual acuity falls as the off-axis angle is increased. Within a full field of about 40 deg, visual acuity will be 3 arc minutes or less, representative of good image quality. Beyond that point, to the edge of the visual field, the level of image quality falls rapidly to a point where visual acuity is about 20 arc minutes for a full field of 100 deg. The fall-off in image quality with increased field angle is due to a combination of off-axis aberrations in the eyes' optics, and the structure of the retina, i.e., the distribution of rods and cones away from the fovea.

## 2.8 Review and Summary

The human eye may be described (approximately) as a 1-inch-diameter water-filled sphere with a focusing lens assembly, adjustable iris, and a high-resolution sensor (the retina) at its image surface. The *typical* eye has a focal length of 17.3 mm, a variable  $f$ -number from  $f/2.5$  to  $f/17$ , and adjustable focus from infinity down to 10 inches. While the full field of view of the eye is approximately 140 deg, the area of useful imagery is limited to about 90 deg. The optics of the eye are configured to reduce residual spherical aberration, while chromatic aberration remains uncorrected. The area of optimum resolution at the retina is referred to as the fovea. In most cases, when forming an image at the fovea, the optics of the eye exhibit image quality (spot size) that is from 2 to 4 times worse than the diffraction limit. Normal visual acuity is 1 arc minute, meaning that under normal conditions the eye will resolve a high-contrast, repeating pattern of equal width bars and spaces, when each element of that pattern subtends an angle of 1 arc minute to the eye. In order to be effective, the designer of optical instruments for visual applications must take into account all of the physical and optical characteristics that have been presented here.

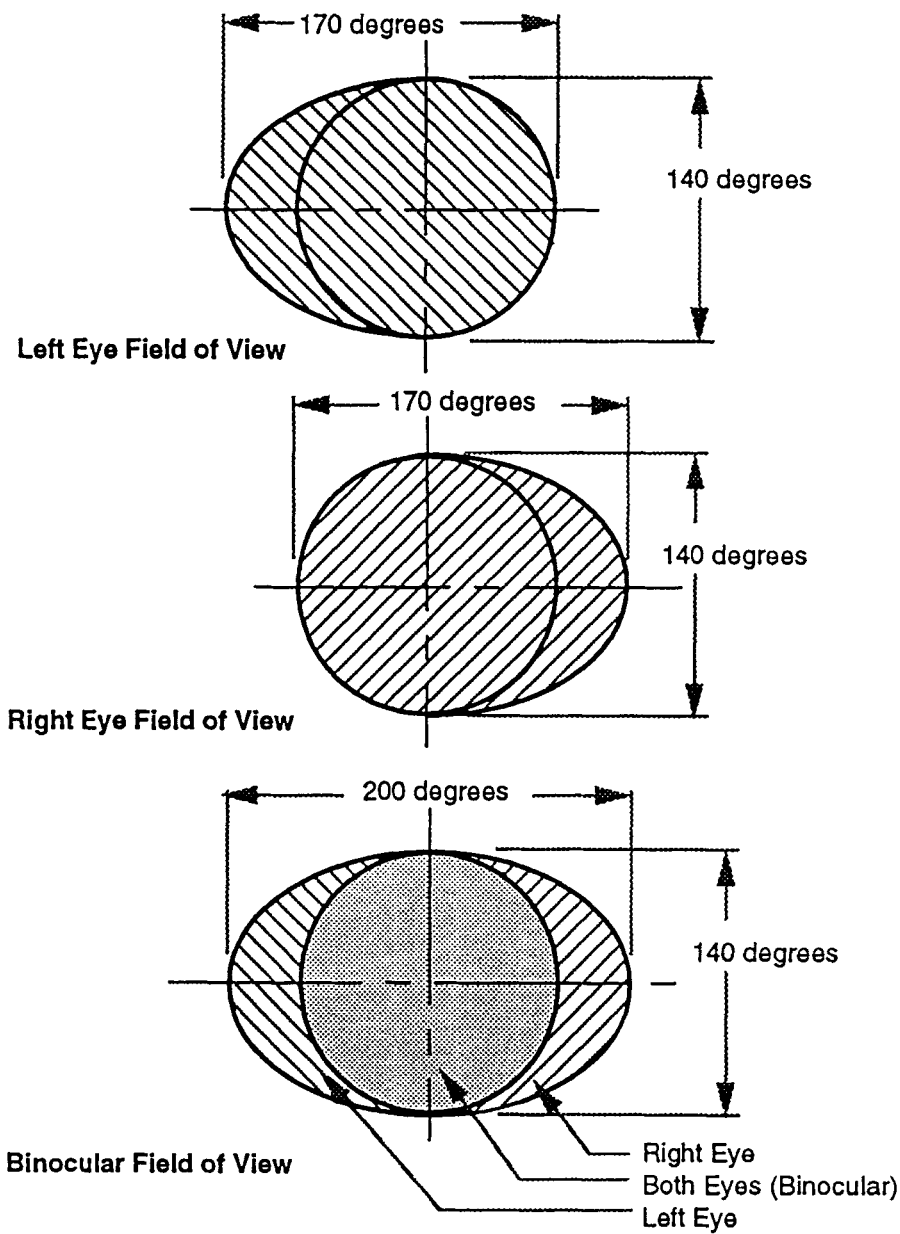


Figure 2.6 The approximate monocular visual field of view for each eye, and the combined binocular field.

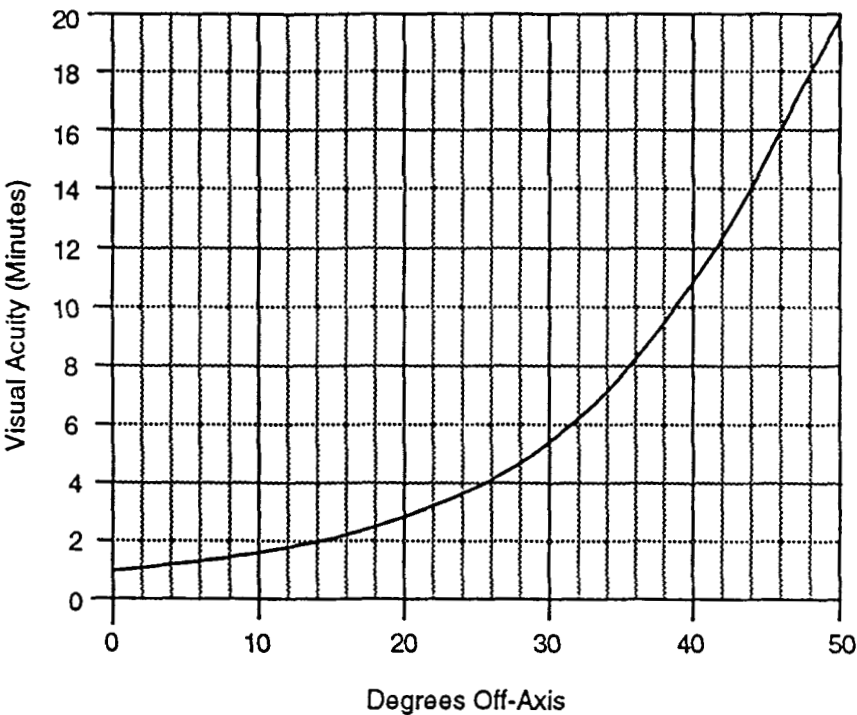


Figure 2.7 The visual acuity (resolution) of the eye is very much dependent on the location of the image on the retina. Maximum acuity is achieved over a very small field (about 1.0-deg diameter), limited by the 0.3-mm diameter of the eye’s fovea.

## 3

## Magnification and Vision

---

### 3.1 Introduction

In the preponderance of cases, the primary reason for introduction of an optical system to be used with the eye is to increase the size of the final image on the retina, thus allowing the viewer to resolve greater detail within that image than would be possible with the naked eye. The term for this increase of final image size is *magnification*. While frequently used when describing the function of an optical device or system, the term magnification is often misinterpreted or applied incorrectly. This chapter contains information and examples that will allow the reader to better understand the true meaning and proper application of the term magnification.

### 3.2 Near Object Standard

A near object is one that can be placed at a comfortable distance from the eye for purposes of visual examination. In order to discuss the magnification factor introduced by an optical system it is essential that we first establish a reference case for comparison purposes. For that reference case, let's consider the typical unaided eye, accommodated to view an object at the near point of vision, which is 254 mm (10 inches).

When the typical eye is focused at 254 mm, the eyelens is accommodated for maximum lens power (Fig. 2.1). In this case the effective focal length of the eye is found to be 16.56 mm and the object to image magnification is  $0.067\times$ . These data have been derived by setting up a computer model of the eye focused at the near point as described in Fig 2.1 and Fig. 3.1(a).

For purposes of this and subsequent examples we will assume that the target being viewed is a 20-mm-diameter USAF resolution target [Fig. 3.1(b)] containing 3-bar patterns ranging from 1 cycle/mm (group 0, element 1), to 228 cycles/mm (group 7, element 6). Using the eye's established maximum resolution value of 110 cycles/mm at the retina, the magnification factor of  $0.067\times$  can be applied to determine the maximum resolution at the target, which will be:  $110 \text{ cycles/mm} \times .067 =$

7.4 cycles/mm (group 2, element 6). As a further point of reference, the 20-mm-diameter object being viewed will subtend an angle of 4.5 deg to the eye and the resulting image at the retina will be 1.34 mm in diameter. Any magnifying optics to be considered will be expected to increase this apparent angle and the corresponding final image size at the retina.

### 3.3 Loupe Magnification

If we wish to resolve more detail in the target being viewed, our first instinct would be to bring it closer to the eye, thus increasing the angle that it subtends and the size of the image on the retina. It has been established, unfortunately, that the typical eye is unable to focus on an object that is closer than 254 mm. This situation can be dealt with by the introduction of a positive lens near the eye. This most basic optical device for enhanced viewing of objects located inside the near point of vision is the loupe, or magnifying glass.

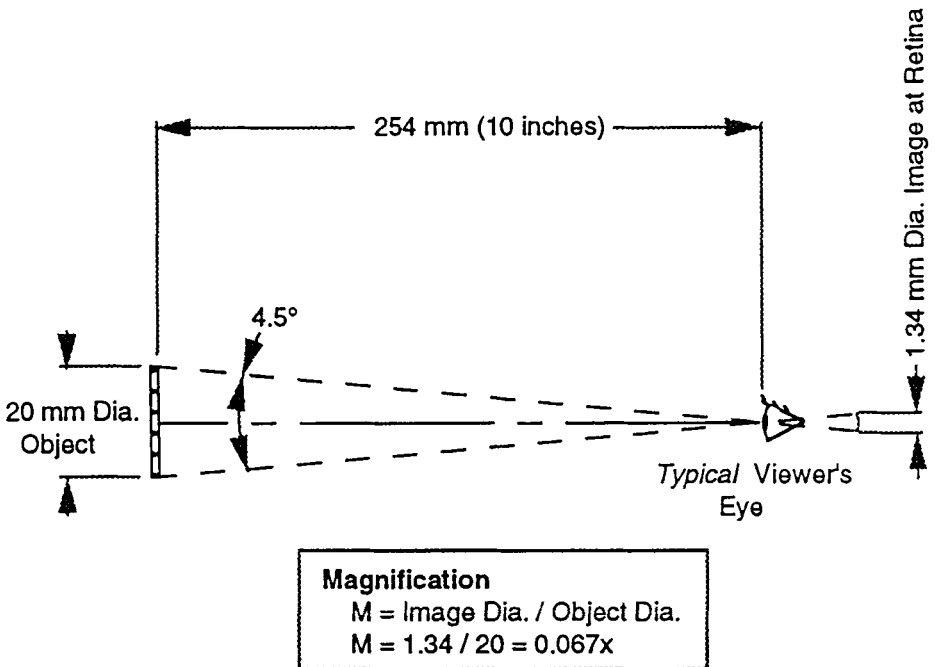
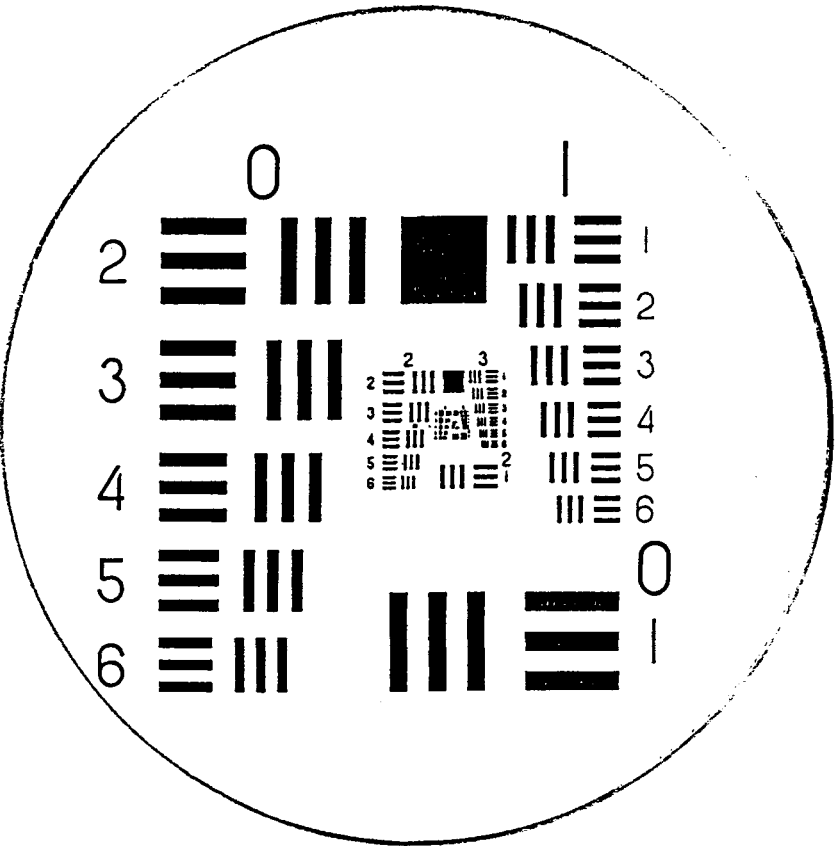


Figure 3.1(a) The standard used in discussing magnification of near objects references the size of the object, its angular subtense, and the final image size on the retina, when the object is located at the near point of vision (10 inches, or 254 mm).



Element Number	Group Number							On Transparent Targets Only
	0	1	2	3	4	5	6	7
1	1.00	2.00	4.00	8.00	16.00	32.00	64.00	128.0
2	1.12	2.24	4.49	8.98	17.96	35.92	71.84	143.7
3	1.26	2.52	5.04	10.08	20.16	40.32	80.63	161.3
4	1.41	2.83	5.66	11.31	22.63	45.25	90.51	181.0
5	1.59	3.17	6.35	12.70	25.40	50.80	101.6	203.2
6	1.78	3.56	7.13	14.25	28.51	57.02	114.0	228.1

Figure 3.1(b) USAF 1951 resolving power test target.



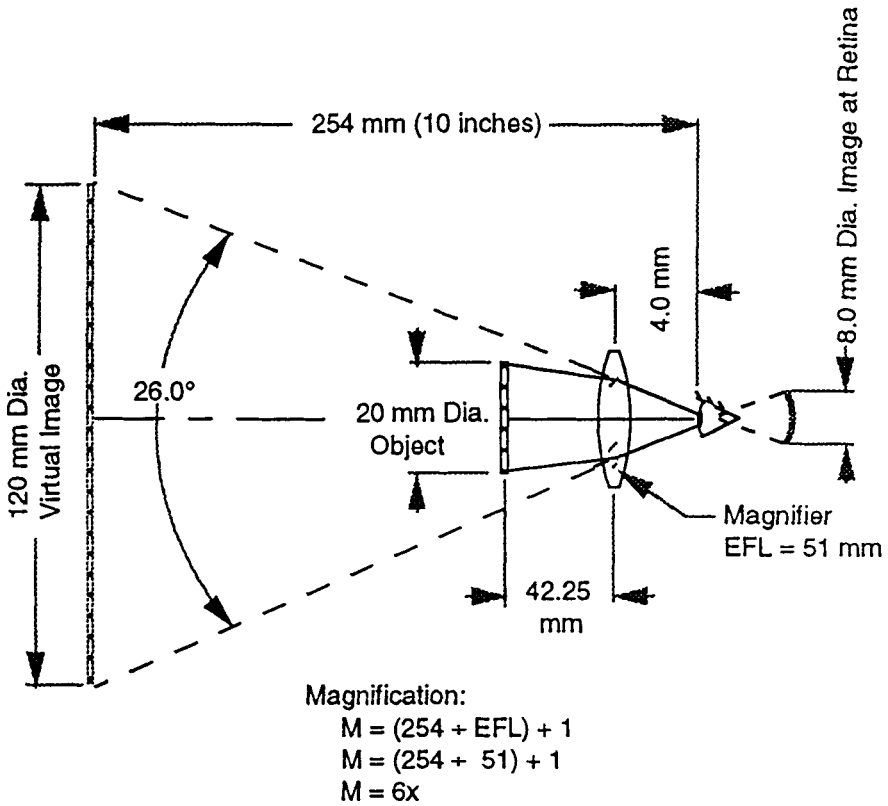


**Figure 3.2** A simple lens, or loupe, can be used as a magnifier to increase the apparent size of a near object, as well as the image size at the retina and the amount of detail that can be resolved at the object.

Figure 3.2 illustrates the function of a magnifying glass as it might be used to view the resolution target described earlier. The approximate (thin lens) magnification power of a magnifier can be determined by the following formula:

$$\text{Mag.} = (254 / \text{focal length}) + 1$$

For the 51-mm focal length thin lens shown in Fig. 3.2, the corresponding magnification would be

$$(254 / 51) + 1 = 6\times.$$

Viewing the 20-mm-diameter target with this thin lens, it can be seen that, with the object at the position shown, the resulting virtual image produced by the lens at a distance of 254 mm from the eye will be: 20 mm

$\times 6.0 = 120\text{-mm}$  diameter. Having established earlier that the magnification from the near point of vision (254 mm) to the retina is  $0.067\times$ , it can be concluded that the final image at the retina, when this magnifier is used, will be:  $120\text{ mm} \times 0.067 = 8.0\text{ mm}$ , or 6 times larger than the image formed without the magnifier.

Note that in forming the 120-mm-diameter virtual image, the magnifier has increased the apparent size of all detail within the target. As a result, the eye will now be able to resolve 7.4 cycles per mm at the virtual image, which corresponds to  $6 \times 7.4 = 44$  cycles per mm (group 5, element 3) at the target being viewed. Several actual magnifier design exercises will be presented in the next chapter.

### 3.4 Microscope Magnification

There is a practical limit of about  $25\times$  to the magnification that can be achieved using a simple magnifier. To achieve magnifications greater than  $25\times$  it is necessary to use a pair of lenses in the form of a microscope as illustrated in Fig. 3.3. In the case of the microscope, the first lens (the objective) forms a real image of the object at magnifications ranging from  $4\times$  to  $100\times$ . The real image formed by the objective is then viewed with the aid of an eyepiece, which acts as a magnifier. Eyepiece magnification in a microscope will typically range from  $5\times$  to  $20\times$ . The total magnification of the microscope is found by multiplying the objective lens magnification by the eyepiece magnification.

The specific example shown in Fig. 3.3 describes a  $50\times$  microscope with a  $10\times$  objective and a  $5\times$  eyepiece. Eyepiece design data will determine the size of its field stop, in this case 18 mm. This field-stop diameter is divided by the objective lens magnification to determine the size of the object that will be seen. In the example shown in Fig. 3.3, the 18-mm-diameter field stop is divided by the  $10\times$  magnification of the objective to determine that a 1.8-mm-diameter spot on the object will be imaged by this microscope. Without the microscope, this 1.8-mm-diameter spot (at the eye's near point) will subtend an angle of 0.4 deg to the eye and will form a 0.12-mm-diameter image on the retina. The  $5\times$  eyepiece will increase the apparent size of the 18-mm-diameter field stop such that it subtends an angle of about 20 deg to the eye and forms a 6.0-mm-diameter image on the retina. The resulting total magnification will then be

$$\begin{aligned}\text{Magnification} &= \text{Image dia. with microscope} / \\ &\quad \text{Image dia. without microscope} \\ &= 6.0 / .12 = 50\times.\end{aligned}$$

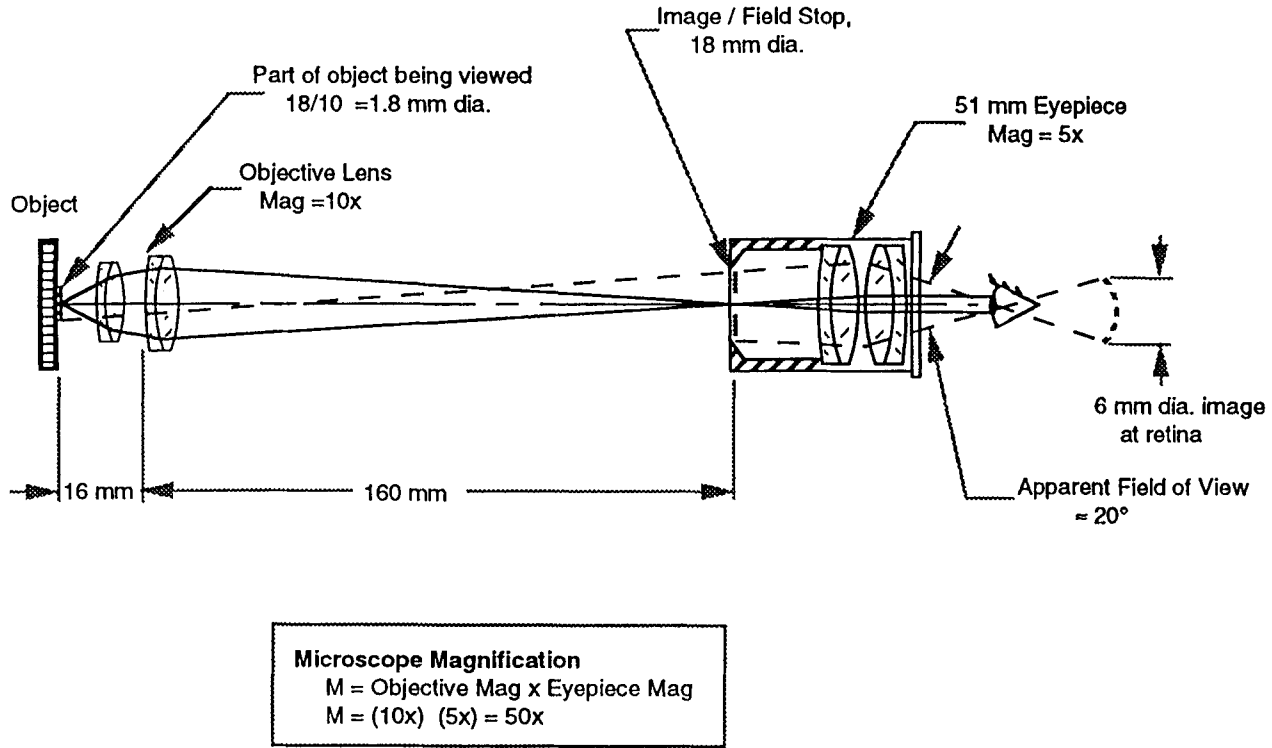


**Figure 3.3** When a simple magnifier cannot provide the required magnification, it is possible to introduce a system with two stages of magnification. Shown here is a basic microscope system with a total magnification of 50.

Regarding resolution, it has been stated that the naked eye can resolve 7.4 cycles per mm when viewing the USAF target at the near point of vision, under ideal conditions. The microscope will increase that limit by a factor of 50 $\times$ , making it about 370 cycles per mm. This means that the entire pattern (maximum frequency = 228 cycles per mm) will be resolved using the 50 $\times$  microscope. A term frequently used to describe a microscope's resolving capability is the minimum size element that can be resolved. In this case, if the eye with microscope can resolve 370 cycles per mm, this would correspond to 740 elements per mm, or .0014 mm (1.4 micron) per resolved element at the object.

Thin lens analysis leads us to the conclusion that the apparent field of view (to the eye) will be about 20 deg and the exit pupil diameter will be 2.55 mm. Other more specific system design parameters will be determined in a later chapter, where an actual microscope optical system design will be developed.

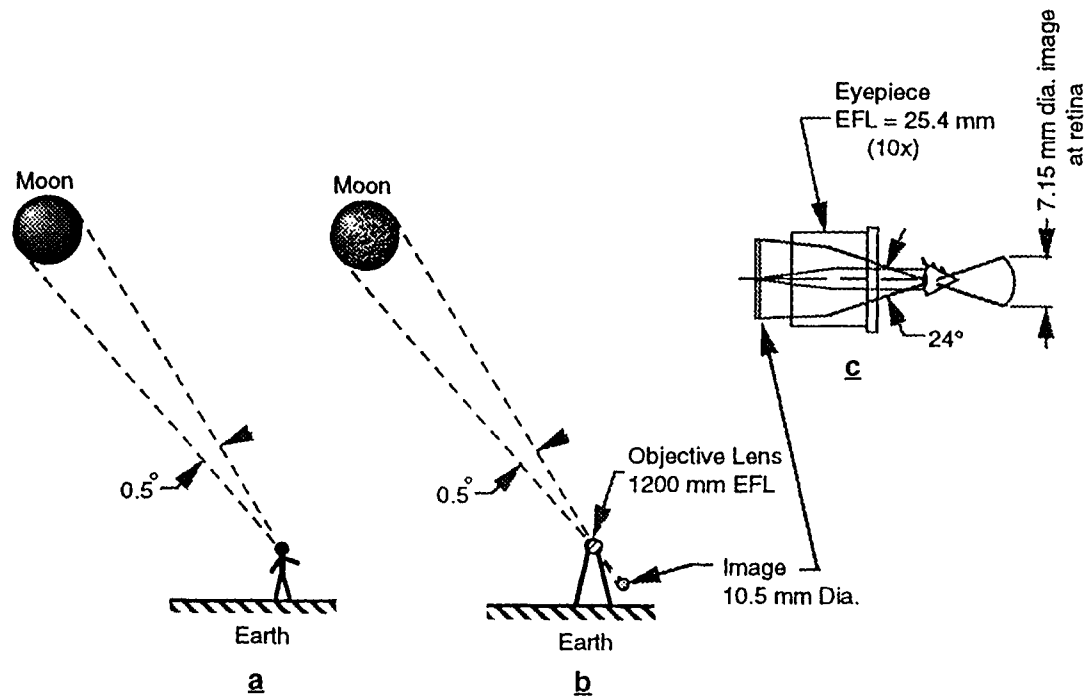
### 3.5 Distant Object Magnification

With the magnifier and the microscope we have been dealing with the viewing of near objects—objects that can be placed close to the eye and the optics being used. Another situation frequently encountered deals with distant objects that cannot be brought physically close to the viewer. A typical example, which we will address in this discussion, would be the moon, which is frequently viewed and recorded at some magnification.

Figure 3.4(a) illustrates the condition where the moon is being viewed by the naked eye. The full moon subtends an angle of about 0.5 deg when viewed from earth. For the typical eye this would result in a 0.15-mm-diameter image on the retina. Knowing that the eye will resolve .0045-mm elements at the retina, this would indicate that we can only resolve  $0.15/.0045 = 33$  elements across the image of the moon. This corresponds to elements that are about 60 miles across. Obviously, some considerable magnification will be required in order to resolve a more interesting and useful level of detail on the moon's surface.

Figure 3.4(b) illustrates the result when a 1200-mm (48-inch) focal length, f/8 telescope objective lens is used to form a 10.5-mm-diameter image of the moon. For a perfect lens, at optimum focus, the resolution limit at that image would be

$$\begin{aligned}\text{Res.} &= 1 / (\lambda \times \text{f-number}) \\ &= 1 / (0.00056 \times 8) = 224 \text{ cycles per mm.}\end{aligned}$$



**Angular Magnification:**

$M = \text{Angle from Telescope} + \text{Angle into Telescope}$

$$M = 24.0^\circ + 0.5^\circ = 48x$$

Figure 3.4 (a) When considering magnification of a distant (as opposed to near) object, the moon is a convenient subject. (b) An objective lens with a focal length of 1200 mm will form an image of the moon that is 10.5 mm in diameter. (c) Viewing that 10.5-mm-diameter image with a 10 eyepiece, the final image will subtend an angle of 24 deg to the eye.

Design experience indicates that residual aberrations, manufacturing tolerances, and focus error will contribute about one-half wave of wavefront error to the image, which will reduce the resolution by about 50%, to approximately 112 cycles per mm.

If, as is shown in Fig. 3.4(c), a 25.4-mm focal length (10×) eyepiece is used to view the image formed by the objective lens, then the final image at the retina will be

$$\begin{aligned}\text{Image Dia. at Retina} &= (\text{Eye efl} / \text{Eyepiece efl}) \\ &\quad \times \text{Eyepiece Image Dia.} \\ &= (17.3 / 25.4) \times 10.5 \\ &= 7.15\text{-mm-dia. Image at Retina.}\end{aligned}$$

The original image at the retina (without the telescope) was 0.15-mm diameter. Thus the magnification factor due to the telescope is  $7.15 / 0.15 = 48\times$ . This corresponds well with the more common method used to calculate telescope magnification, where the focal length of the objective (48 inches) is divided by the focal length of the eyepiece (1 inch), again yielding a magnification of  $48\times$ .

The resolution of this system will be limited by the eye. It was determined earlier that the resolution at the image formed by the objective will be about 112 cycles per mm. We have established that the typical resolution limit at the retina is 110 cycles/mm. Knowing the efl of the eye to be 17.3 mm, and the efl of the eyepiece to be 25.4 mm, it can be concluded that the best visual resolution achievable at the objective/eyepiece image plane will be  $(17.3 / 25.4) \times 110 = 75$  cycles/mm. Since the objective lens delivers a resolution of 112 cycles/mm, telescope performance will be eye limited.

While we have established previously that the naked eye is limited to resolving 60-mile element size on the moon's surface, introduction of this  $48\times$  telescope will reduce this minimum resolved element size to about 1.25 miles.

An alternate approach to visualization of the telescope's function might deal with the apparent viewing distance that is achieved. With the unaided eye we see the moon as it appears from a distance of about 226,000 miles. With the  $48\times$  telescope, we see the moon as it would appear to the unaided eye from a distance of  $226,000 / 48 = 4708$  miles. Addition of the telescope to the visual system may be thought of as being equivalent to a journey of more than 221,000 miles through space.

### 3.6 Photographic Systems

In discussing the magnification associated with a photographic system, it is essential that all of the contributing factors involved in generating and viewing the final image be considered.

For this example we will assume that the moon is again being imaged by the 1200-mm focal length objective described in the previous section. In this case the eyepiece will be replaced by a 35-mm camera body with the primary 10.5-mm-diameter image being formed directly onto the film (Fig. 3.5). Following processing, the film (or a contact print from the negative) can be viewed with the naked eye or with a magnifier. Applying the near point magnification factor of  $0.067\times$  for the naked eye, we can conclude that this will result in an image diameter on the retina of 0.7 mm. It was found earlier that the size of the moon's image when viewed with the naked eye was 0.15 mm. From this we can conclude that recording the image on film with a 1200-mm lens will result in a visual magnification factor of  $0.7 / 0.15 = 4.7\times$ . In a subsequent step we might choose to generate an  $8\times 10$  print using this negative (magnification factor of  $8.5\times$ ). This would result in a final image size on that print of 89 mm for the moon's diameter. When viewed at the near point, this image would subtend a 20-deg angle to the eye and the final image on the retina would be about 5.9-mm diameter. Again, reverting back to the diameter of the moon's image of 0.15 mm at the retina for the naked eye, we can now calculate the magnification of the photographic system as follows:

$$\begin{aligned}\text{Mag.} &= \text{Final Image Dia. at Retina} / \text{Original Image Dia. at Retina} \\ &= 5.90 / 0.15 = 39\times.\end{aligned}$$

Regarding ultimate resolution, if we assume that the film and print paper do not limit resolution, we can apply the  $.0045\text{mm}$  / element resolution limit at the retina to the final image and conclude that  $5.9 / .0045 = 1311$  elements will be resolved across the 1972-mile diameter of the moon. The resulting resolved element size would then be  $1972 \text{ miles} / 1311 \text{ elements} = 1.5 \text{ miles per element}$ . As might be expected, because the final magnification factors are nearly the same ( $39\times$  vs.  $48\times$ ), this is quite close to the resolution found using the  $48\times$  telescope to view the moon directly.

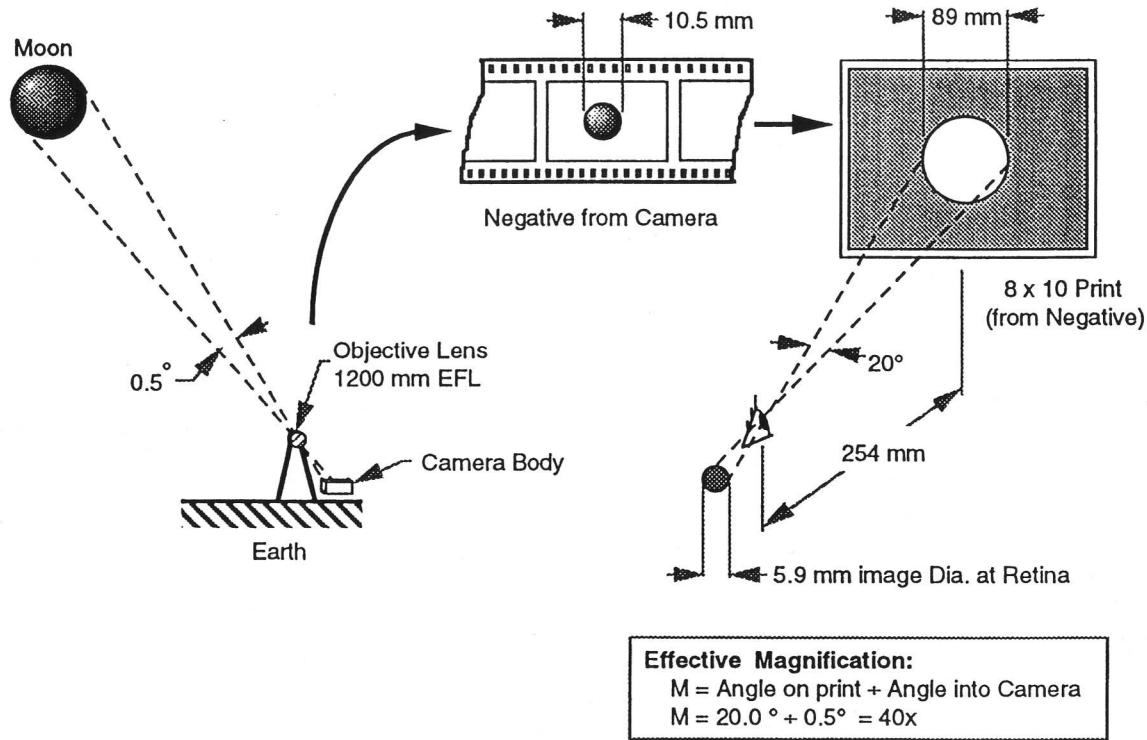


Figure 3.5 The effective magnification of a photographic system will depend upon several factors, including the focal length of the taking lens, the size of the photographic print, and the distance at which that print is viewed.



### 3.7 Video Systems

For one final example of magnification, this section will consider a video (television) system and the multitude of factors that are involved in determining the ultimate magnification factor as we view the TV screen in our living room (Fig. 3.6).

First, in the studio, let's assume that the subject is recorded using a camera with an 18-mm focal length lens (Fig. 3.6). The camera sensor is a half-inch CCD with dimensions of  $4.8 \times 6.4$  mm. The 6-ft tall subject being recorded is standing 25 feet from the camera. The resulting image of the subject at the sensor will be,  $(6 / 25) \times 18 = 4.3$  mm high. Note that this image is about 90% of the 4.8-mm maximum vertical format size at the CCD.

The image is then broadcast to our home where it is viewed on a 32-inch monitor at a distance of 6 ft (1829 mm) from the eye. The height of the display on a 32-inch monitor will be approximately 488 mm. The image of our subject will be 90% of that, or about 439 mm. Finally, the magnification from the monitor to the retina will be:

$$\text{Eye efl} / \text{viewing distance} = 17.3 / 1829 = .0095\times.$$

As a result, the final image size of the subject on the retina will be

$$.0095 \times 439 = 4.17 \text{ mm}.$$

As shown in Fig. 3.6, the angular subtense of the subject to the viewer at home is the same as the angular subtense of the subject to the camera in the studio. In this case the magnification of the system is  $1.0\times$ , or unity.

While a discussion of resolution is not particularly useful in this case, we can look at a few points of interest. First, if we were in the studio viewing the subject from the camera position, the 1-minute-per-element resolution capability of the typical eye would mean that the subject would be visually resolved into 810 one-minute elements over its height. When viewing the subject's picture on our 32-inch monitor, we can assume a high quality system capable of 500 TV lines per picture height. This would mean that the subject's picture (which it will be recalled is 90% of the picture height) would be made up of 450 TV lines, or 450 picture elements. It can be concluded that the television system in this specific case (Fig. 3.6), has degraded our ability to resolve detail on the subject by about 45%.

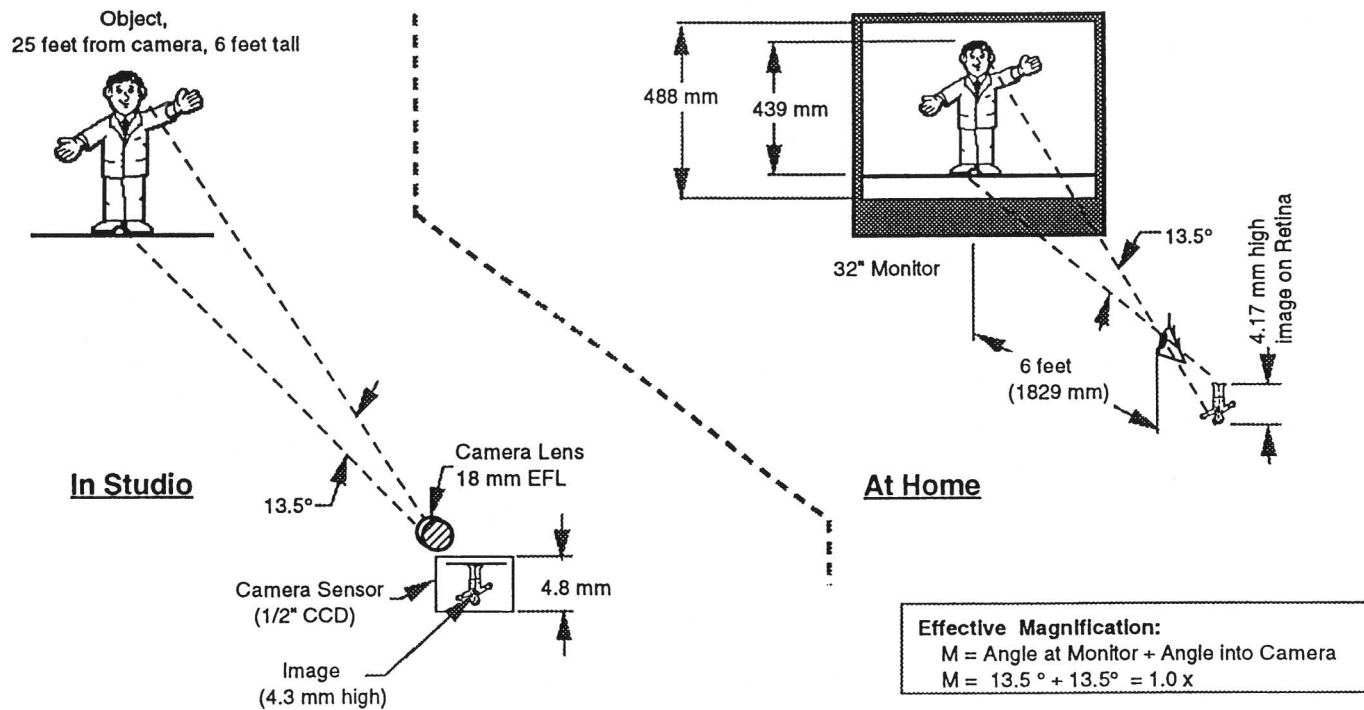


**Figure 3.6** The magnification of a television system is dependent on the camera lens focal length, the camera sensor size, the monitor size, and the final viewing distance. All of these enter into the determination of effective system magnification.

### 3.8 Review and Summary

While the subject of magnification may seem complex initially, it is possible to simplify each example, making the topic relatively easy to understand. In this chapter we have dealt with the final image size on the retina, with and without the optical system, as a basis for determining the final visual magnification factor. For near objects, we have utilized the magnification factor of  $0.067\times (1/15^{\text{th}})$  for the fully-accommodated eye, viewing an object at the near point of vision (254 mm) as the base reference.

The magnifier and the microscope were then introduced and their magnification was determined by finding and comparing the ratio of the final image size on the retina with and without these optics. Optics of the telescope were then described and the ability of the telescope to magnify the apparent size of a distant object was covered.

Finally, two systems were discussed that were somewhat more complex than the direct viewing visual systems. They were the photographic system and the television system. In both of these cases, several additional factors were found that required consideration. However, as in previous cases, the resulting magnification factor was ultimately found by comparison of the final image size on the retina, before and after the introduction of these systems.

## 4

## The Magnifier—Design

---

### 4.1 Introduction

The simplest of optical devices intended to enhance our visual capability is the *magnifier*. This is a simple positive lens with a focal length of 100 mm or less. (Biocular, Sherlock Holmes-type magnifiers, which may have longer focal lengths, will not be covered.) When a simple positive lens is placed close to the eye, it permits the object being viewed to be moved inside the near point of the eye, thus increasing the apparent size of that object along with the final image size on the retina.

The most common lens forms used for magnifiers are the biconvex element, the achromatic doublet, and the Hastings triplet. While all of these are commercially available at reasonable prices, we will consider the optical design of each in order to gain some insight into their performance characteristics.

Several more complex, multicomponent lens forms are used as magnifiers. The design and performance of one such magnifier will also be covered. In every case the final visual image quality, in terms of on-axis and off-axis resolution, will be determined and compared.

### 4.2 The Biconvex Magnifier

The simplest of all magnifiers would be the biconvex lens element with equal radii, made from a common crown glass type. For most of the examples to be presented in this chapter we will assume that a nominal magnification of 6× is required. It will further be assumed that the closest optical surface of the magnifier will be 10 mm from the eye's cornea, the pupil diameter of the eye will be 4 mm, and that the eye will be fully accommodated, i.e., focused at a distance of 254 mm.

Figure 4.1 contains lens data from the OSLO lens design program for the eye model viewing a near object (top) and for that same eye model working in conjunction with a biconvex 6× magnifier made from BK7 optical glass to view that same object. In both cases, the object being viewed is 20 mm in diameter. The working wavelengths and indices of refraction are also shown.

**\*PARAXIAL CONSTANTS**  
Effective focal length: 16.561359 Lateral magnification: -0.067127  
Numerical aperture: 0.116299 Gaussian image height: 0.671273  
Working F-number: 4.299257 Petzval radius: -15.409421

**\*LENS DATA**  
**EYE MODEL (NEAR OBJECT)**

SRF	RADIUS	THICKNESS	APERTURE RADIUS	GLASS	NOTE
OBJ	--	254.000000	10.000000	AIR	
1	7.800000	0.600000	6.000000	CORNEA M	
2	6.400000	3.000000	5.000000	AQUEOUS M	
AST	--	--	1.774924 AS	AQUEOUS P	IRIS
4	5.950000	4.000000	4.000000	LENS M	
5	-6.100000	17.160000	4.000000	VITREOUS M	
6	-12.500000	0.001000	6.000000	RETINA M	
IMS	-12.500000	--	6.000000		

**\*PARAXIAL CONSTANTS**  
Effective focal length: 18.092886 Lateral magnification: -0.412178  
Numerical aperture: 0.116299 Gaussian image height: 4.121781  
Working F-number: 4.299259 Petzval radius: -12.639273

**\*LENS DATA**  
**EYE w/6x MAGNIFIER**

SRF	RADIUS	THICKNESS	APERTURE RADIUS	GLASS	NOTE
OBJ	--	38.200000	10.000000	AIR	
1	48.000000	4.000000	10.000000	BK7 C	6X
2	-48.000000 P	10.000000	10.000000	AIR	MAGNIFIER
3	7.800000	0.600000	6.000000	CORNEA M	
4	6.400000	3.000000	5.000000	AQUEOUS M	
AST	--	--	1.775098 AS	AQUEOUS P	IRIS
6	5.950000	4.000000	4.000000	LENS M	
7	-6.100000	17.160000	4.000000	VITREOUS M	
8	-12.500000	0.001000	6.000000	RETINA M	
IMS	-12.500000	--	6.000000		•

**\*WAVELENGTHS**  
CURRENT    WV1            WV2            WV3  
1    0.560000    0.510000    0.610000

**\*REFRACTIVE INDICES**

SRF	GLASS	RN1	RN2	RN3	VNBR
0	AIR	1.000000	1.000000	1.000000	--
1	BK7	1.518032	1.520769	1.515909	106.590319
2	AIR	1.000000	1.000000	1.000000	--
3	CORNEA	1.377000	1.379340	1.375210	91.300000
4	AQUEOUS	1.336000	1.338085	1.334405	91.300000
5	AQUEOUS	1.336000	1.338085	1.334405	91.300000
6	LENS	1.411000	1.413551	1.409049	91.300000
7	VITREOUS	1.337000	1.339091	1.335400	91.300000

Figure 4.1 Tabulated lens data for the model eye accommodated to view an object at 254 mm (top). The same eye model with a simple biconvex 6x magnifier (bottom).

The *design* of such a simple lens is governed by the variables available to produce improved image quality. In this case, since lens power (6 $\times$  magnification) is fixed, the only variables available to the designer are the lens shape and lens material. It has been concluded that the economies of making both radii the same, and using a popular crown glass type, far outweigh any advantages that can be realized by a more complex shape and/or material.

Figure 4.2 contains lens drawings of the two systems tabulated in Fig. 4.1. In viewing the “eye with magnifier” layout it should be remembered that the lens will form a virtual image of the object. That virtual image will be located at the eye’s near point (254 mm) and it will be approximately six times larger than the object.

Figure 4.3 contains results of ray trace analysis of both systems. While reviewing these aberration curves the reader should note the changes in scale factors that exist between them. The most apparent differences between the two are the increase in astigmatism and distortion that occur due to the increased field angle involved when the magnifier is introduced. These results are interesting, but not significant. Most important is the residual spherical and chromatic aberration introduced by the biconvex lens. From the MTF data shown in Fig. 4.4, it can be concluded that these residual aberrations will result in a resolution loss of about 10%.

While the nominal on-axis performance of the biconvex lens is *respectable*, let’s now examine its off-axis performance. We will assume that the relationship between object, magnifier, and the eye are fixed (as in a slide viewer). Now, if we wish to examine a point that is 10 mm from the center of the object, the eye will rotate in its socket about a point that is about 13.5 mm inside the first surface of the cornea. When the eye rotates through a 13-deg angle (Fig. 4.5, top), the object point that is 10 mm from the center will be imaged at the center of the retina. Due primarily to off-axis chromatic aberration in the magnifier, the resolution at this point will be reduced to about 87 cycles per mm (Fig. 4.5, bottom). This result would lead one to believe that overall performance could be improved by the introduction of a color-corrected (achromatic) magnifier.

### 4.3 The Doublet Magnifier

Design of a 6 $\times$  achromatic doublet magnifier is a relatively basic exercise. The most important steps in this process involve thin lens setup, starting lens selection, creation of a realistic set of optimization goals, and, finally, lens optimization and evaluation.

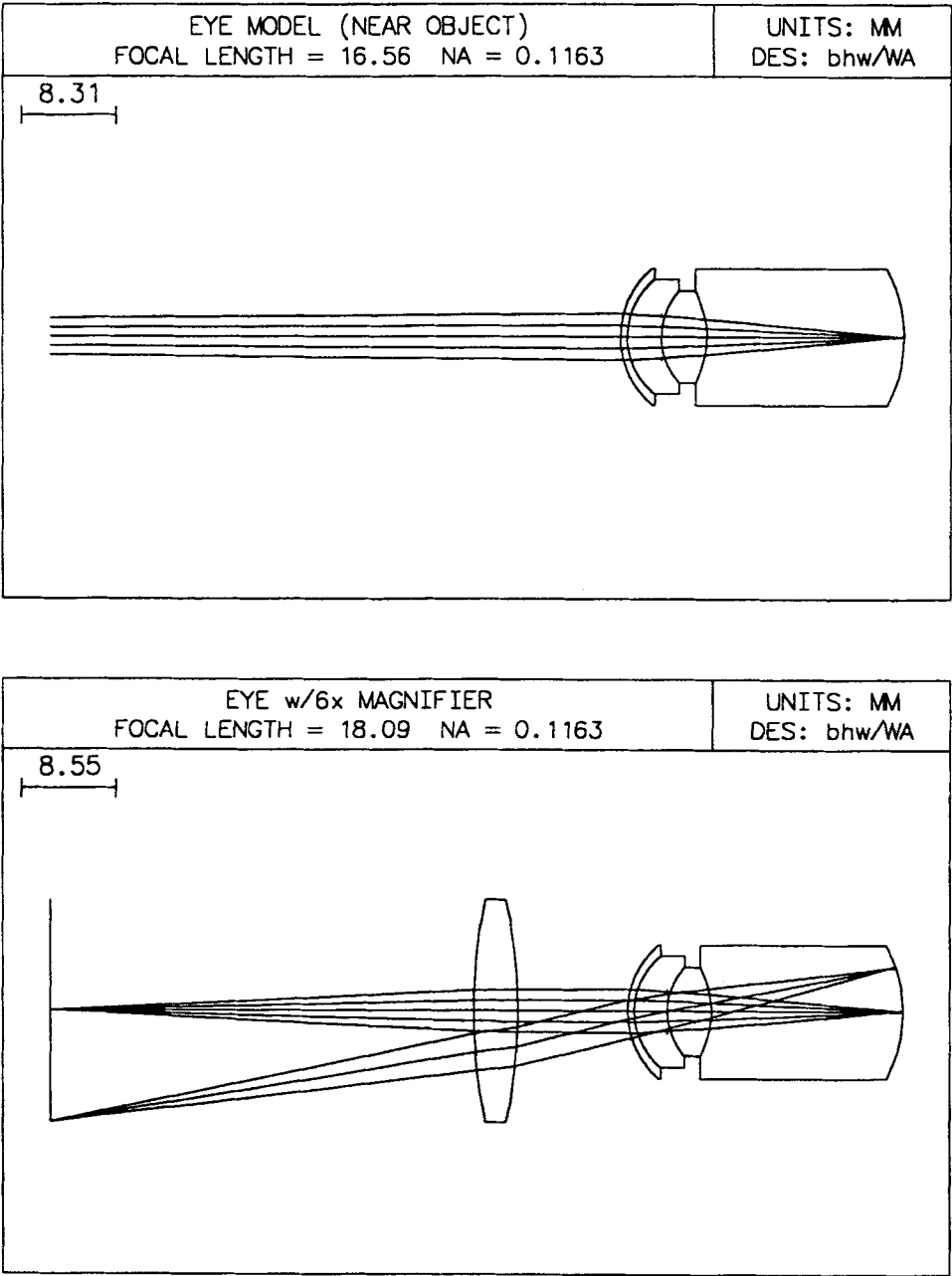


Figure 4.2 Lens layouts showing the model eye accommodated to view an object at 254 mm (top) and the same model eye with a simple biconvex 6× magnifier (bottom).

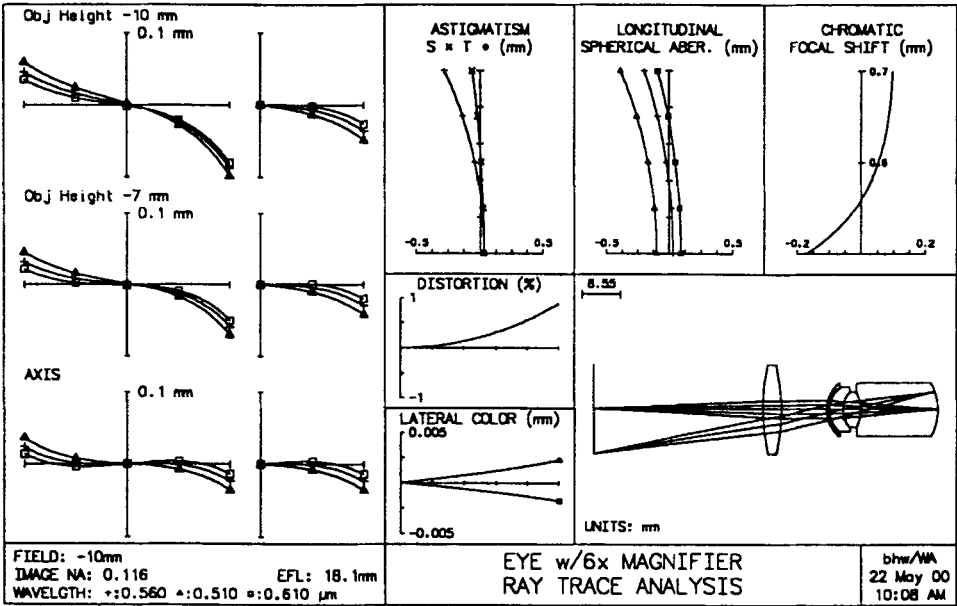
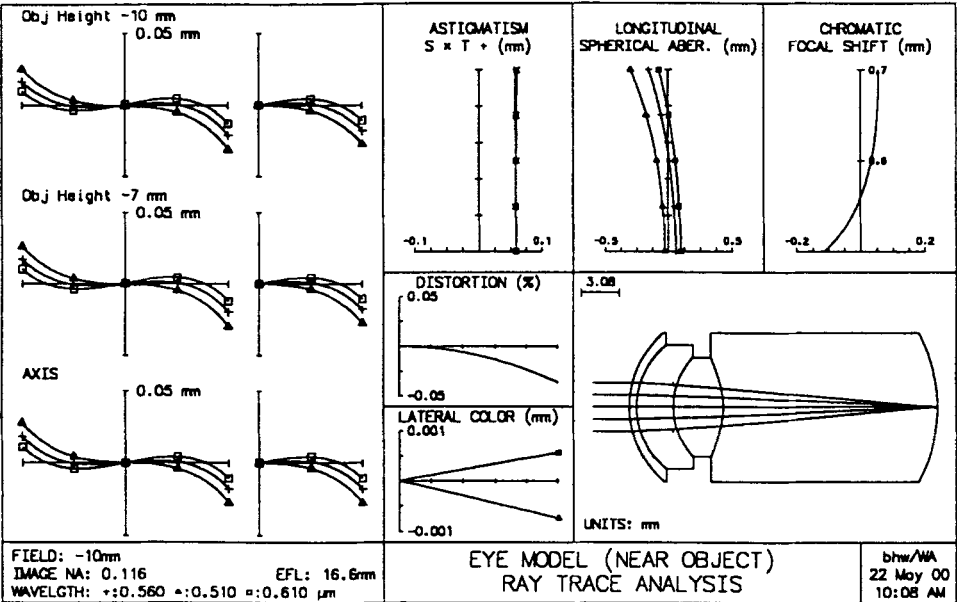


Figure 4.3 Ray trace analysis (aberration curves) for the model eye accommodated to view an object at 254 mm (top) and the same model eye with a simple biconvex 6× magnifier (bottom).



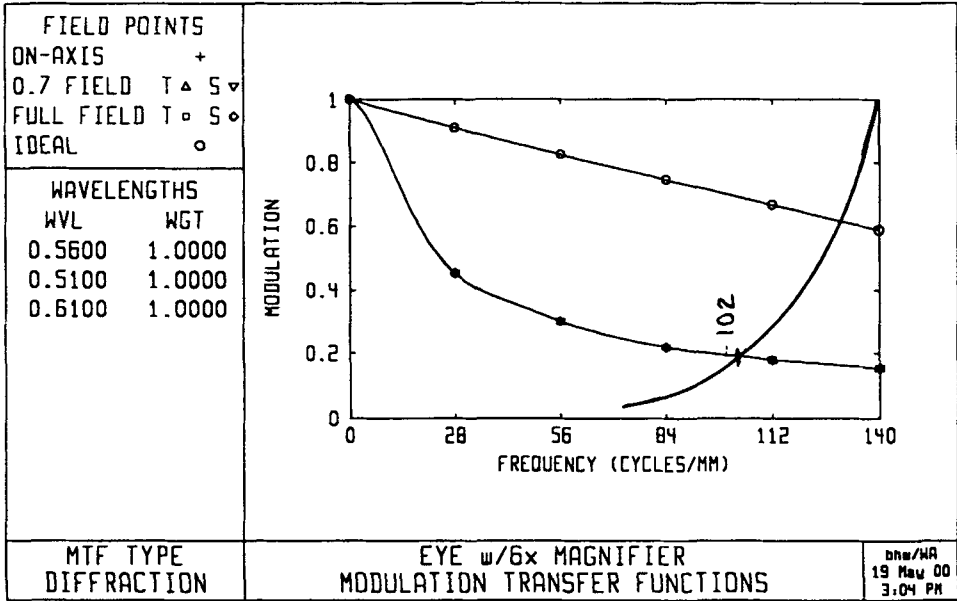
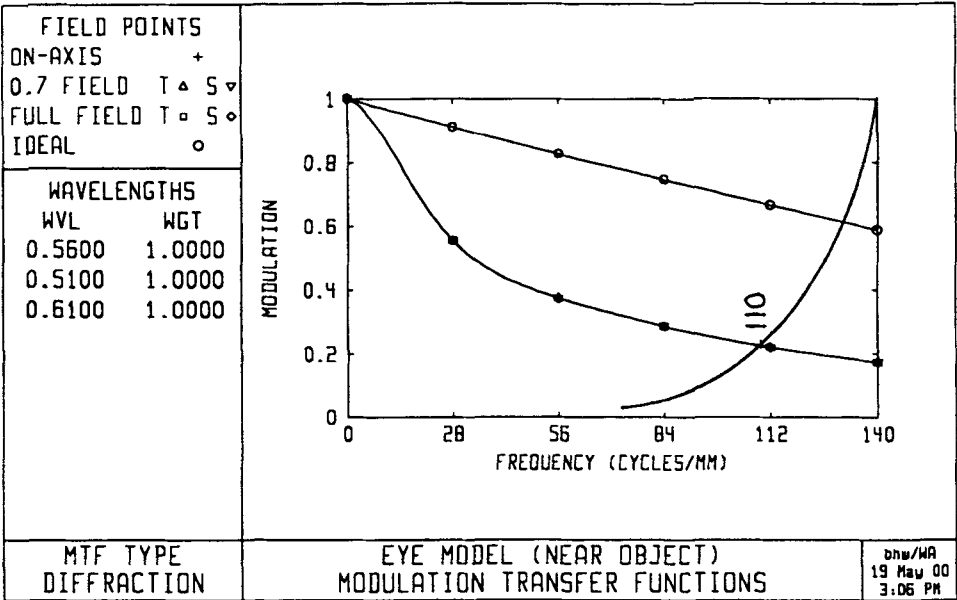


Figure 4.4 MTF curves for the model eye accommodated to view an object at 254 mm (top), and the same model eye with a simple, biconvex 6x magnifier (bottom).

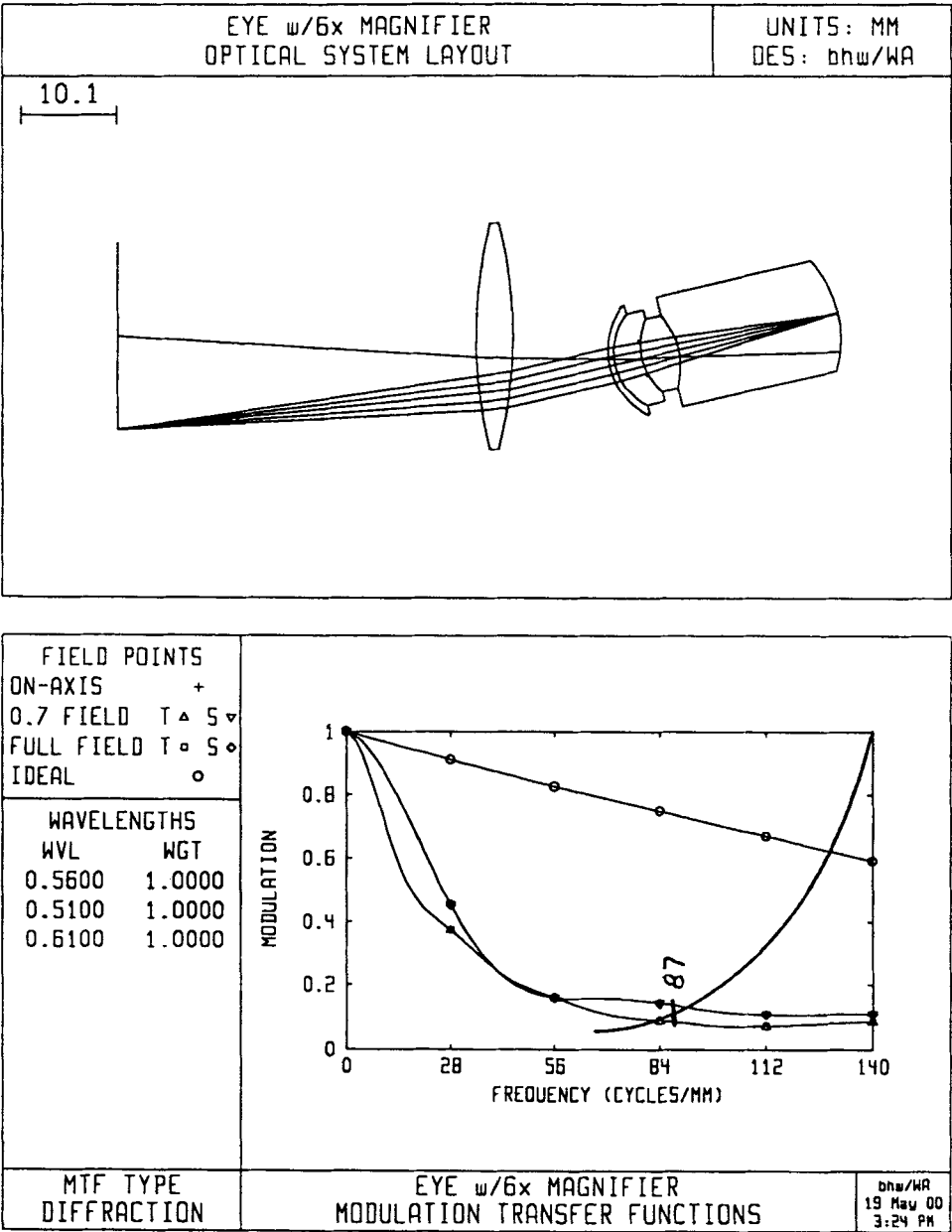


Figure 4.5 Model eye with a simple 6× magnifier viewing an off-axis point. Lens layout (top) and MTF data (bottom).

For our thin lens setup, we will assume the layout shown in Fig. 4.6, where we have a lens with a 50-mm focal length, an object distance of 44 mm, an exit pupil location 22 mm from the lens and an image distance of -261 mm from that pupil. Making this image distance 7 mm greater than the near point will allow the exit pupil to be located inside the eye by that amount. The eye is shown in Fig. 4.6 for reference only; it is not a part of the thin lens setup. Next, a real doublet is substituted for the thin lens. The source for such a starting design will depend on the designer. Many commercially available catalog lenses are included in most lens design packages. This would represent one obvious source. In this case, based on the designer's recent experience, the starting doublet parameters were assigned as shown in Fig. 4.7.

The lens was set up such that the optimization variables were limited to the three lens curvatures. Optimization goals were set so that the chosen image plane would be the paraxial image plane, and spherical, astigmatism, and chromatic third-order aberrations were minimized. Following each optimization run, the magnification of the final design was checked. If not close enough (within 2%) to the 6 $\times$  goal, the object distance was fine tuned and the lens was re-optimized. The final optimized 6 $\times$  achromatic magnifier doublet is shown in Fig. 4.8.

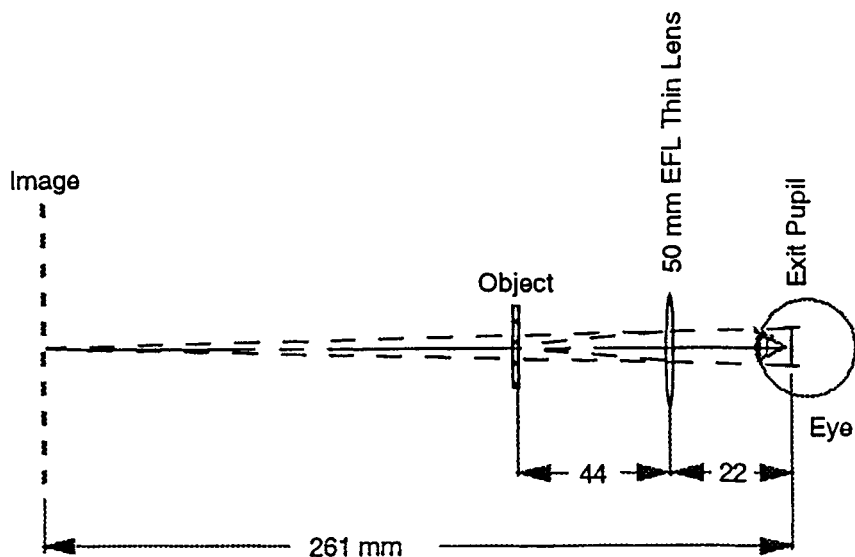
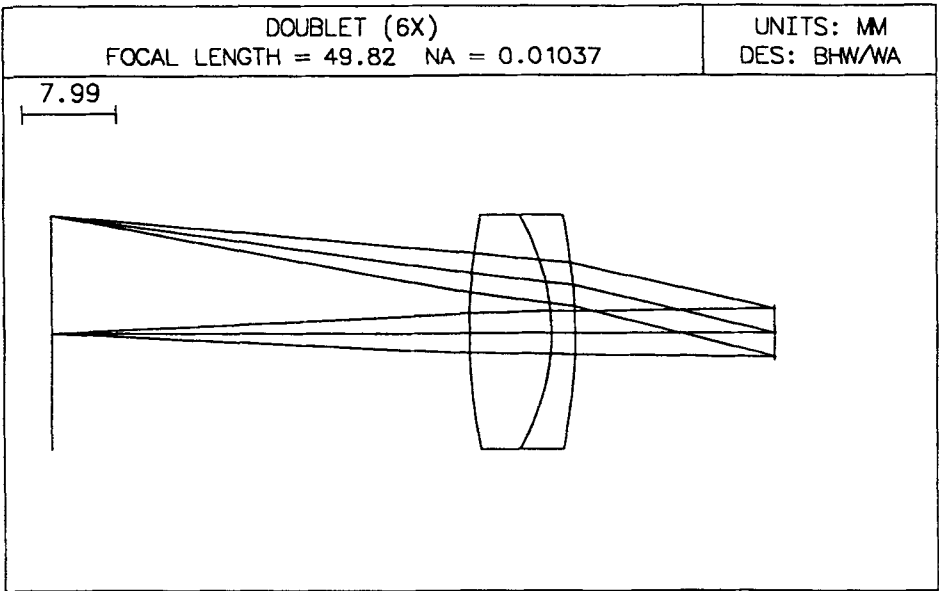


Figure 4.6 Thin lens layout for the design of a 6 $\times$  achromatic doublet magnifier.



**\*PARAXIAL CONSTANTS**

Effective focal length:    49.822249    Lateral magnification:    5.801000

Numerical aperture:    0.007514    Gaussian image height:    58.010004

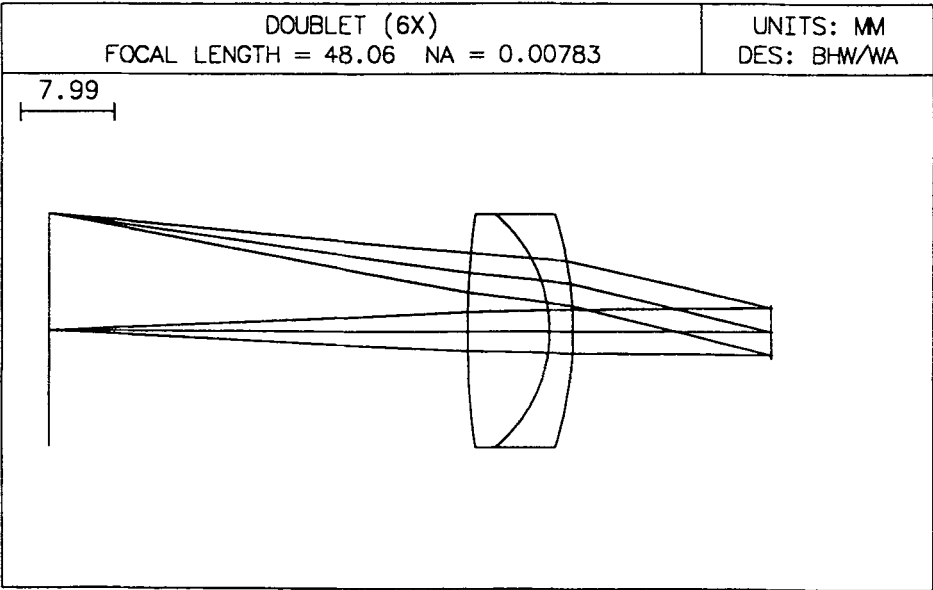
Working F-number:    66.500000    Petzval radius:    -72.975169

**\*LENS DATA**

**DOUBLET (6X-START)**

SRF	RADIUS	THICKNESS	APERTURE RADIUS	GLASS	SPE
OBJ	--	38.400000	10.000000	AIR	*
1	50.000000 V	7.000000	10.000000	BAK1	C
2	-20.000000 V	2.000000	10.000000	SF2	C
3	-50.000000 V	17.000000	10.000000	AIR	
AST	--	-261.000000	1.949518 AS	AIR	*
IMS	--	--	58.423101 S		

Figure 4.7 Starting design for optimization of a 6× achromatic doublet magnifier.



\*PARAXIAL CONSTANTS

Effective focal length:	48.056191	Lateral magnification:	5.953419
Numerical aperture:	0.007830	Gaussian image height:	59.534186
Working F-number:	63.855815	Petzval radius:	-69.227836

\*LENS DATA

OPTIMIZED DOUBLET (6X)

SRF	RADIUS	THICKNESS	APERTURE RADIUS	GLASS	SPE
OBJ	--	35.900000	10.000000	AIR	•
1	74.800000 V	7.000000	10.000000	BAK1	C
2	-13.000000 V	2.000000	10.000000	SF2	C
3	-33.300000 V	17.000000	10.000000	AIR	
AST	--	-261.000000	2.012954 AS	AIR	*
IMS	--	--	60.541252 S		

Figure 4.8 Final design form following optimization of a 6× achromatic doublet magnifier.

The next step in this design process involves combining this lens with the model eye to confirm its performance in terms of both magnification and image quality. The eye model, accommodated for focus at the near point, was added to the doublet lens with a clear distance of 10 mm between the lens and the eye. The object distance was adjusted to bring the on-axis image to the point of best focus. The resulting lens and eye combination is shown in the lens layout in Fig. 4.9 (top). Note that the doublet lens is located such that there is a 10-mm space from the lens to the cornea of the eye and that the 4-mm-diameter pupil of the eye is set to be the limiting aperture for the combination. As shown in the MTF data (Fig. 4.9, bottom), this lens-eye combination will result in an on-axis resolution of 108 cycles per mm on the retina. The resolution loss due to introduction of the doublet magnifier is a negligible loss—less than 2%.

In designing the doublet the amount of residual astigmatism and off-axis color were reduced relative to the simple magnifier. The resulting improvement in off-axis image quality can be determined by rotating the eye by about 12 deg to view the 10-mm field point. This results in the layout shown in Fig. 4.10 (top). The accommodation of the eye was then adjusted for best focus and the MTF data were then computed. As can be seen in Fig. 4.10 (bottom), the resulting off-axis resolution limit at the retina is 104 cycles per mm. This represents a significant improvement relative to the resolution limit of 87 cycles per mm that was found with the simple magnifier (Fig. 4.5).

#### 4.4 The Triplet Magnifier

Another common lens form frequently used as a magnifier is the symmetrical cemented triplet (*Hastings Triplet*). For this example, in lieu of a lens design exercise, the OSLO catalog lens system was used to locate a commercially available cemented triplet. In scanning available lenses, a 51-mm efl, 25-mm-diameter triplet was found in the JML catalog (similar lenses are available from alternate sources). This lens was substituted into the lens data tabulation, replacing the achromatic doublet. The object distance was adjusted to the point where best on-axis focus was found at the retina. In this case, the on-axis image quality was found to be essentially the same as that of the achromatic doublet (108 cycles per mm). The symmetry of the triplet would lead us to expect some improvement in off-axis performance. Again, the model eye was tilted through about 12 deg and the eye accommodation was fine-tuned to produce best focus at the retina. The resulting lens layout is shown in Fig. 4.11 (top). The MTF calculation was again executed and when combined

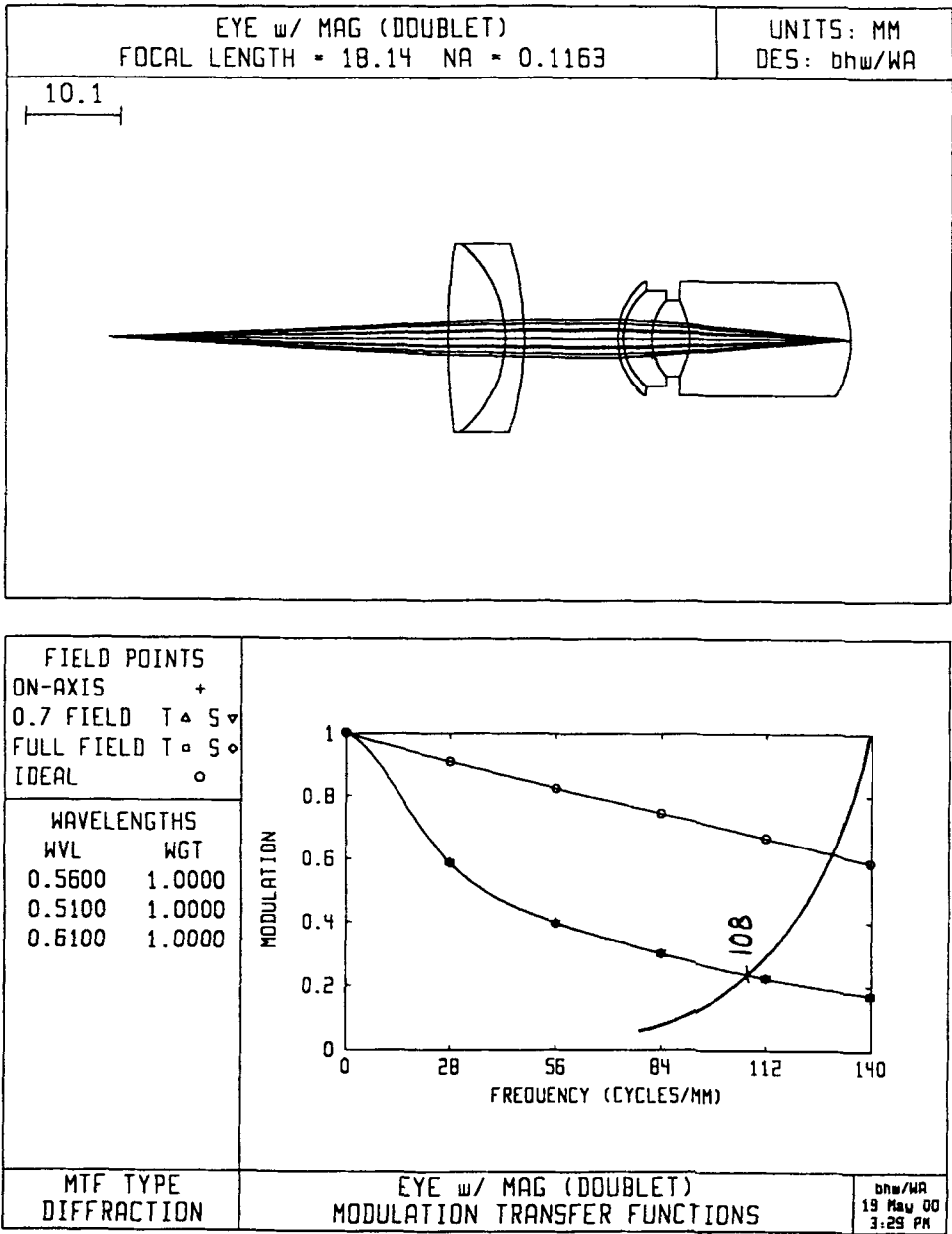


Figure 4.9 Lens layout and MTF data for the optimized 6× achromatic doublet magnifier combined with the model eye.

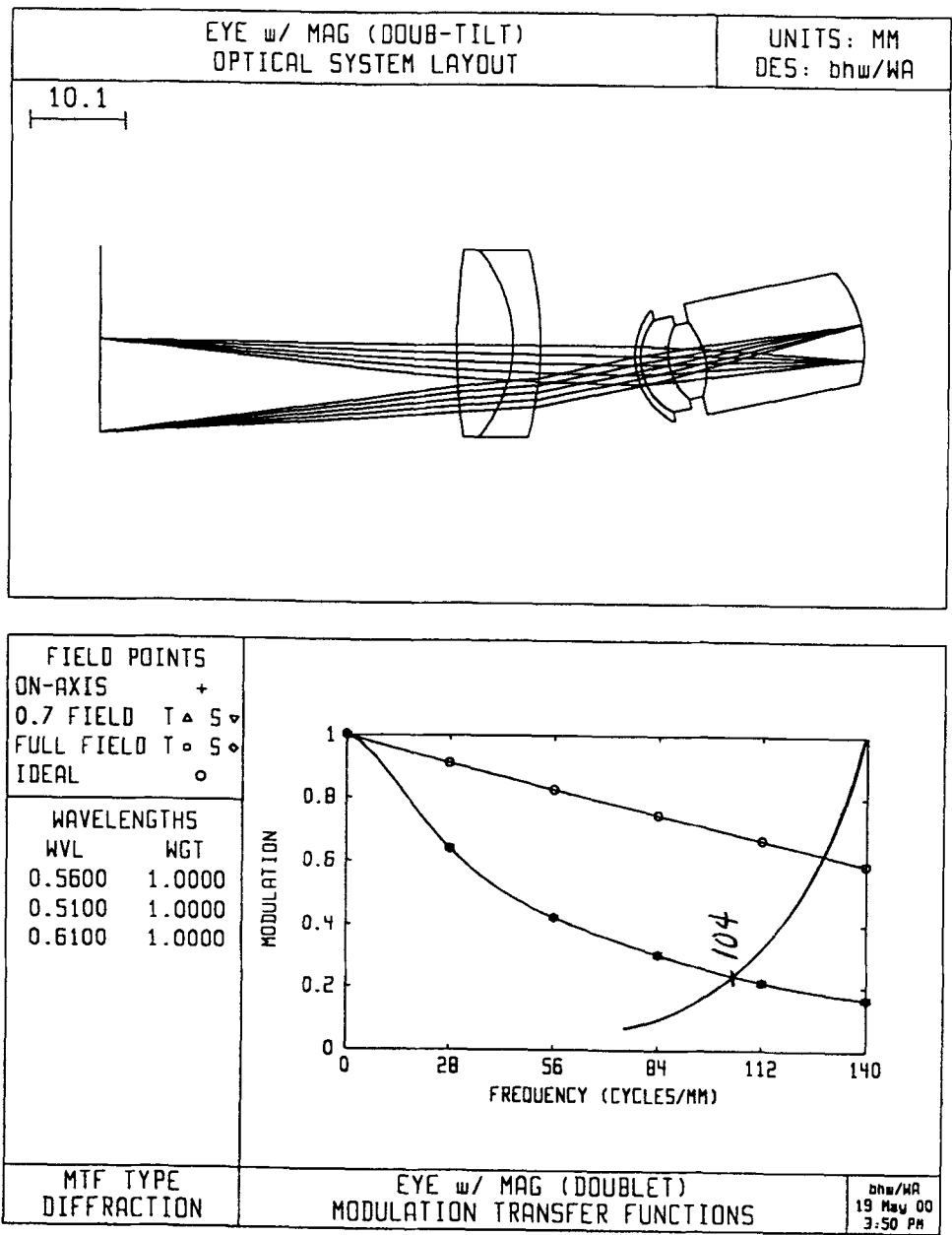


Figure 4.10 Lens layout and MTF data for the optimized 6× achromatic doublet magnifier, with tilted eye viewing an off-axis point.



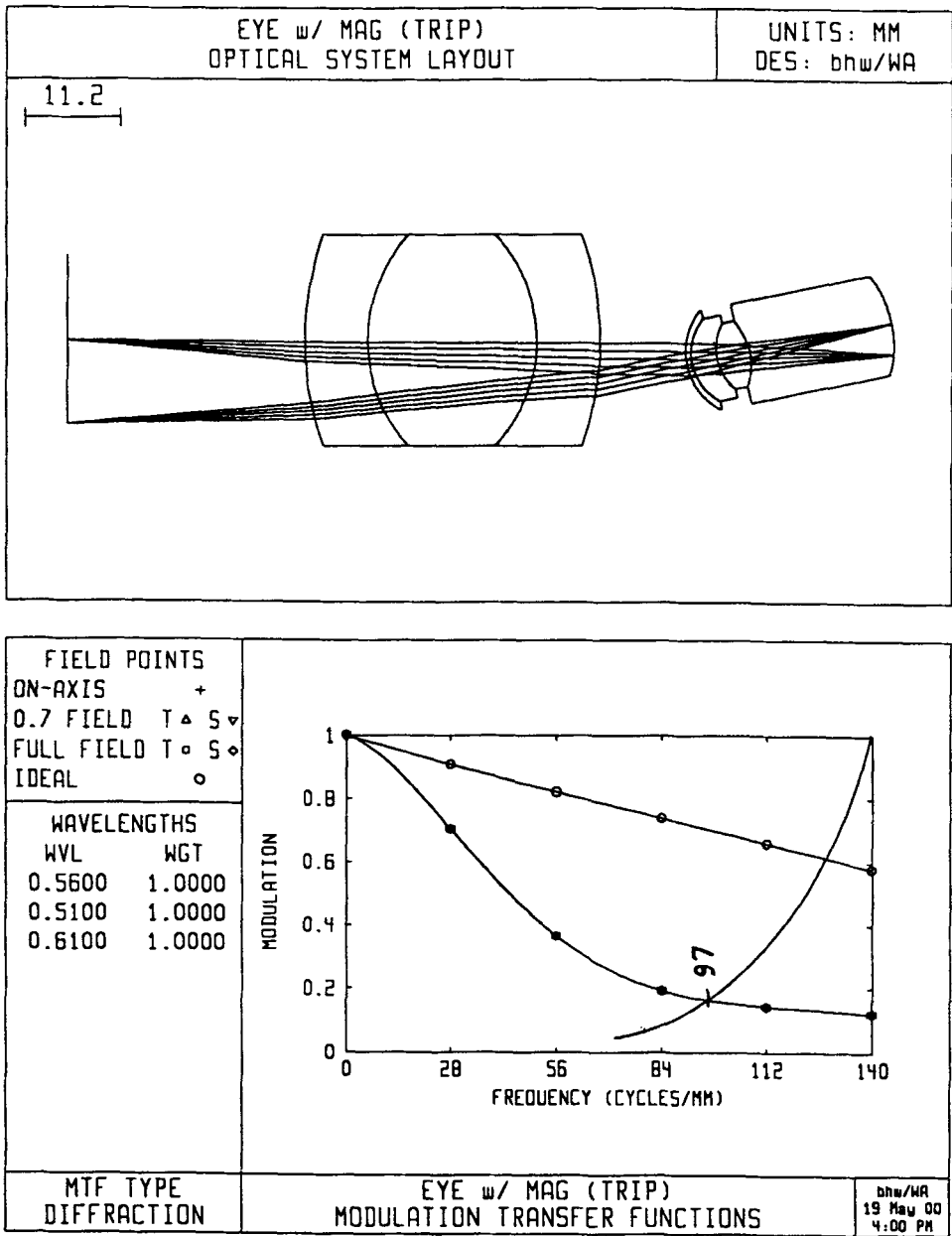


Figure 4.11 Lens layout and MTF data for a 6× Hastings triplet magnifier, with tilted eye viewing an off-axis point.

with the visual AIM curve, the resolution limit was found to be 97 cycles per mm. This level of image quality, combined with its commercial availability, would seem to make the triplet a good choice for our 6× magnifier application.

#### 4.5 The Symmetrical Two-Doublet Magnifier

One final magnifier lens configuration worth consideration consists of two identical cemented doublets, arranged to face each other with a small airspace between lenses. In the case of the 6× magnifier, where a final focal length of about 50 mm is required, we can achieve such a design by selecting two identical 100-mm doublets from the catalog lenses and arrange them such that they face each other with a 1-mm air space between. A search of the catalog lens files of OSLO reveals the lens #32327 from Edmund Scientific Co., Inc. will meet our basic requirements. (again, similar lenses are available from alternate sources).

The doublet lenses were placed in the design program, replacing the cemented triplet. The object distance was adjusted for optimum focus at the retina. On-axis resolution was again found to be 108 cycles per mm at the retina. The model eye was then tilted by 12.5 deg so that the image of the 10-mm off-axis point was centered on the retina (Fig. 4.12, top). The accommodation of the model eye was then fine-tuned to optimize focus, and the MTF curve shown in Fig. 4.12 (bottom) was generated. The resulting resolution limit of 102 cycles per mm at the retina indicates that the off-axis performance of this lens configuration is acceptable, and it is competitive with the previous examples shown. It is reasonable to conclude that, if one wishes to construct a 6× magnifier, the use of two commercially available achromatic doublets arranged as described here would probably represent the best configuration.

#### 4.6 Resolution

Throughout this chapter reference is made to the resolution achieved at or on the eye's retina. These values range from 110 cycles per mm for the accommodated model eye (Fig. 4.4, top), to 87 cycles per mm for the eye with the biconvex simple magnifier in the off-axis case (Fig. 4.5, bottom).

It was established in Chapter 2 that the magnification factor (object-to-retinal image) was 0.067× for the fully-accommodated model eye, viewing an object at a distance of 254 mm. This means that the 110 cycles per mm at the retina will translate to  $110 \times .067 = 7.3$  cycles per mm at the object. If the object is a USAF resolution target this would mean that the typical eye would resolve Element 6 in Group 2 on the target.

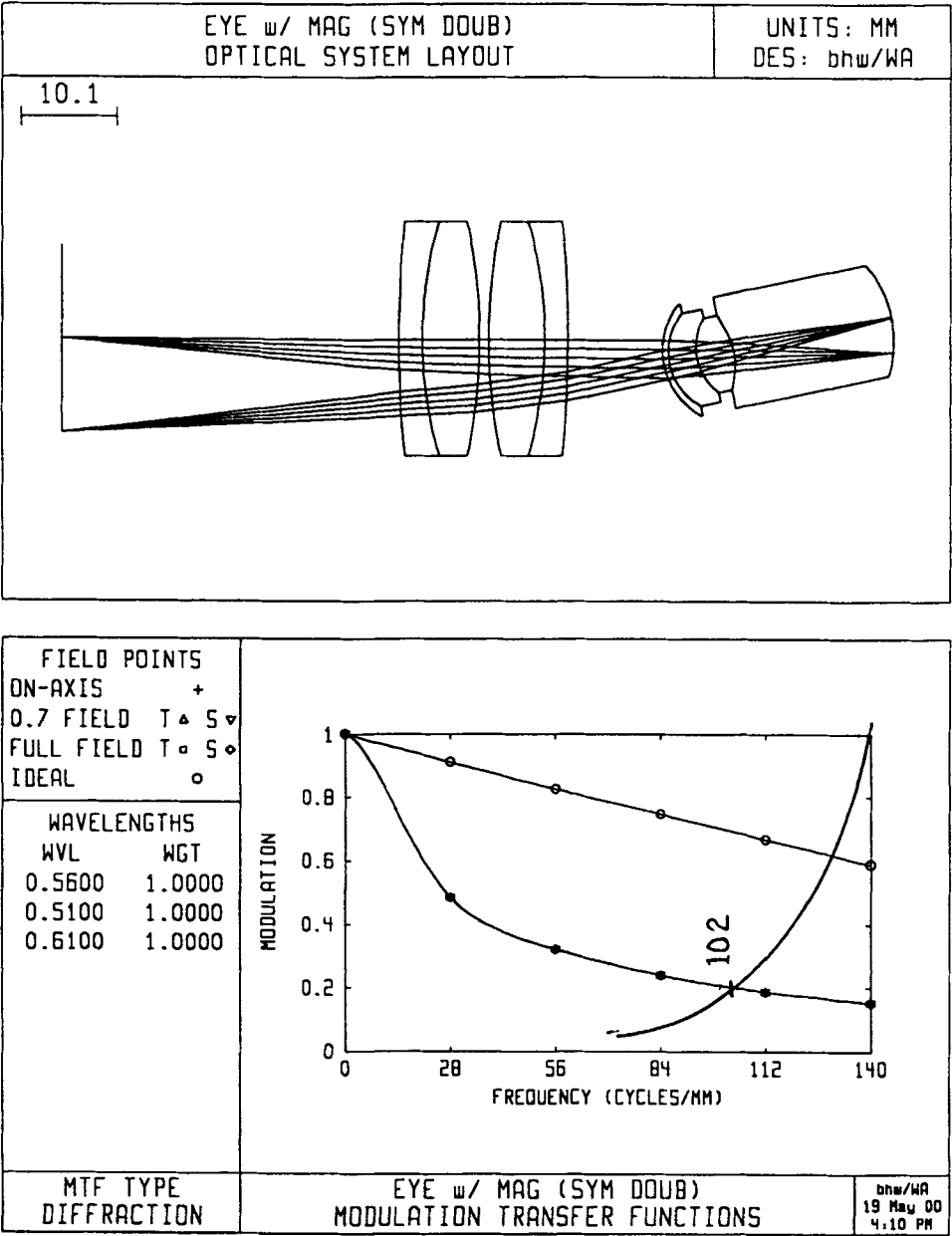


Figure 4.12 Lens layout and MTF data for the optimized Symmetrical doublet 6× magnifier, with tilted eye viewing an off-axis point.

Now, with the introduction of a  $6\times$  magnifier it is found that the nominal magnification factor (object to retinal image) becomes  $0.067 \times 6 = 0.4\times$ . As a result, when we find a  $6\times$  magnifier design that produces a final image at retina with a resolution of 108 cycles per mm, this means that we will resolve  $108 \times 0.4 = 43$  cycles per mm at the target. Again, if the object is a USAF resolution target, this would mean that the typical eye with this magnifier would resolve element 3 in group 5 on the target.

## 4.7 Review and Summary

This chapter has covered the topic of the magnifier—its configuration, design, and layout. Four basic magnifier types have been covered: the biconvex single element, the custom-designed achromatic doublet, a commercially available cemented (Hastings) triplet and finally, a symmetrical assembly containing two low-cost, commercially available achromatic doublets. For each case the design was evaluated for image quality both on axis and at the edge of a 20-mm-diameter object field. As is most often the case, it was found that, as the total number of lens elements was increased, the performance of the magnifier was improved. Considering all factors it was concluded that the economy of using commercially available optics resulted in the two-doublet design offering a very high level of image quality at a very competitive cost.

In the probable case where an *all new* magnifier design is not required (many fine magnifier assemblies are readily available), the value of this chapter will be found in the experience gained in following, and, where possible, duplicating the design exercises described. The resulting familiarity with the design software and the design concepts presented here will be valuable when applied to a variety of future design tasks involving visual systems.

## 5

## The Eyepiece—Design

---

### 5.1 Introduction

The eyepiece is quite similar in function to the magnifier discussed in the preceding chapter. The major distinction is that the eyepiece is used to view a real image that has been formed by optical components located between the eyepiece and the object being viewed (foreoptics). As a result, those foreoptics will define the size, shape, and paths of the ray bundles that will pass through the eyepiece.

While the final design of an eyepiece may be fine-tuned to function with a specific set of foreoptics, the eyepiece will generally be designed as an independent optical device, based on the specifications of the final system. For the examples to be presented here, it will be assumed that all eyepieces have a focal length of 28 mm (approximately 9 $\times$  magnification). The exit pupil diameter will be set to 4 mm ( $f/7.0$ ), and the field of view will be set to an appropriate value, consistent with the eyepiece type. As with most other visual designs presented in this book, equally-weighted spectral wavelengths of 0.51, 0.56, and 0.61 microns will be used.

### 5.2 The Generic Eyepiece

Each eyepiece has a unique set of characteristics that will determine its applicability to a particular task. We will cover nine eyepiece types in this chapter and present design and performance data for each. Figure 5.1 contains tabulated design data on these nine eyepiece types, making meaningful side-by-side comparisons possible. The focal length, entrance pupil size, and exit pupil location (chief ray angle) have been held constant for all designs, while the field of view, eye relief, and image distance will vary depending on eyepiece type. In general terms, the lens or lens group that is located close to the eye is referred to as the *eye* lens, while the lens or lens group that is located close to the image is referred to as the *field* lens. Note that for all eyepiece design work presented here the optical layout is such that the object is assumed to be at infinity and light rays are traced through the exit pupil of the eyepiece, through the lens, and then on to the eyepiece image surface.

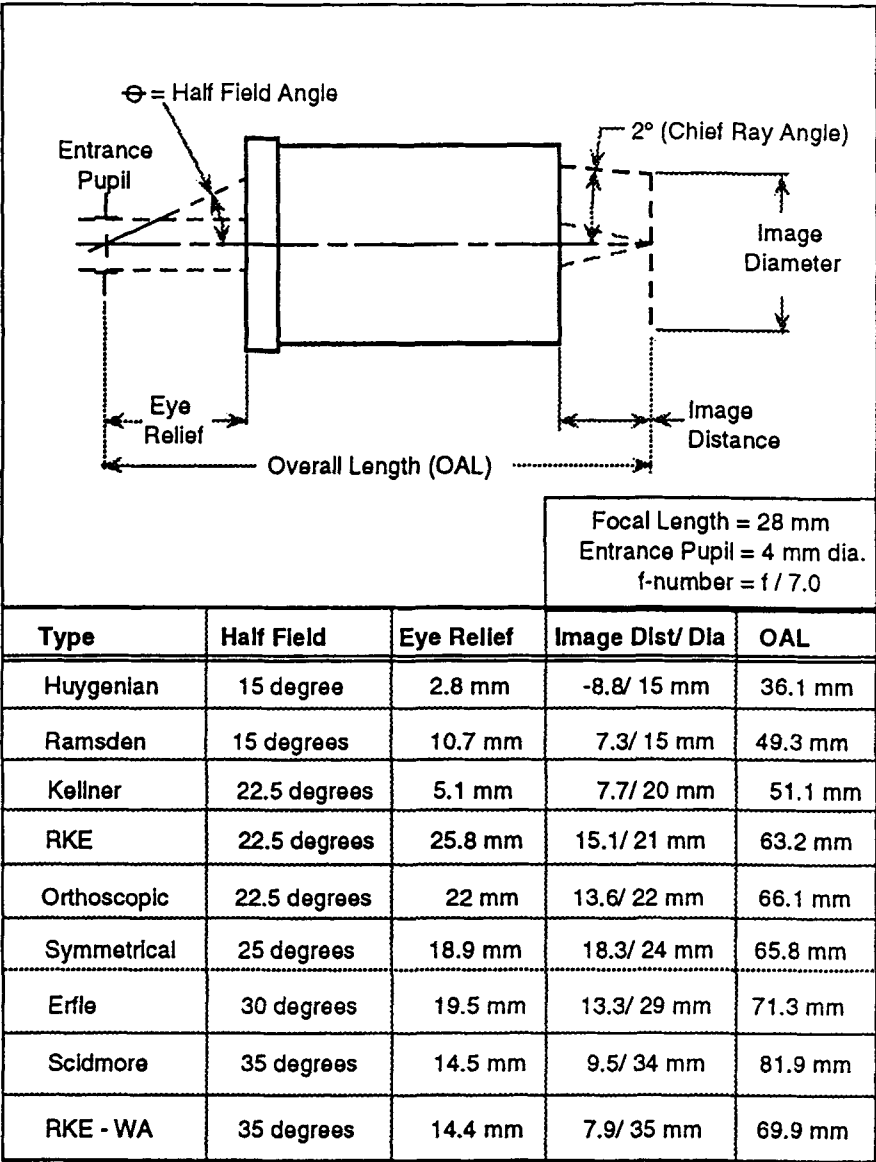


Figure 5.1 Table of eyepiece designs, with major characteristics and dimensions.

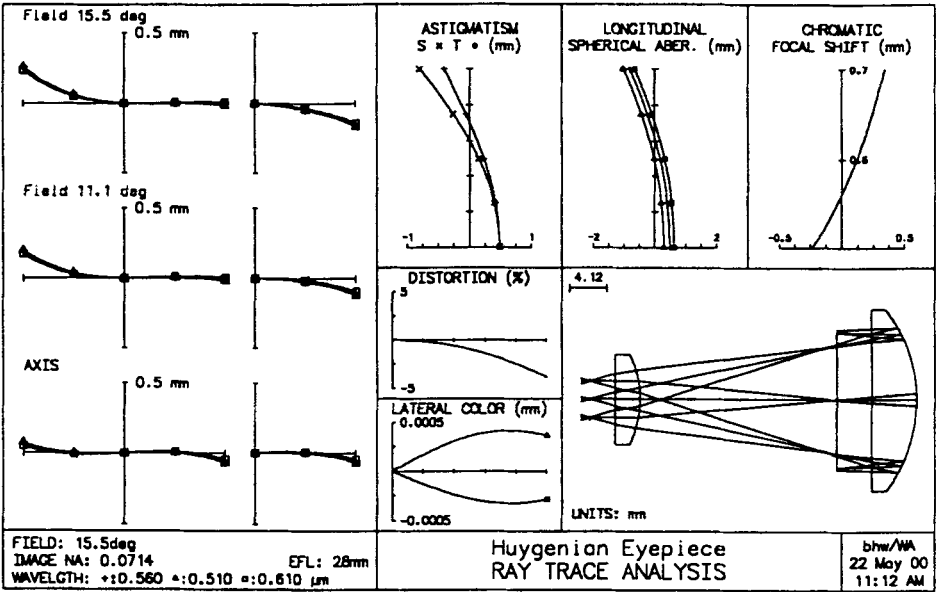
The most logical and common eyepiece optical design procedure begins with selection of a basic eyepiece type, depending primarily upon the field of view that must be covered. The focal length of the chosen design is then scaled to achieve the desired magnification. Finally, the scaled eyepiece design is added to the optical system, where its form can be fine-tuned to compensate for specific ray paths and residual system aberrations.

### 5.3 The Huygenian Eyepiece

The simplest eyepiece type would be the Huygenian. This eyepiece consists of two plano convex elements made from a common crown glass type. These elements are arranged with their plano surfaces facing the eye and the lens separation approximately equal to the final eyepiece focal length. While aberration correction over the 15-deg half field of the Huygenian eyepiece is quite good, there are several features that make this eyepiece form undesirable. In addition to the eye relief being quite small, the image is formed within the eyepiece, making the introduction of a reticle impractical in most cases. Figure 5.2 contains an illustration of a typical Huygenian eyepiece, along with aberration curves and complete design data.

### 5.4 The Ramsden Eyepiece

A second eyepiece form, nearly as simple as the Huygenian, is the Ramsden eyepiece. The Ramsden also consists of two plano convex elements made from a common crown glass type. These elements are arranged with the convex surfaces facing each other and the lens separation approximately 85% of the final eyepiece focal length. While eye relief and image location are improved relative to the Huygenian, the Ramsden eyepiece is afflicted with a considerable chromatic aberration. Figure 5.3 contains an illustration of a typical Ramsden eyepiece, along with aberration curves and complete design data.



**\*PARAXIAL CONSTANTS**

Effective focal length:	27.995436	Lateral magnification:	-9.3318e-20
Numerical aperture:	0.071429	Gaussian image height:	7.790138
Working F-number:	7.000000	Petzval radius:	-19.858577

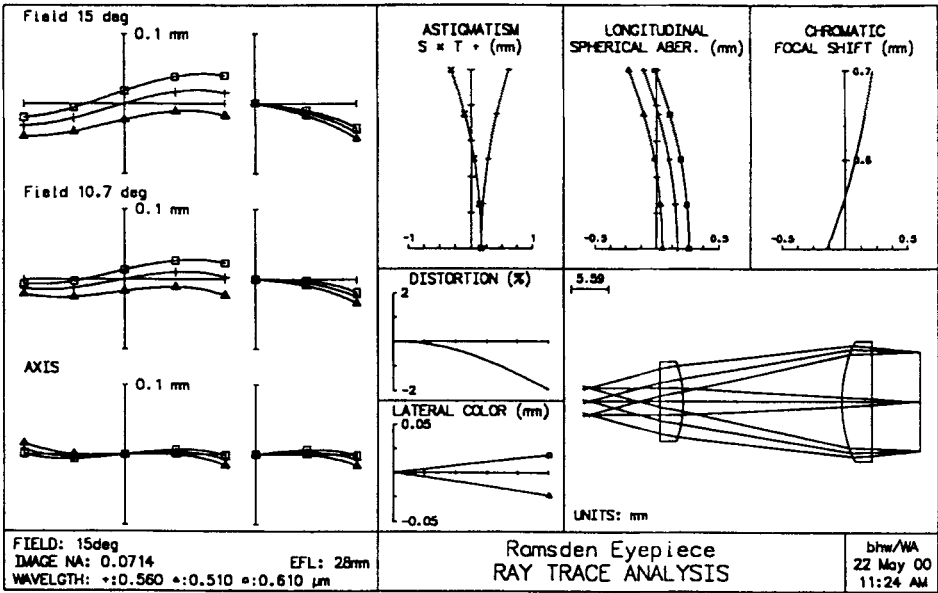
**\*LENS DATA**

**Huygenian Eyepiece**

SRF	RADIUS	THICKNESS	APERTURE RADIUS	GLASS	NOTE
OBJ	--	3.0000e+20	8.3479e+19	AIR	
AST	--	2.800000	2.000000 A	AIR	Ent Pupil
2	--	2.800000	5.000000	BK7 C	
3	-11.500000	25.500000	5.000000	AIR	
4	--	5.000000	10.000000	BK7 P	
5	-16.500000	-8.800000	10.000000	AIR	
IMS	--	--	7.500000		*

Figure 5.2 The Huygenian is the simplest eyepiece form. It will cover a 30-deg field of view and is well corrected for chromatic aberrations. Major drawbacks include an immersed image and limited eye relief.





*PARAXIAL CONSTANTS			
Effective focal length:	27.995782	Lateral magnification:	-9.3319e-30
Numerical aperture:	0.071429	Gaussian image height:	7.501447
Working F-number:	7.000000	Petzval radius:	-29.933504

\*LENS DATA

Ramsden Eyepiece						
SRF	RADIUS	THICKNESS	APERTURE RADIUS	GLASS	SPE	NOTE
OBJ	--	3.0000e+30	8.0385e+29	AIR		
AST	--	10.700000	2.000000 AK	AIR		Ent Pupil
2	--	3.400000	6.000000	BK7 C		
3	-19.300000	23.400000	6.000000	AIR		
4	21.700000	4.500000	9.000000	BK7 P		
5	--	7.280000	9.000000	AIR		
IMS	--	--	7.300000		*	

Figure 5.3 The Ramsden is another simple eyepiece form. It will cover a 30-deg field of view but it is not well corrected for chromatic aberrations. The image is located outside the eyepiece and eye relief is greatly improved over the Huygenian.

## 5.5 The Kellner Eyepiece

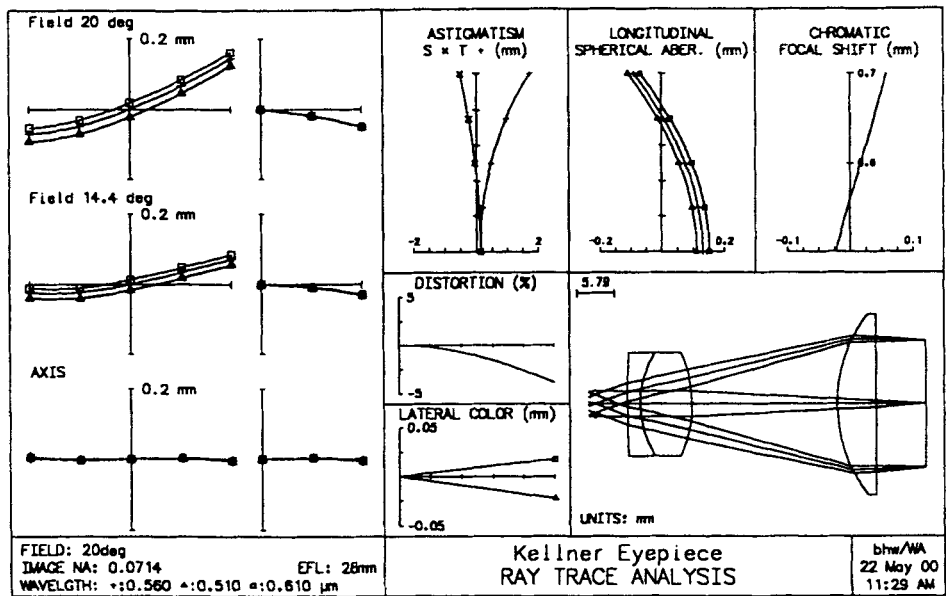
The Kellner eyepiece is quite similar to the Ramsden with the notable change that the eye lens is made into an achromatic doublet. This change permits the correction of axial chromatic aberration and a reduction of off-axis (lateral) color. As a result, a slight increase in the half field of view (from 15 to 22.5 deg) is possible. Eye relief of the Kellner eyepiece is not compatible with a comfortable visual instrument design. Figure 5.4 contains an illustration of a typical Kellner eyepiece, along with aberration curves and complete design data.

## 5.6 The RKE Eyepiece

A family of eyepiece designs has been generated where the arrangement of lenses found in the Kellner eyepiece is reversed and the air space between the lens is dramatically reduced. One very popular manifestation of this design approach is found in the RKE eyepiece, designed and marketed by Edmund Scientific Co., Inc. of Barrington, NJ. As the data in Fig. 5.1 shows, the half field of view of the RKE eyepiece can be extended to 22.5 deg with very comfortable eye relief. Figure 5.5 contains an illustration of a typical RKE eyepiece, along with aberration curves, and complete design data. From the aberration data it can be seen that the off-axis aberrations (lateral color and field curvature) are very well corrected.

## 5.7 The Orthoscopic Eyepiece

This limited presentation dealing with eyepiece design demonstrates the evolution of several design forms based on less complex earlier designs. The Orthoscopic form, for example, is similar to the RKE form, with the achromatic doublet replaced by a cemented triplet. Covering the same half field as the RKE, the Orthoscopic is found to have reduced lateral color and distortion. Some economy in manufacture is realized by making the cemented triplet symmetrical. Figure 5.6 contains an illustration of a typical Orthoscopic eyepiece, along with aberration curves and complete design data. While there is some increase in high-order astigmatism, the improvement in both lateral color and distortion more than offsets that shortcoming.



**\*PARAXIAL CONSTANTS**

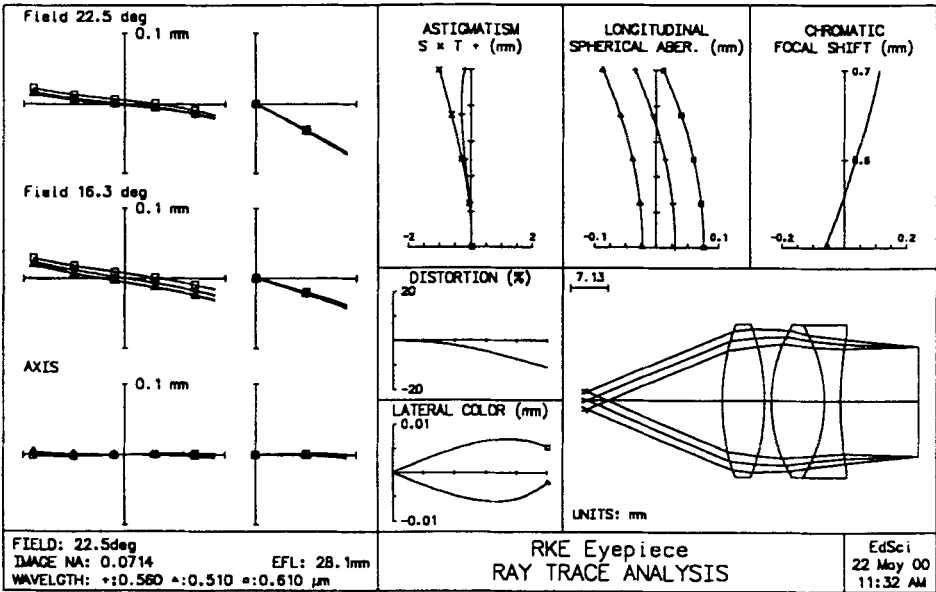
Effective focal length:	27.978997	Lateral magnification:	-1.3989e-29
Numerical aperture:	0.071429	Gaussian image height:	10.183522
Working F-number:	7.000000	Petzval radius:	-30.301751

**\*LENS DATA**

**Kellner Eyepiece**

SRF	RADIUS	THICKNESS	APERTURE RADIUS	GLASS	SPE	NOTE
OBJ	--	2.0000e+30	7.2794e+29	AIR		
AST	--	5.100000	1.958836 A	AIR		Ent Pupil
2	153.000000	2.000000	8.000000	F4	C	
3	14.900000	8.000000	8.000000	BAK2	C	
4	-19.900000	22.300000	8.000000	AIR		
5	23.500000	6.000000	14.000000	BAK2	C	
6	--	7.710000	14.000000	AIR		
IMS	--	--	V 9.750000		*	

Figure 5.4 The Kellner eyepiece is quite similar to the Ramsden but the eyelens has been achromatized, which improves color correction. The Kellner will cover a 45-deg field of view with good image quality and limited eye relief.



**\*PARAXIAL CONSTANTS**

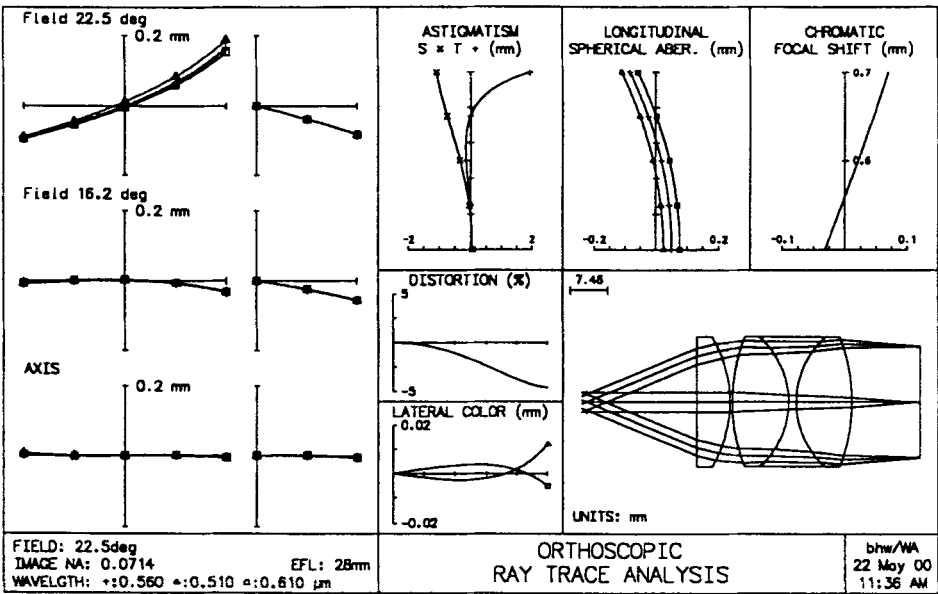
Effective focal length:	28.070574	Lateral magnification:	-1.4035e-29
Numerical aperture:	0.071429	Gaussian image height:	11.627212
Working F-number:	7.000000	Petzval radius:	-45.790405

**\*LENS DATA**

**RKE Eyepiece**

SRF	RADIUS	THICKNESS	APERTURE RADIUS	GLASS	SPE	NOTE
OBJ	--	2.0000e+30	8.2843e+29	AIR		
AST	--	25.800000	2.000000 AK	AIR		Ent Pupil
2	42.700000	8.000000	14.500000	SK5	C	
3	-42.700000 P	1.300000	14.500000	AIR		
4	28.000000	10.000000	14.000000 K	SK5	C	
5	-28.000000 P	3.000000	14.500000	SF4	C	
6	64.800000	15.060000	13.000000 K	AIR		
IMS	--	--	V 10.300000		*	

Figure 5.5 The RKE eyepiece is a derivative of the Kellner, with the field lens rather than the eyelens achromatized. This leads to further improvements in color correction. The RKE will cover a 45-deg field of view with very good image quality and generous eye relief.



**\*PARAXIAL CONSTANTS**

Effective focal length:	27.981394	Lateral magnification:	-1.3991e-29
Numerical aperture:	0.071429	Gaussian image height:	11.590273
Working F-number:	7.000000	Petzval radius:	-34.918470

**\*LENS DATA**

**ORTHOSCOPIC**

SRF	RADIUS	THICKNESS	APERTURE RADIUS	GLASS	SPE	NOTE
OBJ	--	2.0000e+30	8.2843e+29	AIR		
AST	--	22.000000	2.000000 A	AIR		
2	--	6.500000	13.000000	BAK1	C	
3	-25.800000	0.500000	13.000000 K	AIR		
4	36.200000	11.000000	13.000000 K	K5	C	
5	-17.800000	1.500000	13.000000 K	F2	C	
6	17.800000	11.000000	13.000000 K	K5	C	
7	-36.200000 P	13.600000	13.000000 K	AIR		
IMS	--	--	11.000000		*	

Figure 5.6 The Orthoscopic eyepiece is a traditional design where the field lens takes the form of an achromatic cemented triplet. This design offers greatly reduced distortion. The Orthoscopic eyepiece will cover a 45-deg field of view with very good image quality and generous eye relief.

## 5.8 The Symmetrical Eyepiece

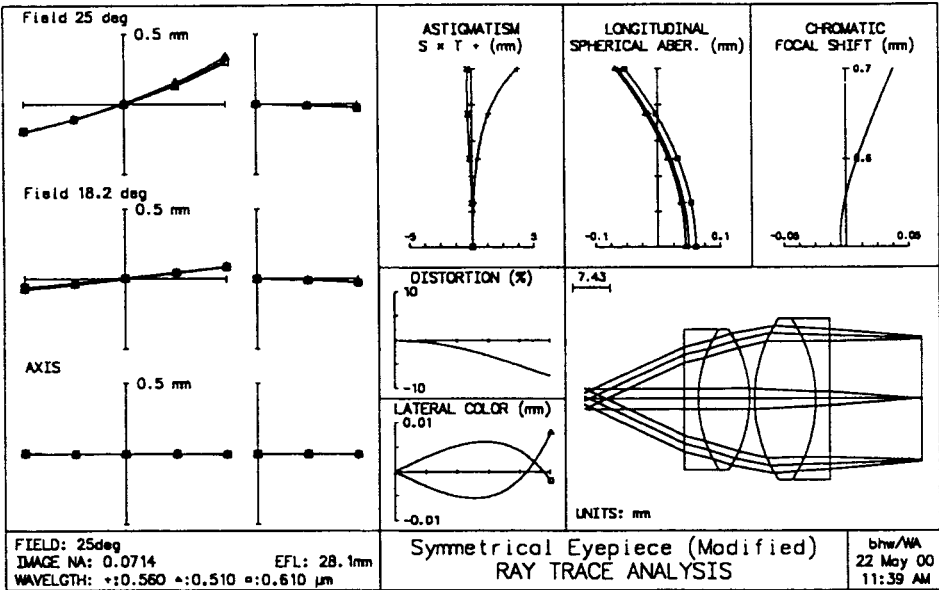
The requirement that an eyepiece's pupil be located outside the lens precludes the possibility of a truly symmetrical design. However, there is a class of eyepiece designated *symmetrical* by virtue of its use of two nearly symmetrical doublets facing each other. This arrangement permits an eyepiece design that will cover a 25-deg half field with very good image quality. Figure 5.7 contains an illustration of a typical Symmetrical eyepiece, along with aberration curves and complete design data. The image quality is essentially the same as that of the Orthoscopic, in spite of an increased half-field angle and a configuration that will probably be less expensive to manufacture.

## 5.9 The Erfle Eyepiece

The Erfle eyepiece design has been around for many years. This form may be thought of as a Symmetrical design, with a biconvex singlet inserted between the two doublets. The Erfle design permits the half field to be increased to 30 deg, with all residual off-axis aberrations held to acceptable levels. Figure 5.8 contains an illustration of a typical Erfle eyepiece, along with aberration curves and complete design data. The image quality is essentially the same as that of the Symmetrical, with a slight increase in lateral color and distortion.

## 5.10 The Scidmore Eyepiece

The Scidmore eyepiece is a contemporary design generated for use in high-performance military instrumentation. This form may be thought of as an Erfle design, with an additional positive (plano-convex) singlet inserted between the two doublets. The choice of optical glass types used in the Scidmore design has been greatly simplified. This design configuration permits the half field to be increased to 35 deg, with all residual off-axis aberrations held to acceptable levels. Figure 5.9 contains an illustration of a typical Scidmore eyepiece, along with aberration curves and complete design data. The image quality is essentially the same as that of the Erfle, with a slight increase in lateral color and distortion.



**\*PARAXIAL CONSTANTS**

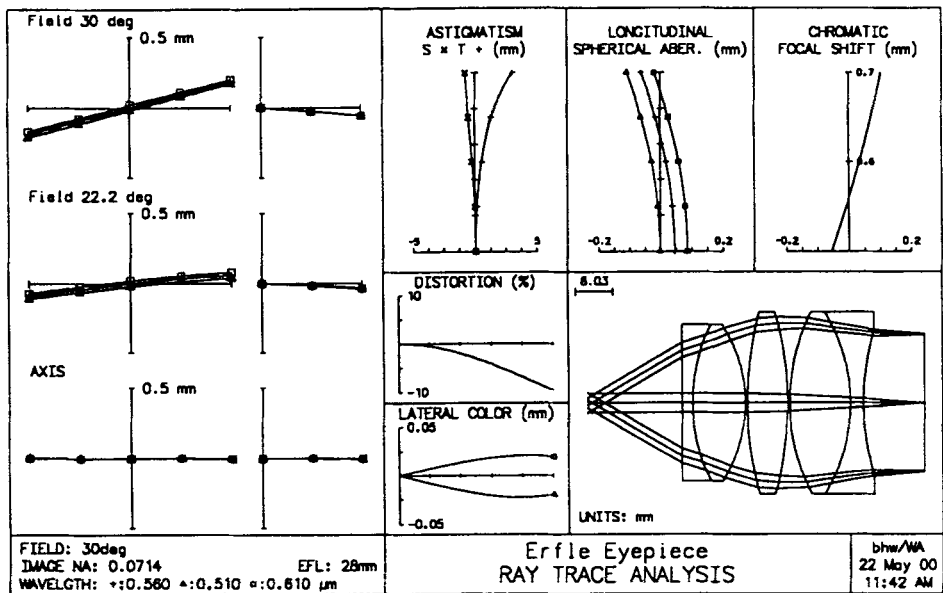
Effective focal length:	28.053728	Lateral magnification:	-1.4027e-29
Numerical aperture:	0.071429	Gaussian image height:	13.081668
Working F-number:	7.000000	Petzval radius:	-42.582514

**\*LENS DATA**

**Symmetrical Eyepiece (Modified)**

SRF	RADIUS	THICKNESS	APERTURE RADIUS	GLASS	SPE	NOTE
OBJ	--	2.0000e+30	9.3262e+29	AIR		
AST	--	18.900000	2.000000 A	AIR		Ent Pupil
2	--	2.800000	14.000000	SF5	C	
3	26.000000	10.000000	14.000000	BAK1	C	
4	-26.000000 P	1.000000	14.000000	AIR		
5	29.800000	12.000000	16.000000	BAK1	C	
6	-29.800000 P	2.800000	16.000000	SF5	C	
7	--	18.360000	15.658604	AIR		
IMS	--	--	12.000000		*	

Figure 5.7 The Symmetrical eyepiece is another traditional design with both the eyelens and the field lens taking the form of cemented achromatic doublets. The symmetrical eyepiece will cover a 50-deg field of view with very good image quality and generous eye relief.

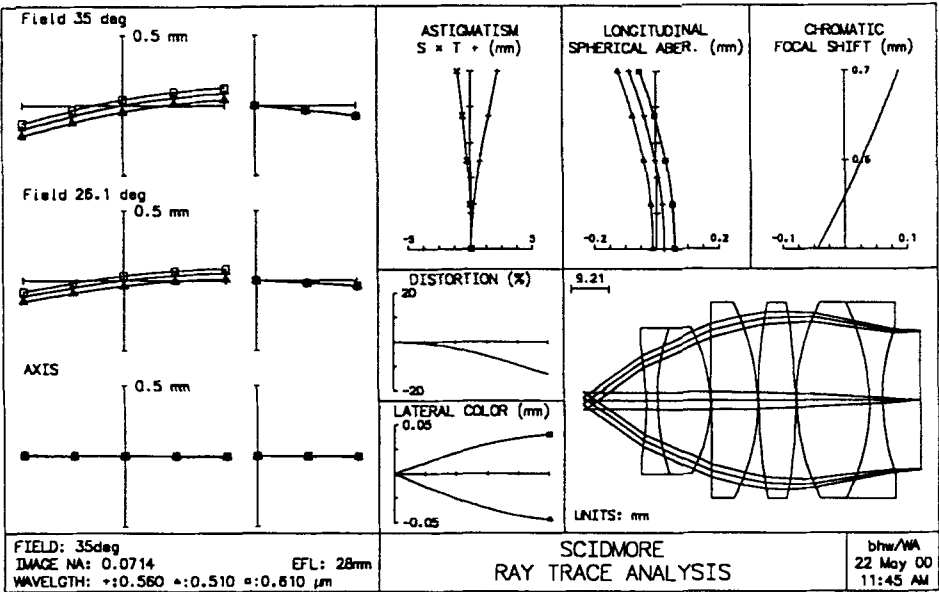


*PARAXIAL CONSTANTS			
Effective focal length:	28.000483	Lateral magnification:	-9.3335e-30
Numerical aperture:	0.071429	Gaussian image height:	16.166086
Working F-number:	7.000000	Petzval radius:	-48.563641

*LENS DATA						
Erfile Eyepiece						
SRF	RADIUS	THICKNESS	APERTURE RADIUS	GLASS	SPE	NOTE
OBJ	--	3.0000e+30	1.7321e+30	AIR		
AST	--	19.500000	1.958669 A	AIR		Ent Pupil
2	--	2.250000	16.788589	F2	C	
3	37.940000	11.200000	16.788589	BK7	C	
4	-31.650000	0.500000	16.788589	AIR		
5	75.400000	8.400000	19.586687	SK10	C	
6	-75.400000 P	0.500000	19.586687	AIR		
7	43.550000	12.900000	19.586687	SK4	C	
8	-37.940000	2.800000	19.586687	SF2	C	
9	51.540000	13.250000	15.669349	AIR		
IMS	--	--	14.600000		*	

Figure 5.8 The Erfle eyepiece is similar to the Symmetrical design with a singlet element added between the doublets. The Erfle eyepiece will cover a 60-deg field of view with very good image quality and generous eye relief.





\*PARAXIAL CONSTANTS

Effective focal length:	27.995615	Lateral magnification:	-1.3998e-29
Numerical aperture:	0.071429	Gaussian image height:	19.602741
Working F-number:	7.000000	Petzval radius:	-56.715454

\*LENS DATA  
SCIDMORE

SRF	RADIUS	THICKNESS	APERTURE RADIUS	GLASS	SPE	NOTE
OBJ	--	2.0000e+30	1.4004e+30		AIR	
AST	--	14.540828	1.957419 A		AIR	Ent Pupil
2	-78.800000	2.800000	14.000000		SF2 C	
3	56.600000	12.900000	18.000000		SK16 C	
4	-37.780000	0.300000	18.000000		AIR	
5	--	11.200000	24.000000		SK16 C	
6	-52.600000	0.300000	24.000000		AIR	
7	132.500000	8.900000	24.000000		SK16 C	
8	-132.500000 P	0.300000	24.000000		AIR	
9	52.600000	17.900000	24.000000		SK16 C	
10	-52.600000	3.300000	24.000000		SF2 C	
11	52.600000	9.450000	18.000000		AIR	
IMS	--	--	17.000000			*

Figure 5.9 The Scidmore eyepiece is similar to the Erfle design with a second singlet element added between the doublets. The Scidmore eyepiece will cover a 70-deg field of view with very good image quality and adequate eye relief.

## 5.11 The RKE Wide-Angle Eyepiece

The RKE Wide-Angle (WA) eyepiece is another contemporary design. This form may be thought of as an Erfle design, with a third achromatic doublet substituted for the biconvex singlet. Like the Scidmore design, this permits the half field to be increased to 35 deg, with all residual off-axis aberrations held to acceptable levels. Figure 5.10 contains an illustration of a typical RKE WA eyepiece, along with aberration curves, and complete design data. The image quality is essentially the same as that of the Scidmore, with the significant advantage that both axial and lateral chromatic aberration are well corrected. Of course another major advantage stems from the commercial availability of this eyepiece, which permits one to realize the cost benefits of manufacture in large quantities.

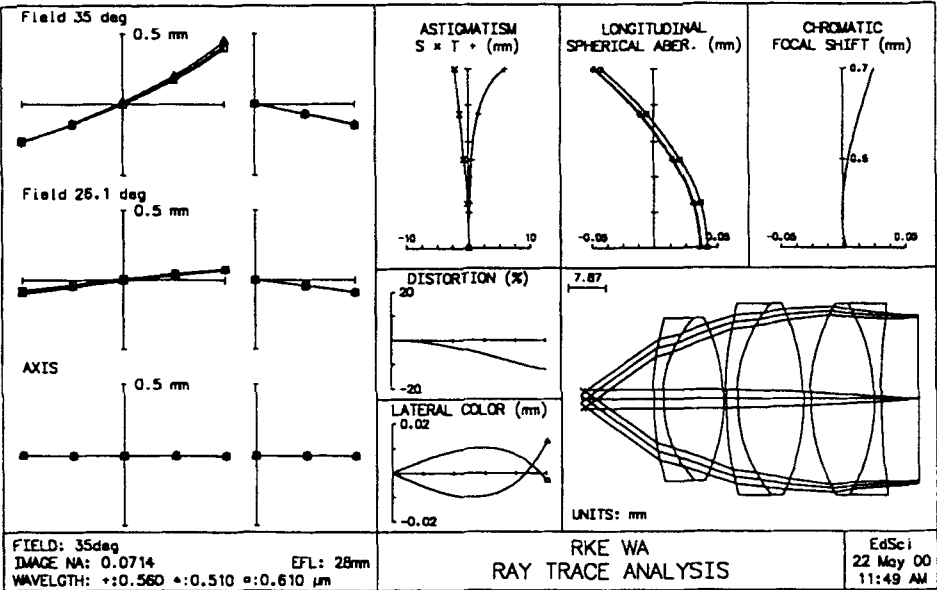
## 5.12 Eyepiece Focus

After an eyepiece design has been generated within an instrument it is necessary to then either set the focus of that eyepiece, or to establish the eyepiece focus adjustment travel that will be required. In the case of a fixed focus instrument, the eyepiece is generally set so that the image being viewed appears at a distance of from 1 to 2 meters from the eye. This corresponds to a setting of from  $-0.5$  to  $-1.0$  diopters, where the diopter value is equal to the reciprocal of the final image distance in meters. In the case of an instrument with an adjustable eyepiece, the adjustment range will ultimately be determined by final instrument specifications. A typical eyepiece focus range would be from  $-4.0$  to  $+3.0$  diopters. This range will permit the instrument to be used by most of the general population, without eyeglasses, regardless of their individual eye correction.

The amount of axial eyepiece travel required to introduce 1 diopter of focus is found using the following formula:

$$D = f^2 / 1000.$$

For the 28-mm-focal-length eyepiece this formula would indicate that the eyepiece must be adjusted axially 0.78 mm (0.031 inch) per diopter. For the fixed focus instrument set at  $-0.75D$  this would mean the eyepiece must be moved 0.59 mm toward the image relative to the nominal zero diopter setting. For the instrument with an adjustable eyepiece range from  $-4$  to  $+3$  diopters, the eyepiece travel would need to range from



**\*PARAXIAL CONSTANTS**

Effective focal length:	28.007191	Lateral magnification:	-1.4004e-29
Numerical aperture:	0.071429	Gaussian image height:	19.610846
Working F-number:	7.000000	Petzval radius:	-35.691114

**\*LENS DATA**

RKE WA							
SRF	RADIUS	THICKNESS	APERTURE RADIUS	GLASS	SPE	NOTE	
OBJ	--	2.0000e+30	1.4004e+30	AIR			
AST	--	14.400000	2.000514 AS	AIR			
2	62.700000	2.000000	17.000000 K	SF2	C		
3	25.500000	12.500000	17.000000 K	BK7	C		
4	-38.300000	0.500000	17.000000 K	AIR			
5	78.100000	2.400000	20.000000 K	SF2	C		
6	31.800000	13.700000	20.000000 K	BK7	C		
7	-48.200000	1.500000	20.000000 K	AIR			
8	40.000000	13.500000	20.000000 K	BK7	C		
9	-40.000000	1.500000	20.000000 K	SF2	C		
10	142.000000	7.870000	19.000000 K	AIR			
IMS	--	--	17.300000		*		

Figure 5.10 The RKE wide-angle (WA) eyepiece is similar to the Erfle design with the central element taking the form of a cemented doublet. The RKE WA eyepiece will cover a 70-deg field of view with very good image quality and adequate eye relief.

-3.12 mm to +2.34 mm relative to the nominal zero diopter setting. Figure 5.11 illustrates the diopter focus setting of an eyepiece. When measuring this setting, an instrument known as a *Dioptrimeter* is used. For most accurate results the entrance pupil of the dioptrimeter should be located at the exit pupil of the eyepiece.

### 5.13 Eyepiece with the Eye

It will be informative to take one of the eyepiece designs and combine it with the model eye for analysis. For this exercise we will work with the Symmetrical eyepiece from Section 5.8. The basic lens configuration must be reversed prior to addition of the model eye. The first surface (the entrance pupil) of the resulting lens combination is set at a distance of -343.6 mm from the object. This results in the chief rays entering the eyepiece at a +2-deg angle, consistent with the original eyepiece design data. The model eye is located with its first surface (outer surface of the cornea) 3 mm inside the exit pupil of the eyepiece. This results in the entrance pupil of the eye being superimposed on the exit pupil of the eyepiece. The resulting lens system is shown in Fig. 5.12, along with aberration curves and complete lens data.

The 50-deg full field of the eyepiece will essentially fill the useful field of view of the eye. The aberration curves indicate that image quality over the central 60% of the field (30 deg) is consistent with the capability of the eye. If an object is located outside of that region, the direction in which the instrument is pointed will need to be altered to bring the image of that object close to the center of the visual field.

Figure 5.13 contains two graphic outputs from the OSLO program (Rev. 6.1) that describe additional performance characteristics of the eyepiece-eye combination. First, the plot of RMS spot size and wavefront error (OPD) illustrates the uniform state of correction over the central 60% of the field. Second, a plot of the level of image distortion on the retina confirms that the 5% residual distortion will not have a significant impact on image quality.

While the results will not be investigated here, it is clear from Fig. 5.14 that simple rotation of the eye about its center of rotation, to view an off-axis field point, will result in significant clipping of the image presented to the retina. This problem will be dealt with by the viewer instinctively, by changing the location of the eye axially and decentering it relative to the optical axis of the system. Since this adjustment process is quite unpredictable, the final design will be best served by assuring the nominal coincidence of pupils (as described earlier) and the optimization of image quality over the central portion of the field of view.

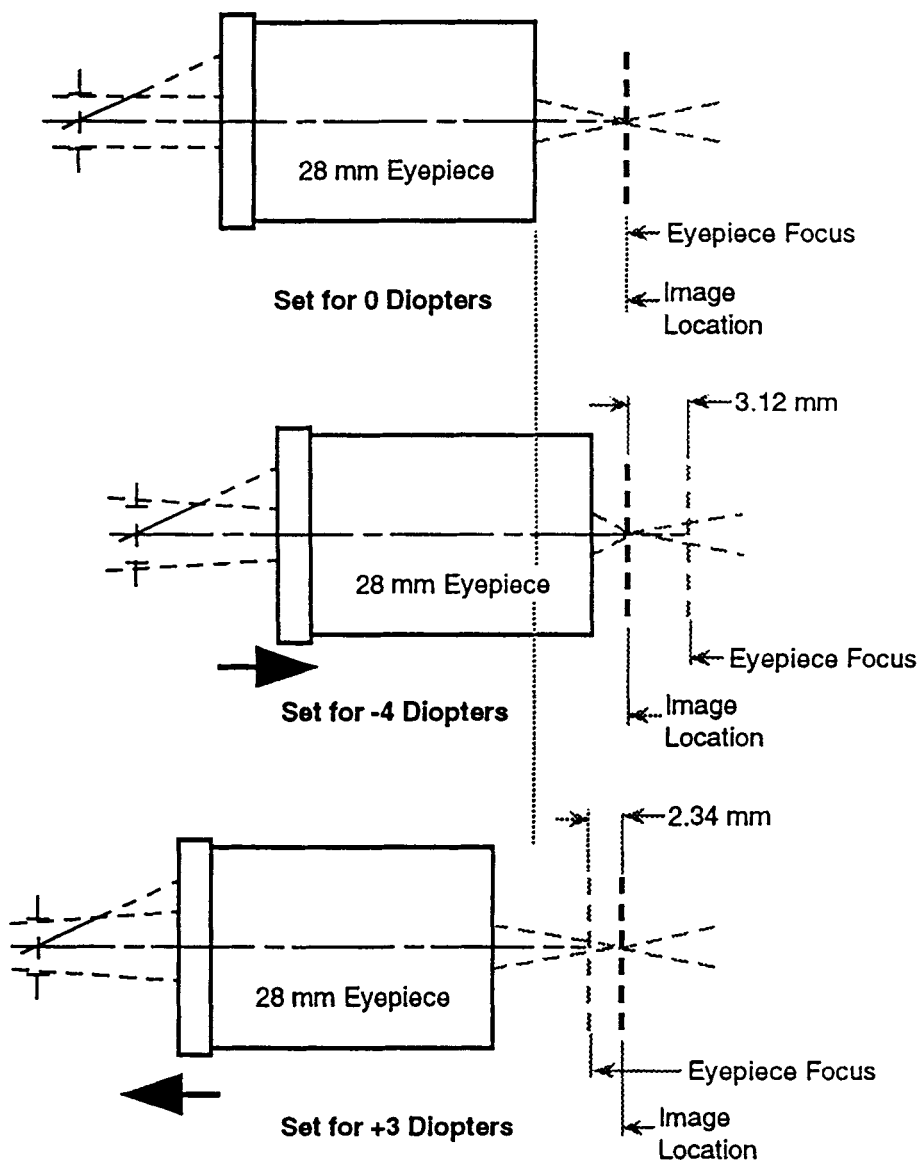
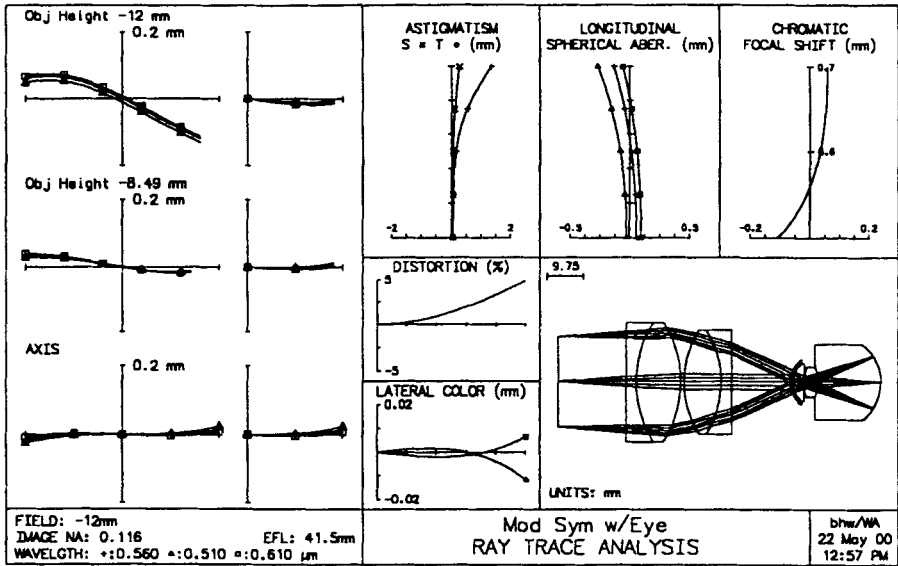


Figure 5.11 The degree of beam divergence or convergence emerging from the eyepiece is determined by the diopter focus setting. A common range of diopter focus settings is shown here.



**\*PARAXIAL CONSTANTS**

Effective focal length:	41.495898	Lateral magnification:	-0.615110
Numerical aperture:	0.116279	Gaussian image height:	7.381325
Working F-number:	4.300000	Petzval radius:	-11.672703

**\*LENS DATA**

**Mod Sym w/Eye**

SRF	RADIUS	THICKNESS	APERTURE RADIUS	GLASS	
OBJ	--	-343.640000	12.000000	AIR	*
AST	--	362.130000	24.641778	AS	AIR
2	--	2.800000	16.000000	SF5	C
3	29.800000	12.000000	16.000000	BAK1	C
4	-29.800000	1.000000	16.000000	AIR	
5	26.000000	10.000000	14.000000	BAK1	C
6	-26.000000	2.800000	14.000000	SF5	C
7	--	29.400000	14.000000	AIR	
8	--	-13.500000	6.000000	AIR	*
9	7.800000	0.600000	6.000000	CORNEA	M
10	6.400000	3.000000	5.000000	AQUEOUS	M
11	--	--	1.800000	KX	AQUEOUS P *
12	10.100000	4.000000	4.000000	LENS	M
13	-6.100000	17.160000	4.000000	VITREOUS	M *
14	-12.500000	0.001000	10.000000	RETINA	M
IMS	-12.500000	--	10.000000		*

Figure 5.12 Ray trace data (aberration curves) and lens data for the Symmetrical eyepiece combined with the model eye. The spacing is set such that the exit pupil of the eyepiece is in coincidence with the entrance pupil of the eye.

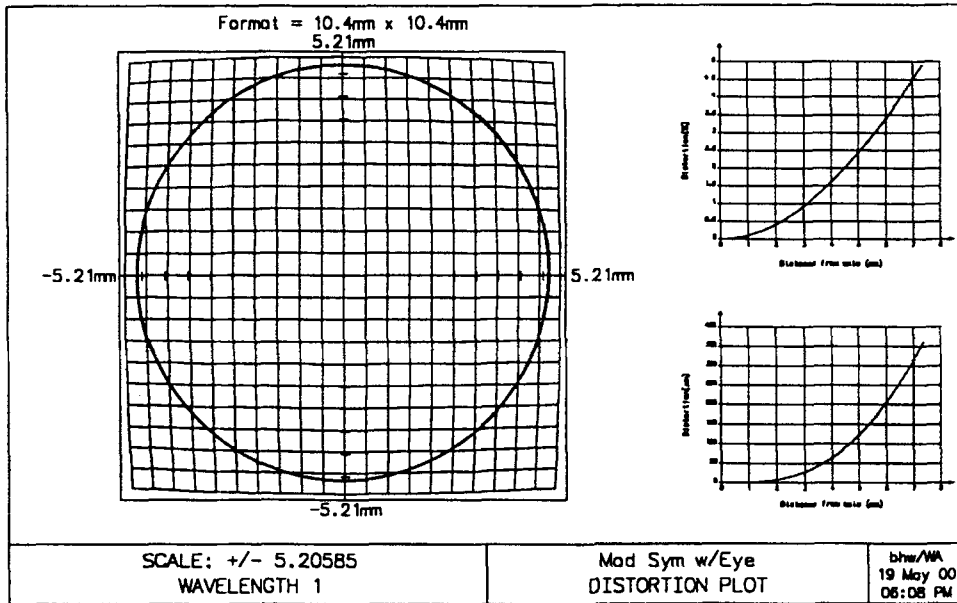
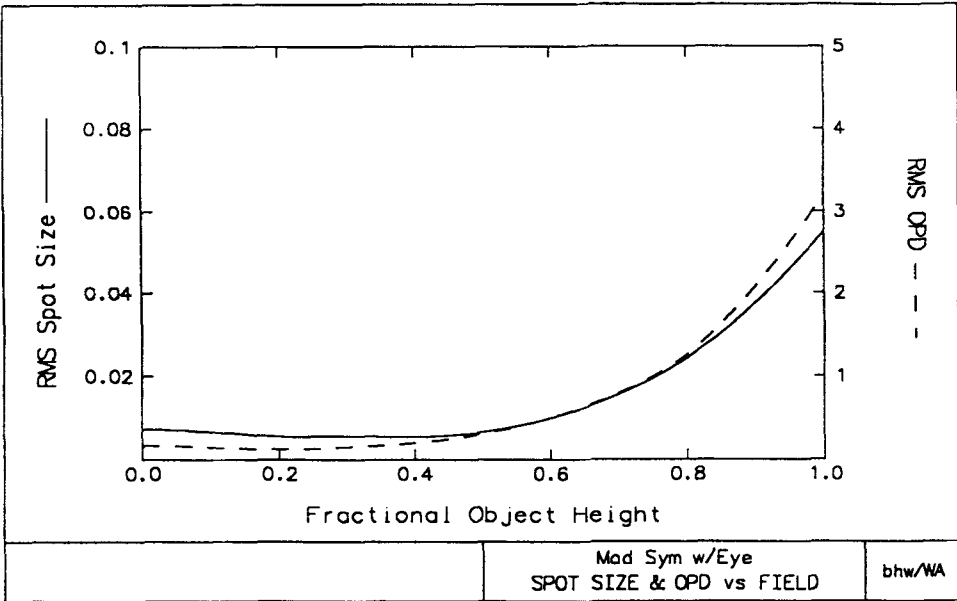


Figure 5.13 Additional OSLO analysis of the Symmetrical eyepiece combined with the model eye. Data at top indicates the uniformity of spot size and OPD over the central 60% of the image. The bottom plot demonstrates the relative freedom from distortion at the final image.

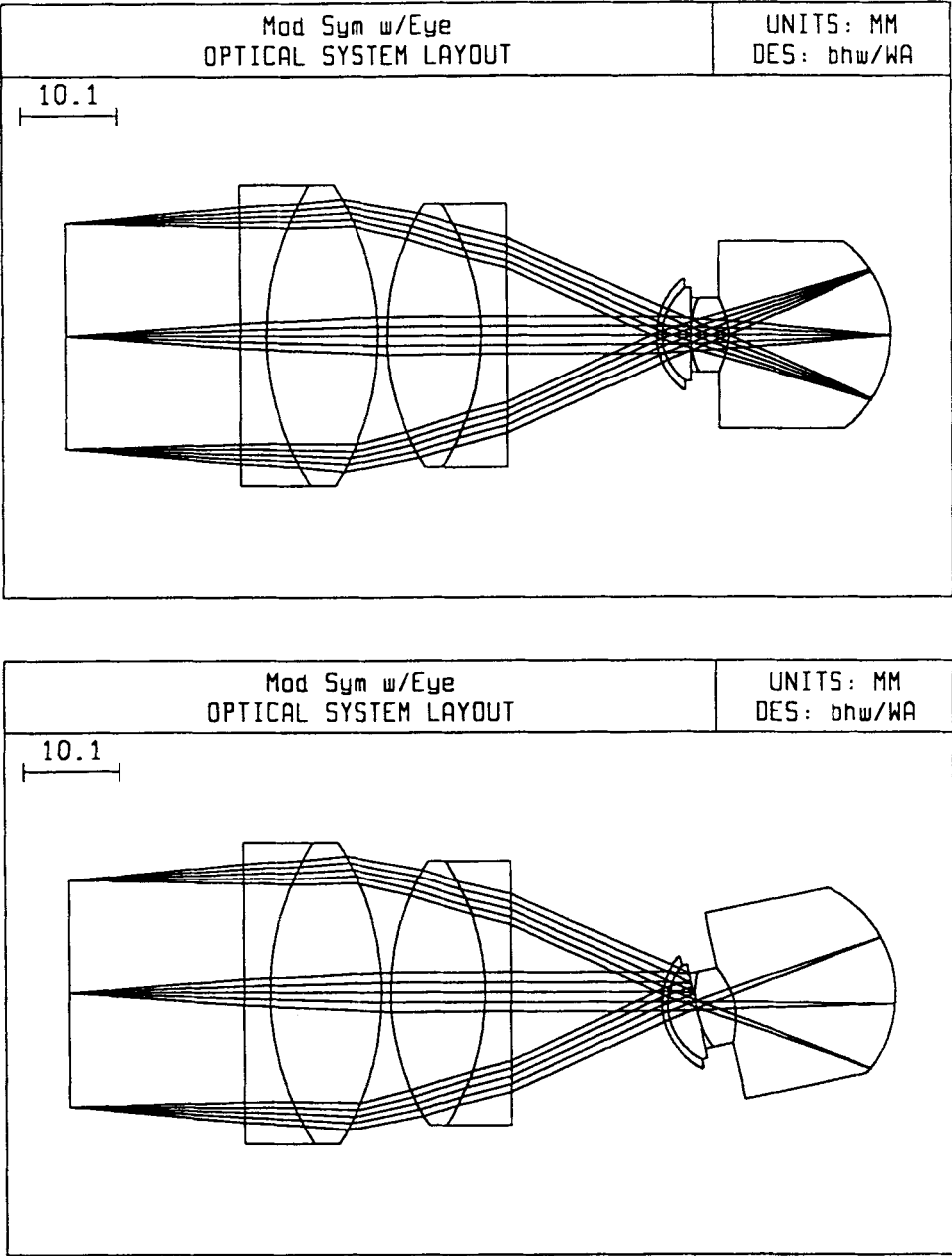


Figure 5.14 Tilt of the eye about its center of rotation will cause significant clipping of the light bundles. The location of the eye relative to the eyepiece will be altered instinctively to minimize this problem while imaging the point of interest at the center of the retina.



## 5.14 Review and Summary

This chapter has covered the eyepiece—its design and implementation into the overall optical system. The evolution of eyepiece complexity has been demonstrated via an in-depth analysis of nine separate and distinct eyepiece types. Each example has been scaled to a common 28-mm focal length to facilitate useful side-by-side comparisons. The recommended method of eyepiece design involves selection of a type that is appropriate to requirements, scaling of that design to provide the desired magnification, and then fine-tuning of the design to make it compatible with the other optics that make up the ultimate complete system.

While the author's initials may be assigned to some of the data presented here, this is not meant to imply that the designs are the creation or property of the author. All of the basic design data for these eyepieces are readily available in contemporary publications, software packages, and patent literature.

## 6

## The Microscope—Design

---

### 6.1 Introduction

When the upper limit of *magnifier* magnification is reached (about 25 $\times$ ), the system known as the *microscope* is considered. The microscope contains two basic optical components—the objective lens and the eyepiece. Each of these has its own magnification factor and the total microscope magnification is the product of the objective lens magnification and the eyepiece magnification.

For this design example we will be designing a microscope with a total magnification of 100 $\times$ . This particular configuration will use a 10 $\times$  objective lens, working with a 10 $\times$  eyepiece. The initial step in the design procedure will be to establish basic system specifications along with a thin lens system layout.

### 6.2 Basic System Specifications

There are a number of established microscope forms. This design will assume the dimensions of a basic Deutsche Industrie Norm (DIN) microscope. In this case the objective lens will have a numerical aperture (NA) of 0.25 ( $f/2$  at the object), and the total track from object to image will be 195 mm. The object diameter will be 1.8 mm, while the image diameter will be 18 mm. This objective lens will be combined with a 25-mm (10 $\times$ ) Orthoscopic eyepiece. Knowing the lens speed at the object to be  $f/2$  and the objective lens magnification to be 10 $\times$ , it follows that the speed of the light bundles at the internal image will be  $f/20$ . The resulting exit pupil diameter will be equal to the eyepiece  $e\text{fl} / 20 = 25 / 20 = 1.25$  mm. Scaling the Orthoscopic eyepiece design shown in Chapter 5 allows the eye relief to be estimated at about 20 mm. The tangent of the apparent half field of view to the eye can be estimated from the maximum image height (9 mm) divided by the eyepiece  $e\text{fl}$  (25 mm):  $\tan^{-1} 9/25 = \tan^{-1} 0.36 = 20$  deg. Having established these basic system specifications (Fig. 6.1.) it is now possible to embark on the lens design phase.

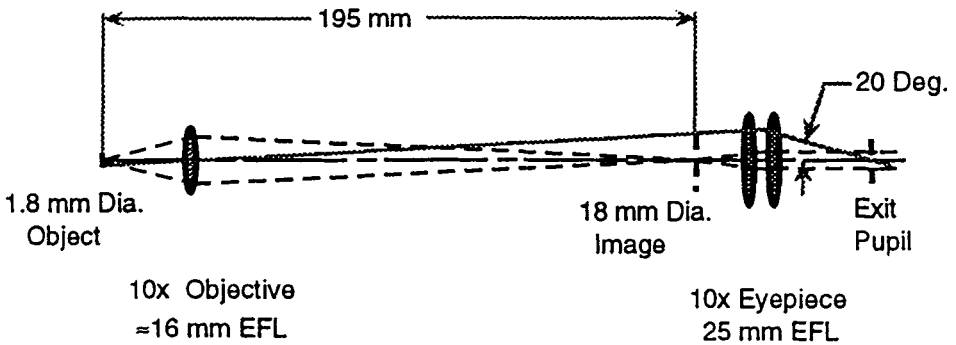


Figure 6.1 Basic thin-lens layout of optics for a 100 $\times$  microscope.

### 6.3 Resolution Goals and Limits

In order to generate a realistic design it is essential that the designer have some notion of the resolution goals and limits of the basic system. In this case, because it is ultimately a visual system, it is reasonable to consider the resolution of the *typical* eye as the limiting factor in ultimate resolution.

From Fig. 2.3 we find that the typical eye with a 1.25-mm pupil diameter is capable of resolving about 6.5 cycles/mm on a target positioned at the near point of vision (254 mm). Knowing this, we can assume that the 10 $\times$  eyepiece magnification will allow the typical viewer to resolve about 65 cycles/mm at the eyepiece image. This value will, in turn, correspond to 650 cycles/mm at the object.

As a point of comparison it will be useful to calculate the diffraction limited resolution limit of the objective lens. We know the f-number of the objective lens is  $f/2$  and the primary wavelength is 0.00056 mm. The diffraction limited cut-off frequency in this case is found using the formula

$$\begin{aligned}\text{Max Resolution (Cutoff)} &= 1 / (\lambda \times f/\#) \\ &= 1 / (.00056 \times 2) = 893 \text{ cycles/mm.}\end{aligned}$$

The conclusion to be drawn is that if we are to utilize all of the eye's resolving capability (650 cycles/mm), the optics will need to be very nearly diffraction limited. Establishing this point of reference allows the designer to decide when the design has reached an acceptable level of image quality.

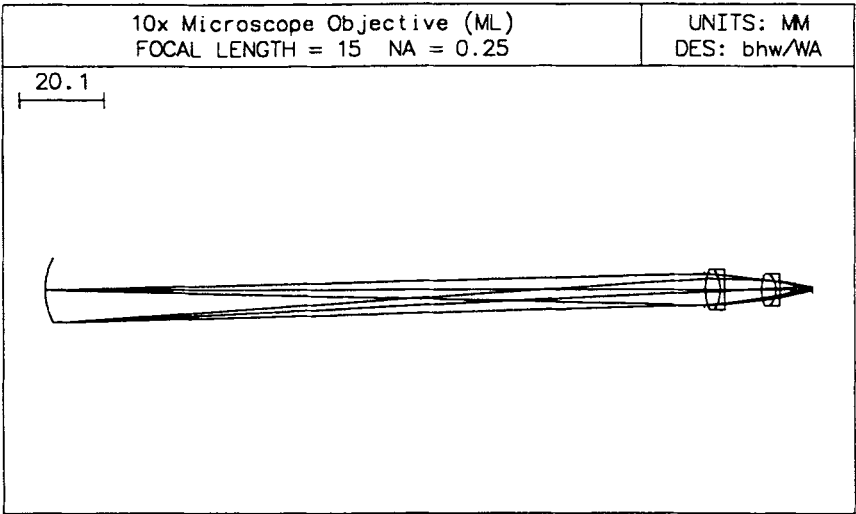
## 6.4 10× Objective, Starting Lens Form

Most lens design projects are initiated by a study of prior designs that are similar in form and performance to the new design. More often than not it is possible to find readily available and legitimate data on an existing design that takes the designer about halfway to a final solution. With the advent of computerized files, often an integral part of the lens design software package, the designer's experience and skill in locating the optimum starting point has become a major factor in the successful design process.

In this case, it is obvious that the 10× microscope objective lens is one that has been extensively worked on over the years, with any number of commercially successful designs resulting. For this example the author has located a design of the *Lister* form that is described in *Lens Design*, a book by Milton Laikin. Design data have been taken from the book, converted to millimeters, and entered into the OSLO software package. The resulting (starting) design is shown in Fig. 6.2. Major differences from our design specifications are the object to image distance (180 vs. 195 mm) and the internal image diameter (16 vs. 18 mm).

Note that for purposes of microscope objective lens design and analysis, the internal image is assumed to be the object, while the actual object plane is assumed to be the image. This reversal has no impact on lens performance, but is merely a matter of tradition and convenience. Also note that the object surface is assumed to have a radius of 18 mm, which eliminates effects of field curvature on the analysis. Ray trace analysis of this design (Fig. 6.3, top) shows it to be limited by high-order spherical aberration and some residual astigmatism. Polychromatic MTF analysis (Fig. 6.3, bottom) indicates that the lens is essentially diffraction limited on axis, with off-axis MTF degraded slightly due to residual astigmatism. On average, the MTF data indicates lens performance with residual wavefront (OPD) errors of about one-quarter wave.

The assumption of a curved field for this design is valid in that the off-axis points will be brought into best focus either by the eye's natural ability to accommodate, or by fine-tuning the focus setting of the microscope. In addition, the movable stage holding the object makes it a simple matter for the viewer to move the object to the optical center of the objective lens. This is a typical example of why it is important that the designer be aware of the manner in which the final instrument is to be used, so that valid and useful trade-offs such as this can be made during the design process.



**\*PARAXIAL CONSTANTS**

Effective focal length:	15.002833	Lateral magnification:	-0.099462
Numerical aperture:	0.250000	Gaussian image height:	0.795695
Working F-number:	2.000000	Petzval radius:	-14.978387

**\*LENS DATA**

**10x Microscope Objective (ML)**

SRF	RADIUS	THICKNESS	APERTURE RADIUS	GLASS	SPE	NOTE
OBJ	18.000000	155.000000	8.000000	AIR	*	
AST	--	0.300000	3.880000	AK	AIR	
2	13.090000 V	3.500000	5.000000	K	K5 C	
3	-9.380000 V	1.130000	5.000000		F2 C	
4	-112.240000 V	8.640000	5.000000		AIR	
5	11.480000 V	3.350000	4.000000		K5 P	
6	-6.000000 V	0.970000	4.000000		F2 P	
7	-21.250000	7.660000	2.100000	K	AIR	
IMS	--	--	0.800000		*	

**\*PARAXIAL TRACE**

SRF	PY	PU	PI	PYC	PUC	PIC
0	--	0.024873	0.024873	-8.000000	0.051613	-0.392832
1	3.855341	0.024873	0.024873	--	0.051613	0.051613
2	3.862803	-0.085119	0.319969	0.015484	0.033464	0.052796
3	3.564887	-0.056799	-0.465171	0.132608	0.032287	0.019327
4	3.500704	-0.111582	-0.087988	0.169092	0.051452	0.030781
5	2.536637	-0.149182	0.109380	0.613636	0.015390	0.104904
6	2.036877	-0.119432	-0.488662	0.665193	0.021203	-0.095475
7	1.921029	-0.250077	-0.209833	0.685759	0.014311	-0.011068
8	0.005436	-0.250077	-0.250077	0.795384	0.014311	0.014311

Figure 6.2    Lens layout and paraxial data for the starting lens form used to generate the final objective lens design.

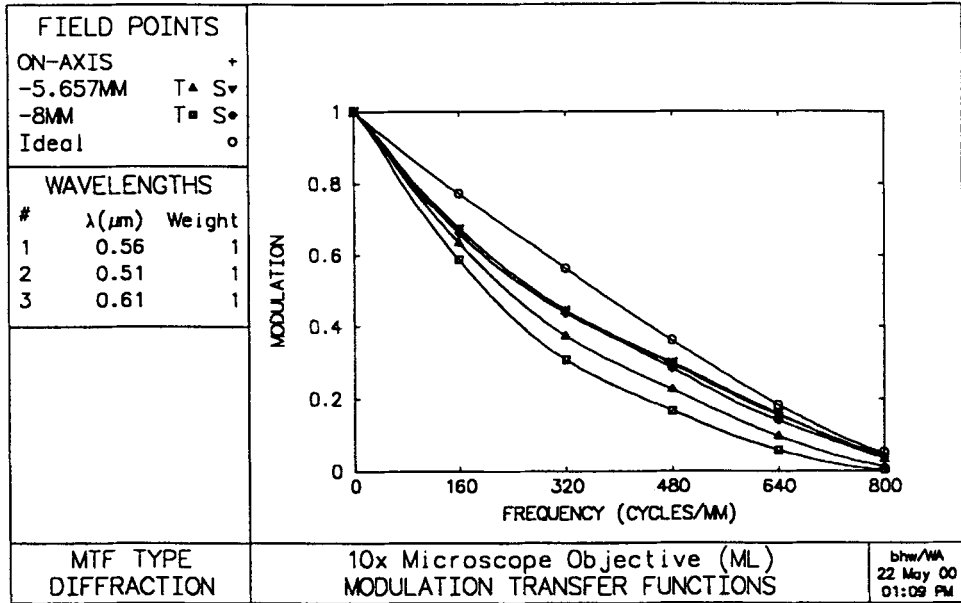
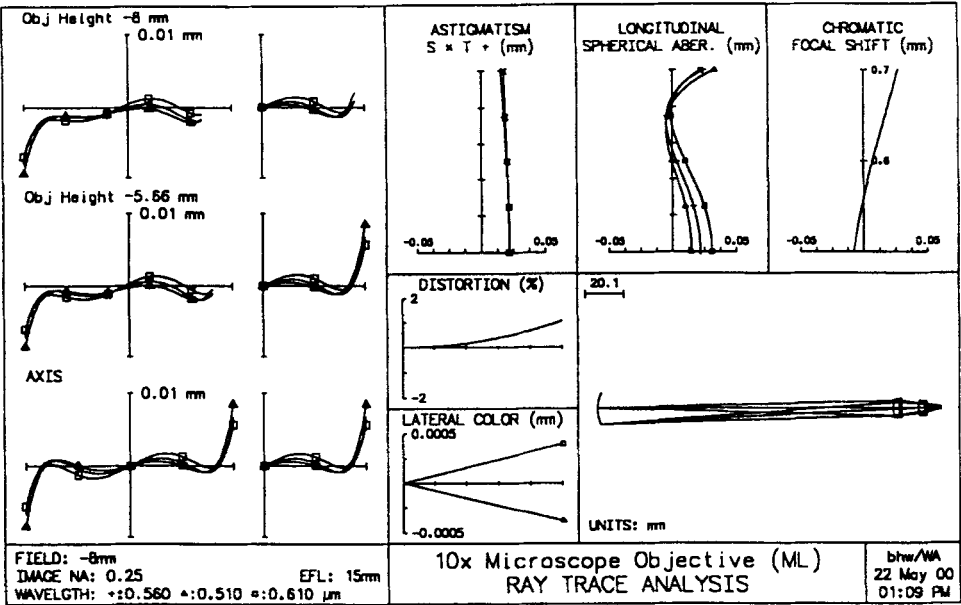


Figure 6.3 Ray trace analysis (aberration curves) and diffraction MTF data for the starting lens form used to generate the final 10× microscope objective lens design.

## 6.5 New 10× Objective Design

The initial step in the design process is to scale the starting lens such that the total track from object to image is 195 mm. This can be accomplished by scaling of the lens efl from the starting value of 15 mm to a value of 16.2 mm. The object diameter is changed at this point from 16 to 18 mm. The lens is then set up for optimization by making all of the curvatures variable. To assure a solution where astigmatism is minimized, the object surface is set to have a radius of 20 mm. (This value is proportional to that of the starting design.)

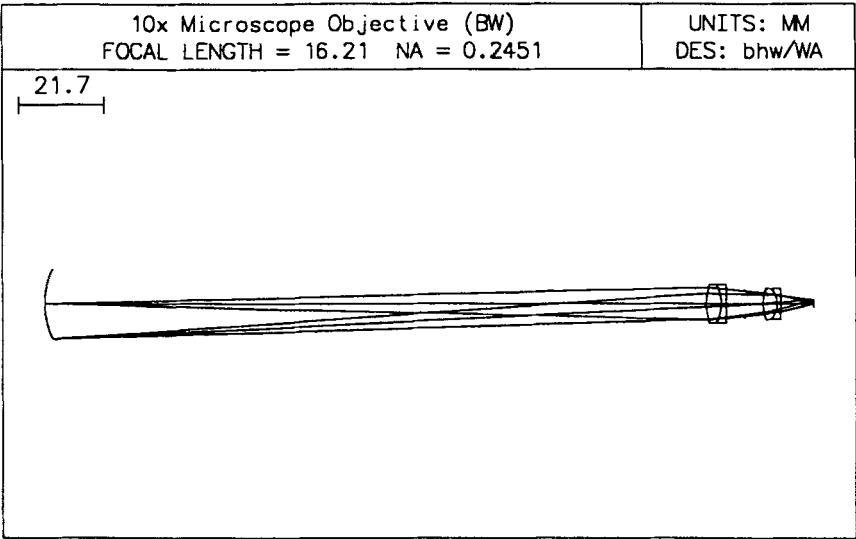
At this point in the lens optimization process, an error function must be constructed that will allow the optimization routine to evaluate the level of image quality after each iteration of the variables. Most software packages will contain several methods of constructing such an error function. During optimization the designer must monitor general lens shapes for producibility, lens apertures as they may impact upon vignetting, and the overall balance of residual lens aberrations. The selection of a good starting design will generally assure a final design that is physically quite similar to the starting form.

In this case, after several rounds of optimization, a final design was generated that met all of the basic lens specifications that had been established. That final lens design is shown, along with final tabulated lens data, in Fig. 6.4. Figure 6.5 contains final ray trace analysis (aberration) data and MTF curves for the new design. It will be noted that the on-axis diffraction limited performance of the starting design has been maintained, while the MTF curves show a slight increase in astigmatism for the off-axis points. Further analysis indicates that this new design has been optimized to yield diffraction limited (1/4 wave OPD) performance over 80% of the field, while meeting all of the established basic lens specifications.

## 6.6 Adding the Eyepiece

The 100× microscope is then created by adding a 10× eyepiece to the 10× objective lens just designed. It has been determined that the eyepiece will need to cover a 40-deg field of view (Fig. 6.1). Data from Chapter 5 indicate that either the RKE (Fig. 5.5) or the Orthoscopic eyepiece (Fig. 5.6) will work well in this application.

The Orthoscopic design was selected and then scaled to 25-mm efl to give us the desired 10× magnification, with an exit pupil diameter of 1.25 mm. This design was then added to the *new* 10× objective lens to produce the final 100× microscope configuration shown in Fig. 6.6. Review of the



\*PARAXIAL CONSTANTS

Effective focal length:	16.213656	Lateral magnification:	-0.099392
Numerical aperture:	0.245098	Gaussian image height:	0.894525
Working F-number:	2.040000	Petzval radius:	-16.097025

\*LENS DATA

10x Microscope Objective (BW)

SRF	RADIUS	THICKNESS	APERTURE RADIUS	GLASS	SPE	NOTE
OBJ	20.000000	167.800000	9.000000	AIR	*	
1	13.300000 V	3.800000	4.200000 K	K5	C	
2	-10.510000 V	1.300000	5.000000	F2	C	
3	-558.000000 V	4.660000	5.000000	AIR		
AST	--	4.660000	3.244549 AS	AIR		
5	11.710000 V	3.600000	4.000000	K5	C	
6	-5.970000 V	1.000000	4.000000	F2	C	
7	-22.940000	8.270000	2.200000 K	AIR		
IMS	--	--	0.900000		*	

\*PARAXIAL TRACE

SRF	PY	PU	PI	PYC	PUC	PIC
0	--	0.024368	0.024368	-9.000000	0.050315	-0.399685
1	4.088940	-0.089694	0.331807	-0.557130	0.047419	0.008426
2	3.748104	-0.062521	-0.446316	-0.376939	0.042348	0.083283
3	3.666826	-0.105540	-0.069093	-0.321886	0.069074	0.042925
4	3.175011	-0.105540	-0.105540	1.1102e-16	0.069074	0.069074
5	2.683196	-0.148027	0.123597	0.321886	0.035880	0.096562
6	2.150297	-0.117087	-0.508211	0.451054	0.038295	-0.039673
7	2.033210	-0.245171	-0.205719	0.489350	0.048857	0.016964
8	0.005647	-0.245171	-0.245171	0.893400	0.048857	0.048857

Figure 6.4 Lens layout and paraxial data for the optimized 10× microscope objective lens modified to meet new system requirements.



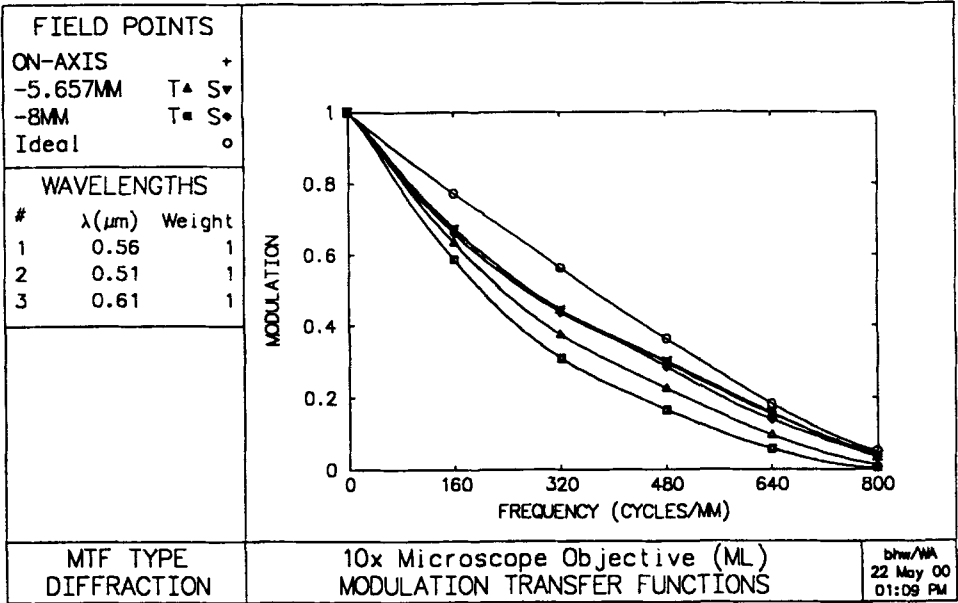
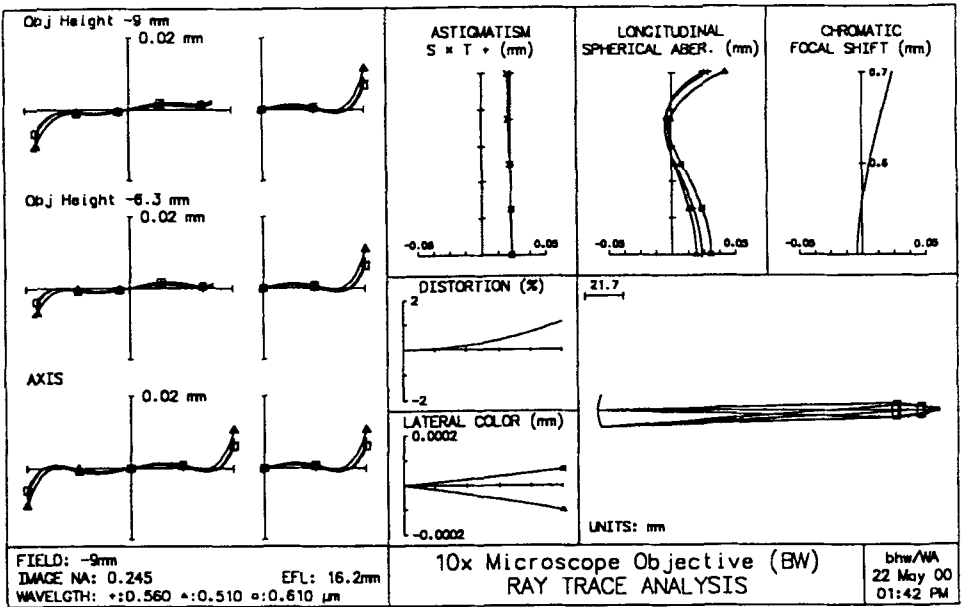
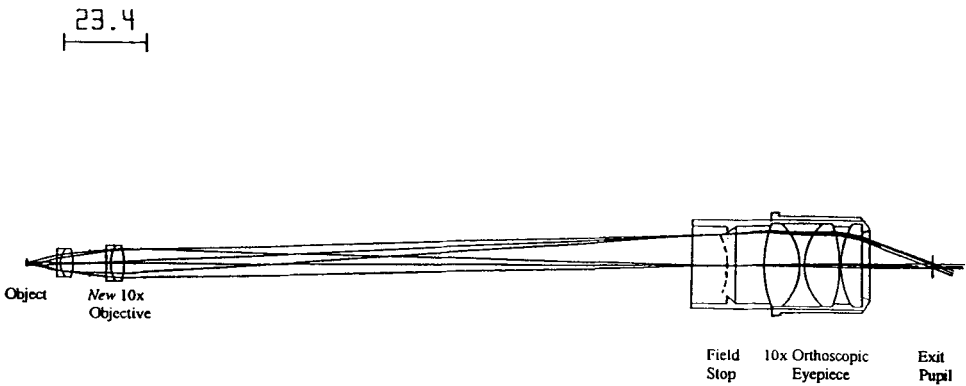


Figure 6.5 Ray trace analysis (aberration curves) and diffraction MTF data for the optimized objective lens modified to meet new system requirements.



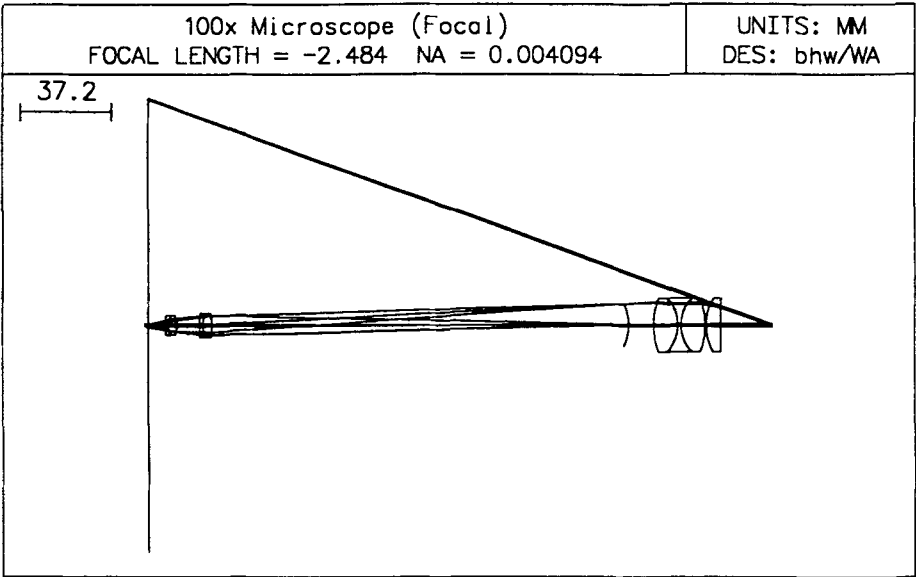
**Figure 6.6** Scale layout of final 100× microscope design with custom-designed 10× objective and 10× Orthoscopic eyepiece.

Edmund Scientific catalog indicates availability of a 25-mm Orthoscopic eyepiece (part # K36161). This is the eyepiece assembly shown in Fig. 6.6. While the details of any commercial eyepiece design will vary from our scaled design, it is safe to assume that the basic performance characteristics of the two will be essentially the same.

**6.7 Performance Evaluation**

For purposes of image quality evaluation the object distance was adjusted to produce a final image that was 254 mm in front of the exit pupil. This simulates the viewer adjusting microscope focus so that the final image is at the near point of vision. This focus adjustment results in the exit pupil diameter being reduced to 1.2 mm. It will be seen that this focus setting results in the object and image surfaces being essentially coincident (Fig. 6.7). This condition conveniently permits us to imagine the situation where the eye is at the exit pupil of the microscope, and that microscope is then taken away. The 100× magnification provided by introduction of the microscope optics is quite easy to visualize. From the data in Fig. 6.7 it is seen that an object size of 0.86 mm will coincide with an image size of 92 mm. This magnification of 107× is a bit larger than the nominal goal of 100×, primarily because of distortion in the eyepiece. Exact ray tracing reveals that the magnification for points close to the axis (paraxial) is actually 102×.

Figure 6.8 (top) contains results of ray trace analysis on the 100× microscope with the final image at the near point. From these aberration curves it can be seen that the high-order spherical aberration of the 10× objective dominates performance. It can also be seen that, due to the



\*LENS DATA

100x Microscope (Focal)

SRF	RADIUS	THICKNESS	APERTURE RADIUS	GLASS	SPE	NOTE
OBJ	--	8.250000	0.860000	AIR		* Object
1	--	0.000100	2.511185 S	AIR		
2	22.940000	1.000000	2.200000 K	F2	C	10x
3	5.970000	3.600000	4.000000	K5	C	Objective
4	-11.710000	4.660000	4.000000	AIR		
AST	--	4.660000	3.244549 A	AIR		
6	558.000000	1.300000	5.000000	F2	C	
7	10.510000	3.800000	5.000000	K5	C	
8	-13.300000	169.750000	4.200000 K	AIR		
9	-20.000000	10.300000	8.750000	AIR		* Field Stop
10	32.340000	9.830000	11.000000	K5	C	
11	-15.900000	1.340000	11.000000	F2	C	10x Ortho
12	15.900000	9.830000	11.000000	K5	C	Eyepiece
13	-32.340000	0.450000	11.000000	AIR		
14	23.050000	5.800000	11.000000	BAK1	C	
15	--	20.800000	11.000000	AIR		
16	--	-254.000000	0.610000	AIR		* Exit Pupil
IMS	--	--	92.000000			* Image

Figure 6.7 Lens layout and lens data for the final 100× microscope design with custom-designed 10× objective and 10× Orthoscopic eyepiece. Microscope focus has been set so that the final image is located at the near point of the eye (254 mm).

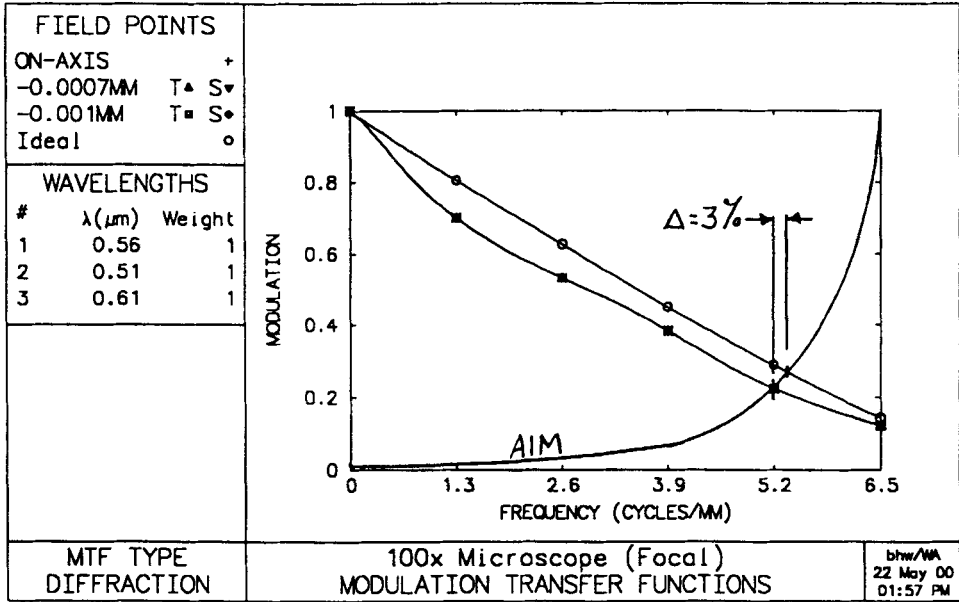
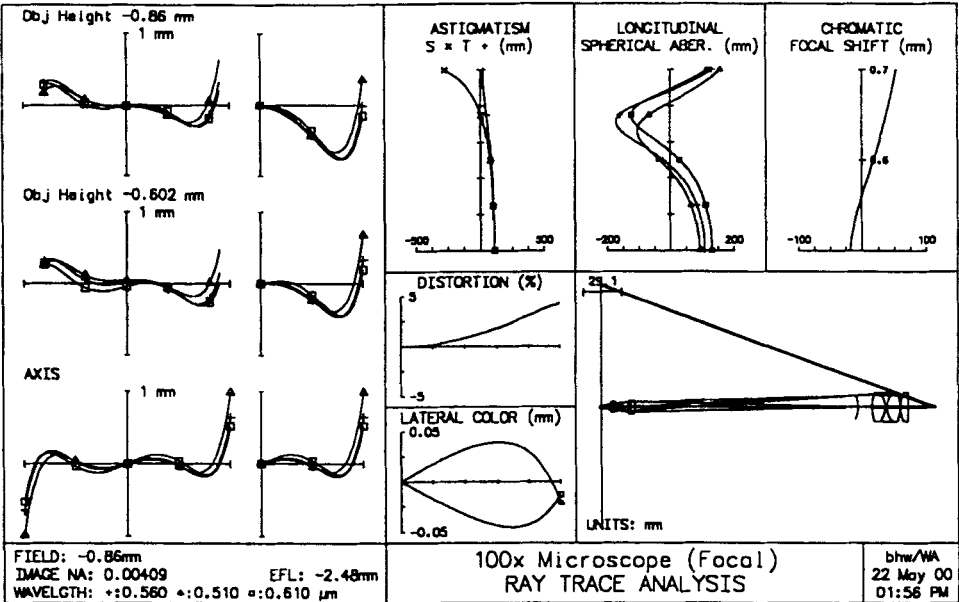


Figure 6.8 Ray trace analysis (aberration curves) and on-axis diffraction MTF curves for the final 100 $\times$  microscope design with custom-designed 10 $\times$  objective and 10 $\times$  Orthoscopic eyepiece. AIM curve shown is based on the expected performance of the model eye with a 1.25-mm pupil diameter.

eyepiece design, lateral color is well corrected and that distortion is less than 5%. The astigmatism curves indicate that the final image is quite flat and free of astigmatism over the central 80% of the field.

It was shown in Chapter 2 (Fig. 2.3), that the typical viewer with a pupil diameter of 1.2 mm is able to resolve 6.5 cycles/mm for a target at the near point of vision. Figure 6.8 (bottom) contains MTF curves for the 100× microscope with the final image at that near point. The AIM curve shown approximates the performance of a typical eye. These MTF results demonstrate that the optics of the 100× microscope will reduce the on-axis resolution by just 4% relative to a diffraction limited (ideal) system.

One might look at this data and conclude that the on-axis resolution achieved (5.2 cycles/mm) isn't all that might be desired. If we assume that the final image consists of a repeating pattern with lines and spaces of equal width, and a frequency of 5.2 cycles/mm, then each line and each space (each element) would have a width of

$$(1/5.2)/2 = 96 \text{ microns.}$$

Having determined earlier that the overall microscope magnification is 102×, this element size at the final image corresponds to a resolved element size of

$$96 \text{ microns} / 102 = 0.94 \text{ microns } (.000037 \text{ inches}) \text{ at the object.}$$

Microscope resolution is often described in terms of the minimum resolved separation of two point sources at the object. Figure 6.9 is a plot of the spread function for the 100× microscope at the final image plane. The Rayleigh criteria states that the two points will be resolved if the energy level between them dips to 74% of the maximum. From Fig. 6.9 it is seen that this is the case when the separation at the image is .144 mm. Applying the 102× magnification factor, the corresponding separation at the object is .0014 mm. If the formula for the Rayleigh criteria is applied we find the following

$$\text{Separation} = .61\lambda / \text{NA} = .61 \times .00056 / 0.25 = .0014 \text{ mm.}$$

This confirms the fact that the microscope is performing at the diffraction limit. Further analysis of this design indicates that the 100× microscope will provide *essentially* diffraction-limited performance over the central 50% of the field, with *very good* image quality over the remainder of the field.

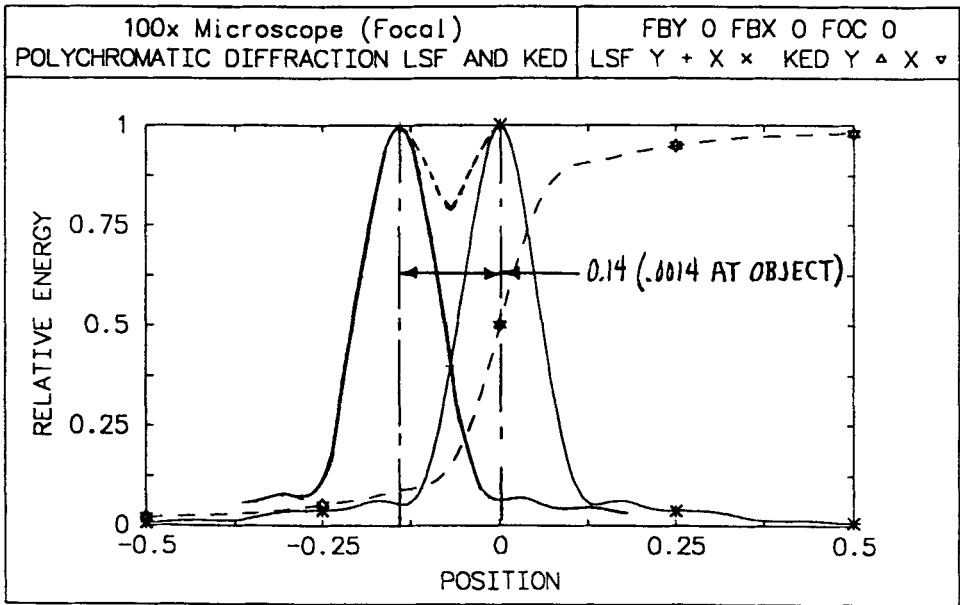


Figure 6.9 On-axis polychromatic line spread analysis shows that the 100× microscope design will permit the viewer to visually resolve two point sources at the object with a separation of just 1.4 microns.

6.8 Review and Summary

The 100× microscope presented here has been designed with a combination of custom design and commercially available optics. This exercise has been configured to expose the reader to a variety of optical design and engineering concepts and techniques. The importance of selecting a good starting design has been demonstrated in the initial stages of objective lens design. We have seen how the use of a quality software package allows the designer to modify and re-optimize that starting design so that it conforms to established performance specifications. It was then shown how the basic eyepiece design data from Chapter 5 can be utilized to complete the system, allowing meaningful analysis of the total system.

Several aspects of the design process described here are unique to the design of a visual instrument. Image quality or resolution goals were established based on the resolving capability of the typical eye. The state of final aberration correction, particularly field curvature and astigmatism, has been determined based upon the accommodation characteristics of the eye, along with an understanding of methods employed by the viewer in use of the final instrument.

## 7

## The Telescope—Design

---

### 7.1 Introduction

The optics of the telescope bear several similarities to those of the microscope. First, an objective lens is used to form an image of the object being viewed. An eyepiece is then introduced to view that image at increased magnification. As with the microscope, the total magnification of the telescope is a result of the individual magnifications of the objective lens and the eyepiece. The major difference between the two systems is that, while the microscope is used to view small (micro) objects and make them appear to be larger than they actually are, the telescope is used to view distant (tele) objects and make them appear closer to the viewer than they actually are. This chapter will cover the optical design considerations involved in the design of two telescope systems intended for distinctly different applications.

### 7.2 The Astronomical Telescope

The astronomical telescope is distinguished by several unique characteristics. The magnification is generally quite high, with the upper limit being typically established by the resolution capability of the eye. The size of the objective lens is generally as large as practical, limited by budget and acceptable overall telescope size and weight. A series of eyepieces is generally part of the telescope package, allowing changes to overall magnification by exchanging the eyepiece being used.

For this exercise we will assume the telescope is being designed for use in a *serious* amateur astronomy application. This would mean that budget and allowable instrument size will be limited. Assuming a refracting design, a limit of about 120 mm on the objective lens clear aperture might be reasonable. For most astronomical observations, a lens speed of  $f/10$  would be typical. This would lead to an  $f/10$  objective lens with an efl of

$$\begin{aligned}\text{Effective Focal Length (efl)} &= \text{Aperture Dia.} \\ &\times f/\# = 120 \times 10 = 1200 \text{ mm.}\end{aligned}$$

The design process started with the selection of a cemented achromat design found on p. 155 of *Optical Engineering Fundamentals* (SPIE Vol. TT30). That design was scaled to 1200-mm focal length and set to a speed of  $f/10$ . The image diameter was set to 24 mm and the design wavelengths were set to 0.56, 0.51, and 0.61 microns. The design was then optimized using all curvatures (including the image), and focus, as variables. All monochromatic aberrations were balanced, while primary color was also corrected. The resulting design, with paraxial and lens data, is shown in Fig. 7.1. The aberration curves and MTF curves for this design are shown in Fig. 7.2. The MTF curves indicate that residual aberrations are in the range of one-half wave. This was not deemed to be an adequate level of image quality for the astronomical telescope being designed.

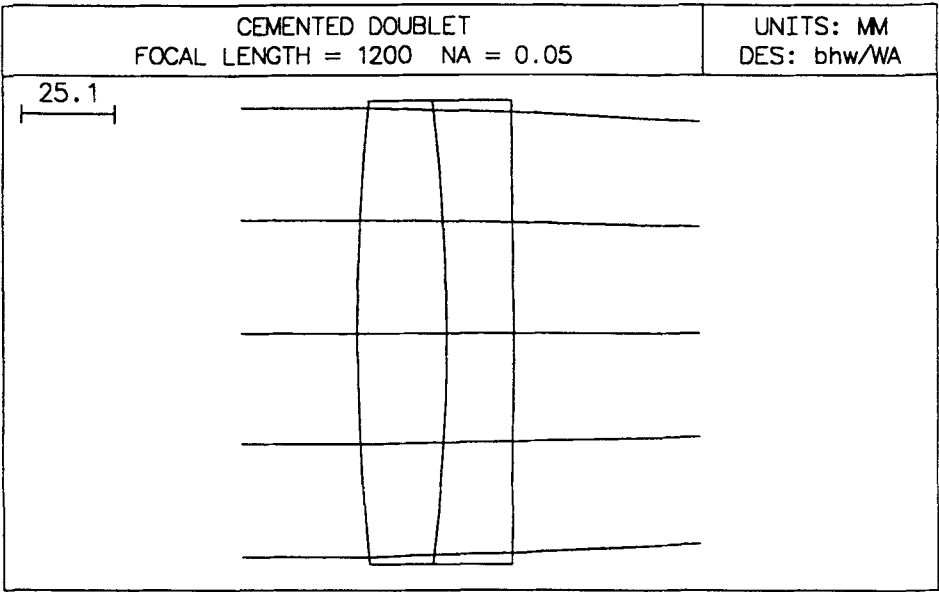
The next step in the design process was to convert the cemented doublet to an air spaced doublet and then to re-optimize the design. A 2-mm air space was added to the design shown in Fig. 7.1 and the glass type of the flint element was changed from F7 to F2, a more common glass type. Whenever the designer is at a point of major change in the design (such as now), this is the ideal time to examine all lens parameters and fine-tune them for optimum cost and producibility. Working again with all curvatures plus focus as variables, the air-spaced doublet was optimized. The resulting lens configuration is shown in Fig. 7.3. Aberration curves and MTF data for this design are shown in Fig. 7.4. From this MTF data it can be concluded that residual aberrations are now less than 0.25 wave. This is indicative of *essentially* diffraction-limited performance and is felt to be acceptable for the application being considered, i.e., serious amateur astronomy.

### 7.3 Resolution Goals and Limits

Examination of the aberration curves in Fig. 7.4 reveals that spherical aberration has been totally eliminated, while the curves for the red and blue light have been made to cross at the 0.7 aperture point. This state of final correction was obtained by careful monitoring and control of the error function during optimization. Note that in some cases the goal is to reduce residuals to zero (spherical aberration), while in other cases the design will benefit by correcting the aberration to a specific nonzero value. This was done for the chromatic aberration to result in a minimum spot size and optimum MTF values. Most of today's optical design software packages are well-suited for this process of aberration balancing.

Another quite common and meaningful method of evaluating the image quality of a telescope objective lens involves the point spread





**\*PARAXIAL CONSTANTS**

Effective focal length:	1200.00700	Lateral magnification:	-4.0000e-23
Numerical aperture:	0.05000	Gaussian image height:	11.65000
Working F-number:	10.00000	Petzval radius:	-1678.01861

**\*LENS DATA**

CEMENTED DOUBLET							
SRF	RADIUS	THICKNESS	APERTURE	RADIUS	GLASS	SPE	NOTE
OBJ	--	3.0000e+25	2.9125e+23		AIR		
AST	--	--	60.00035	AS	AIR		
2	605.70000 V	24.00000	62.00000		BK7	C	
3	-506.10000 V	18.00000	62.00000		F7	C	
4	-3194.80000 V	1175.85000	62.00000		AIR		
IMS	-450.00000 V	--	V	11.65000			

Figure 7.1 Lens layout and data on a cemented achromatic doublet considered and rejected for use as the telescope objective lens.

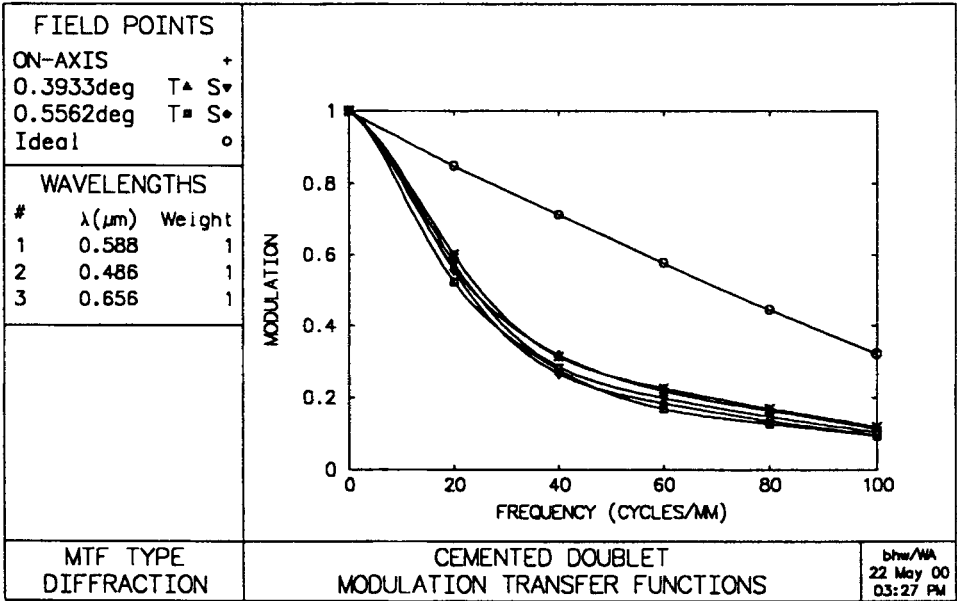
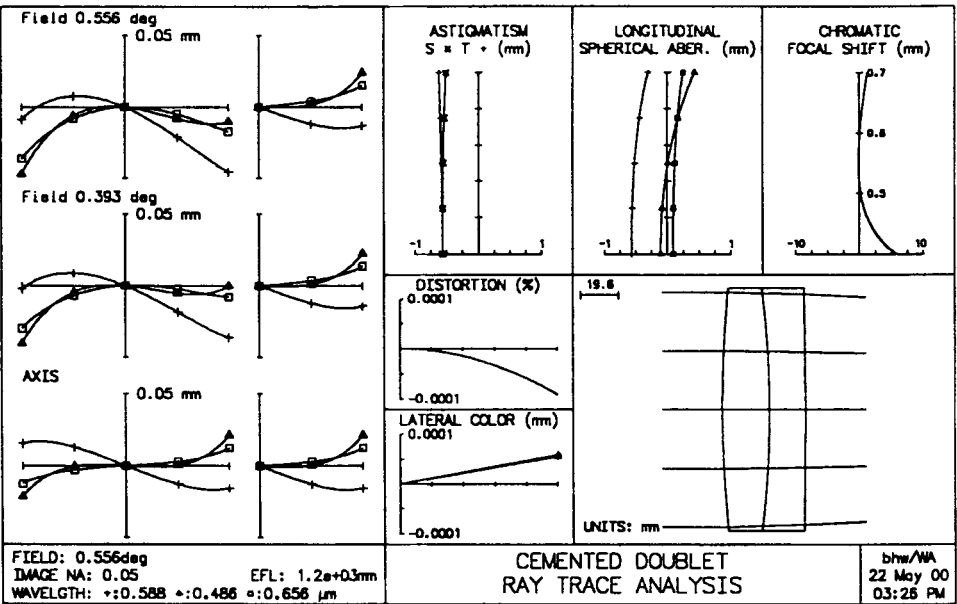
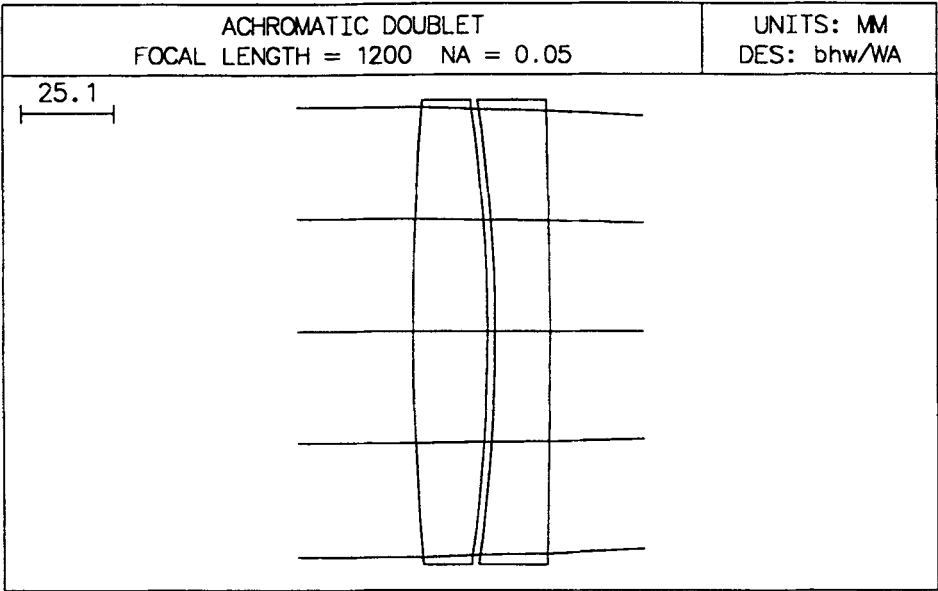


Figure 7.2 Ray trace analysis (aberration curves) and diffraction MTF data for the cemented achromatic doublet considered and rejected for use as the telescope objective lens.



**\*PARAXIAL CONSTANTS**

Effective focal length:	1199.91672	Lateral magnification:	-3.9997e-28
Numerical aperture:	0.05000	Gaussian image height:	11.65000
Working F-number:	10.00000	Petzval radius:	-1681.26911

**\*LENS DATA**

ACHROMATIC DOUBLET						
SRF	RADIUS	THICKNESS	APERTURE RADIUS	GLASS	SPE	
OBJ	--	3.0000e+30	2.9127e+28	AIR		
AST	--	--	59.99584 AS	AIR		
2	711.00000 V	20.00000	62.00000	BK7	C	
3	-428.84000 V	2.00000	60.00000	AIR		
4	-431.46000 V	15.00000	62.00000	F2	C	
5	-1841.20000 V	1178.40000	62.00000	AIR		
IMS	-440.00000 V	--	V 11.65000			

Figure 7.3 Lens layout and data on the optimized air-spaced achromatic doublet accepted for use as the telescope objective lens.

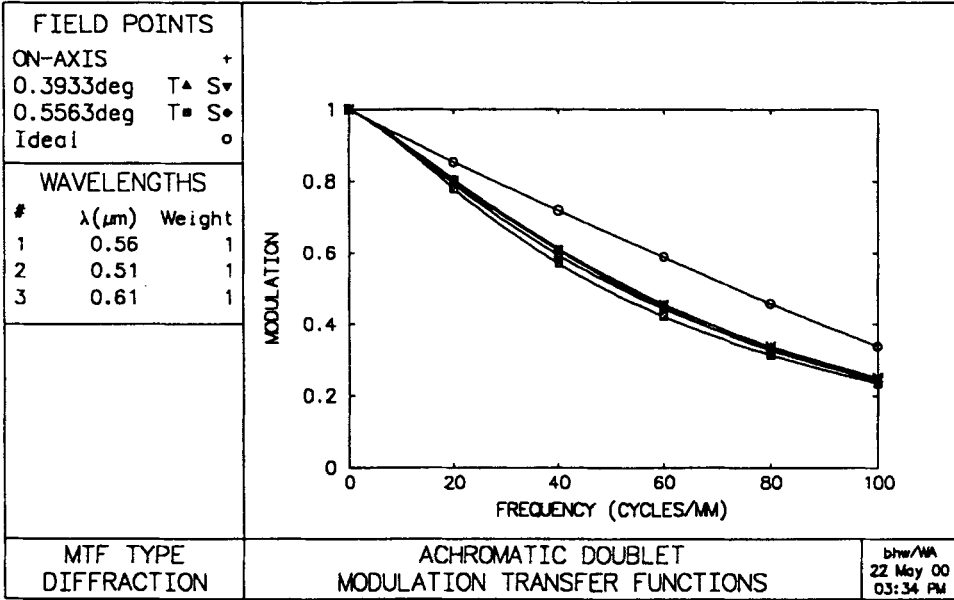
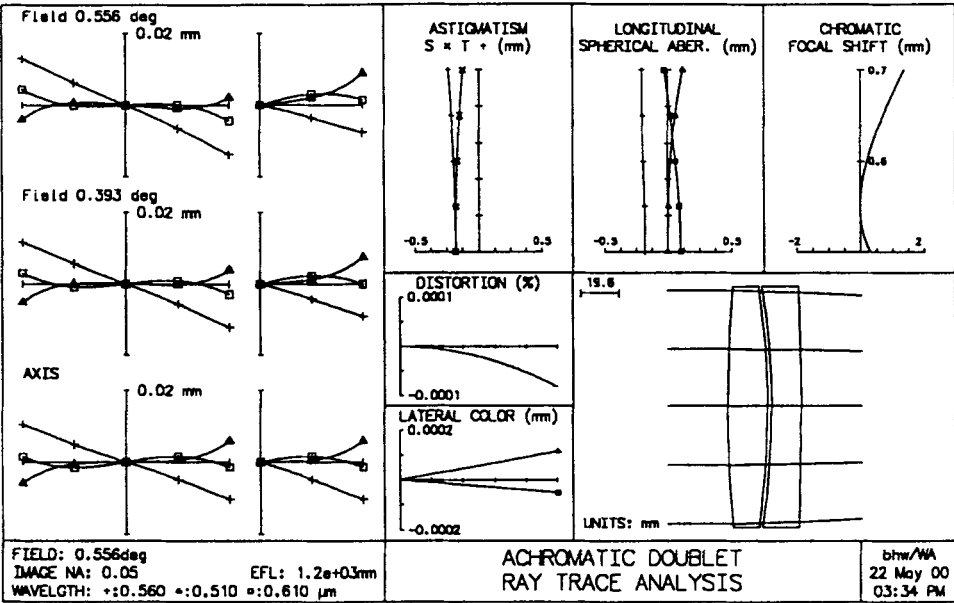


Figure 7.4 Ray trace analysis (aberration curves) and diffraction MTF data for the optimized air-spaced achromatic doublet design accepted for use as the telescope objective lens.

function. Figure 7.5 contains the plotted point spread functions for the image of two point sources that are separated by .007 mm at the image, which corresponds to an angular separation of 1.2 arc seconds in object space. The dip in relative energy to 74% corresponds to the Rayleigh criteria, which states that this is the level of change required for the two points to be resolved. The formula for a diffraction-limited objective (according to Rayleigh) is as follows

Separation at Image =  $1.22 \times \lambda \times f/\# = 1.22 \times .00056 \times 10 = .0068 \text{ mm}$   
Angular Separation =  $.00068 / 1200 = 1.17 \text{ arc seconds}$ .

These results confirm the essentially diffraction-limited performance of the design.

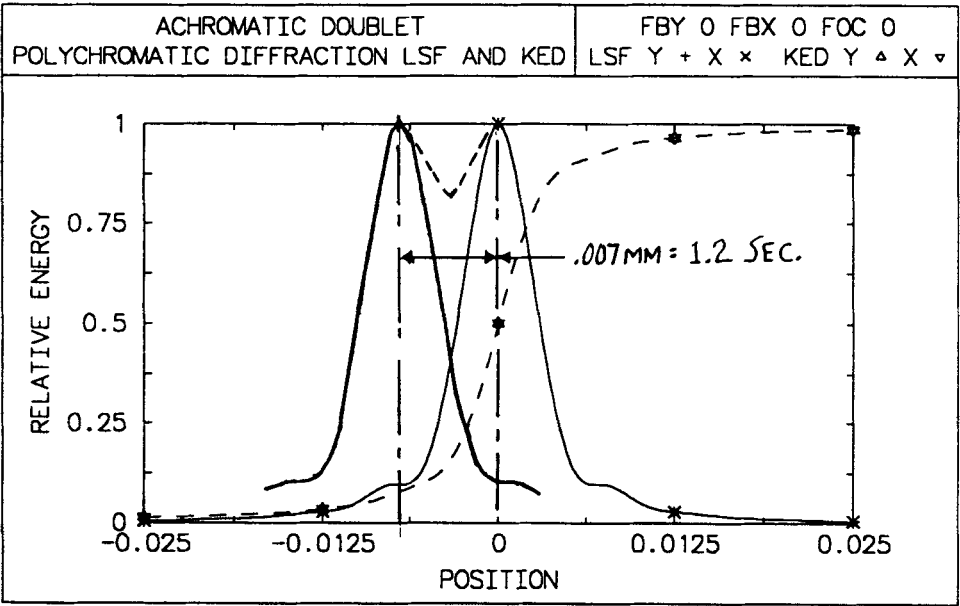


Figure 7.5 Polychromatic line spread analysis shows that the objective lens design will permit the viewer to visually resolve two point source objects imaged with a separation of just 7 microns. This separation is representative of a 1.2-second angle in object space.

While the amateur astronomer will generally be using the telescope for visual observation, a 35-mm camera body may be introduced to record the image formed by the objective lens. In this case, the image (film) surface will be flat, and the image format will be 24 × 36 mm. The air-spaced achromatic objective has been evaluated to determine its

suitability in a photographic application. While the design was done assuming a 23.5-mm-diameter curved image surface, the photographic application has been simulated assuming a 36-mm-diameter, flat-image surface. The resulting MTF data (Fig. 7.6) indicates that, assuming the use of a typical ISO400 black and white film, resolution will be 72, 62, and 40 cycles per mm on film, for field points at the center, top/bottom, and edges of the image, respectively.

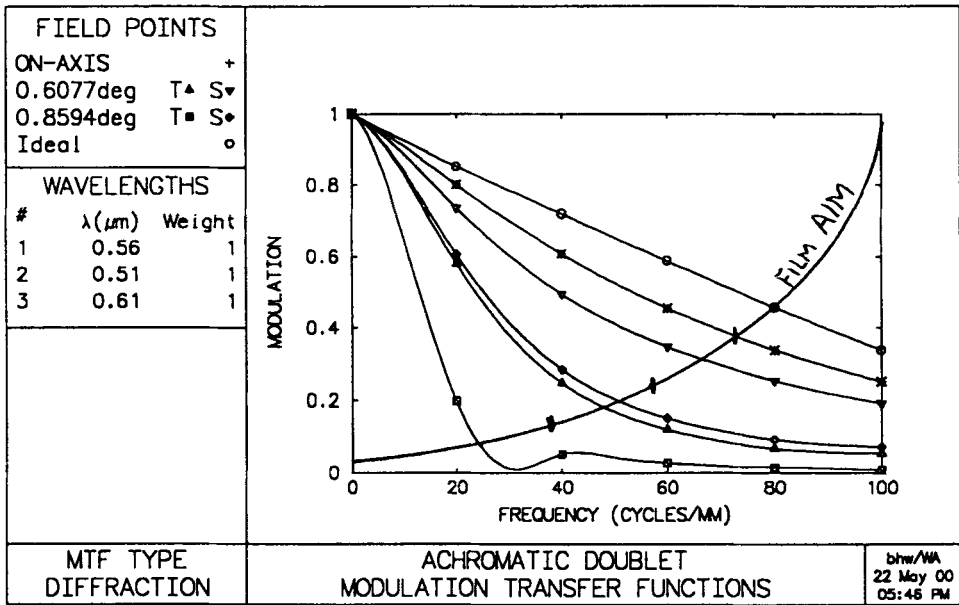


Figure 7.6 Diffraction MTF data for the objective lens illustrating potential performance as a photographic lens over a 35-mm film format. Extending the field of view to cover the film format results in increased astigmatism.

Next, moving on to visual performance of the telescope, the selection of an eyepiece for use with the objective lens is most important. Usually, a set of eyepieces will be used to permit changes in telescope magnification. This author does not advocate the use of a zoom eyepiece to permit magnification change without changing of the eyepiece. While zoom lenses have certainly proven their worth in numerous applications, eyepiece design has not been one of them. A typical set of interchangeable eyepieces would be the RKE eyepieces found in the Edmund Scientific catalog. As we found in Chapter 5, the RKE form is a very good design, well suited for an application such as this, and well within the budget of the serious amateur astronomer. There are five

eyepieces available in this set, with focal lengths of 8, 12, 15, 21, and 28 mm. All of these are designed to cover a field of view of about 44 deg.

Figure 7.7 shows the MTF data for the objective lens, along with AIM curves for each eyepiece combined with the typical eye. These AIM curves take into account the fact that the maximum resolution of the eye will vary as the pupil diameter changes. From the table of optical characteristics (Table 7.1) it is seen that the exit pupil diameter will range from 2.8 mm with the 28 mm eyepiece, down to 0.8 mm with the 8 mm eyepiece. This variation in pupil diameter will cause the resolution of the eye (viewing a target at 254 mm) to range from 7 cycles/mm, down to 4.5 cycles/mm. These values have been combined with the magnification factors of each eyepiece to generate the AIM curves shown in Fig. 7.7. From that figure it is found that the maximum resolution observed by the viewer, at the objective lens image, will range from 63 cycles/mm with the 28-mm eyepiece, to 112 cycles/mm with the 8-mm eyepiece. These resolution values correspond to angular resolutions in object space of 2.7 arc seconds per cycle with the 28-mm eyepiece, down to 1.5 arc seconds per cycle with the 8-mm eyepiece. Other factors that are important to comfortable and effective viewing, such as field of view and eye relief, are presented in Table 7.1.

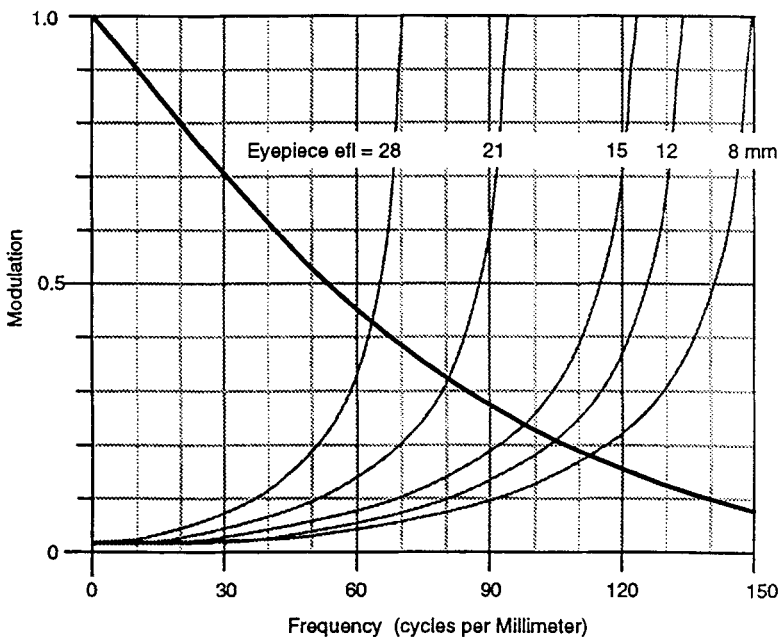


Figure 7.7 On-axis MTF data for the 1200-mm f/10 telescope objective combined with AIM curves of the model eye, viewing the image using eyepieces from the RKE eyepiece family.

**Table 7.1 Table of astronomical telescope optical characteristics assuming use of the custom-designed 1200-mm f/10 objective lens in conjunction with the family of RKE eyepieces.**

Objective Lens = 1200 mm, f/10 Air-Spaced Achromat (  $\lambda/4$  OPD)

Eyepiece = Edmund Scientific RKE Series (efl = 8, 12, 15, 21, and 28 mm)

Eyepiece efl / Image dia.	Telescope Magnification	Exit Pupil Dia.	Eye Relief	Eye + EP Res.	Eye + EP + Obj. Res.	Ang. Res. (Seconds)	Field of View (True / Apparent)
8.0 / 6.6 mm	150x	0.8 mm	6.5 mm	140 ~ /mm	106 ~ /mm	1.6	.32 / 44 degrees
12.0 / 9.7 mm	100x	1.2 mm	10.0 mm	120 ~ /mm	96 ~ /mm	1.8	.46 / 44 degrees
15.0 / 11.9 mm	80x	1.5 mm	12.0 mm	100 ~ /mm	83 ~ /mm	2.1	.57 / 44 degrees
21.0 / 17.3 mm	57x	2.1 mm	17.0 mm	85 ~ /mm	74 ~ /mm	2.3	.83 / 44 degrees
28.0 / 23.3 mm	43x	2.8 mm	23.0 mm	67 ~ /mm	58 ~ /mm	3.0	1.11 / 44 degrees



The apparent field-of-view values shown can be related to the 0.5-deg angle of the full moon to assist in visualizing the effect at each magnification. From all the data presented it might be concluded that two eyepieces, with efls of 12 and 21 mm, would serve well as a starting point, while others might be added later depending on most frequent applications.

## 7.4 The Terrestrial Telescope

The terrestrial telescope is used for viewing objects at distances up to several miles, in common applications, such as sports, boating, and bird watching. This exercise will be geared toward the design of a telescope for such an application. General characteristics of one such telescope might include: reasonable size, moderate magnification, generous field of view, large exit pupil, an erect image, and close focus capability. This design will assume the following specifications:

Magnification: 12×

Entrance Pupil Dia.: 60 mm

Exit Pupil Dia.: 5 mm

Field of View: 4 Deg (True)

48 Deg (Apparent)

Image Orientation: Erect, using a Dual Porro Prism Assembly

The final telescope configuration will evolve from the selection of an eyepiece. In order to cover the 48-deg apparent field, a complex eyepiece design, such as the Erfle type (Fig. 5.8), will be required. The  $f/7$  speed of the eyepiece and the 5-mm pupil requirement lead to an eyepiece focal length of 35 mm. Because the telescope magnification is found by dividing the objective lens efl by the eyepiece efl, it follows that the objective efl will be  $35 \times 12 = 420$  mm. The aperture of the objective will be equal to the 5-mm exit pupil diameter multiplied by the 12× magnification, or 60-mm diameter. The speed of the objective will then be  $420/60 = f/7$ , not surprisingly equal to the value assumed for the eyepiece speed earlier. The intermediate image diameter is derived from knowing the objective lens efl and the true field of view

$$\begin{aligned}\text{Image/Field Stop Diameter} &= 2 (420 \text{ mm} \times \tan 2 \text{ deg}) \\ &= 29.3\text{-mm diameter}\end{aligned}$$

The objective lens design was initiated by scaling the 1200-mm telescope objective designed earlier to a focal length of 420 mm, making the speed  $f/7$ , and the half-field angle 2.0 deg. When optimized, this lens

was found to be afflicted with unacceptable levels of astigmatism and field curvature. The glass block simulating the erecting porro prisms was then added to the design and, at the same time, a doublet field corrector was added between that glass block and the final image plane to deal with off-axis aberrations. This lens was then optimized, resulting in the final form shown in Fig. 7.8.

## 7.5 Resolution Goals and Limits

Aberration curves and MTF data shown in Fig. 7.9 indicate that this objective lens is very well corrected and quite suitable for the application being considered. The AIM curve shown is for the typical eye (with a 5-mm pupil diameter) and a 35-mm eyepiece. The resulting on-axis visual resolution at the objective image plane will be 45 cycles/mm.

The Erfle eyepiece from Chapter 5 was scaled to a 35-mm efl and added to the objective lens to make up the final 12× telescope. Figure 7.10 shows the layout of that telescope with the folding Porro prisms and the Erfle eyepiece. Paraxial constants and tabulated lens data are also shown. Ray trace analysis and MTF data for the 12× telescope were then calculated with the results shown in Fig. 7.11. Note that for this case the evaluation is done in the afocal mode, resulting in angular rather than linear outputs. The final design is afflicted with about 2 diopters of astigmatism. The AIM curve shown is based on a maximum visual angular resolution of 1650 cycles/radian, the approximate limit of the eye with a 5-mm pupil and a 35-mm efl eyepiece. On-axis performance introduces a negligible (2%) degradation relative to ideal diffraction limited performance. Resolution over the central 50% (2 deg) of the field will be greater than 1000 cycles/radian. This falls to 550 and 300 cycles/radian for 3- and 4-deg field points, respectively. This image degradation is due to residual astigmatism and off-axis color in the eyepiece.

From a mechanical perspective, the final telescope will occupy a package that is about 4 inches in diameter by 15 inches long. Total weight of the telescope is estimated at less than 4 pounds. A tripod mount will be provided at the center of gravity to assure steady viewing, although, at 12× magnification, careful *hand held* viewing should be possible. The eyepiece mechanics will provide for rapid focus travel from -10 to +30 mm relative to the infinity setting. In addition to generous diopter adjustment, this will permit the telescope to be focused on objects as near as 25 feet.

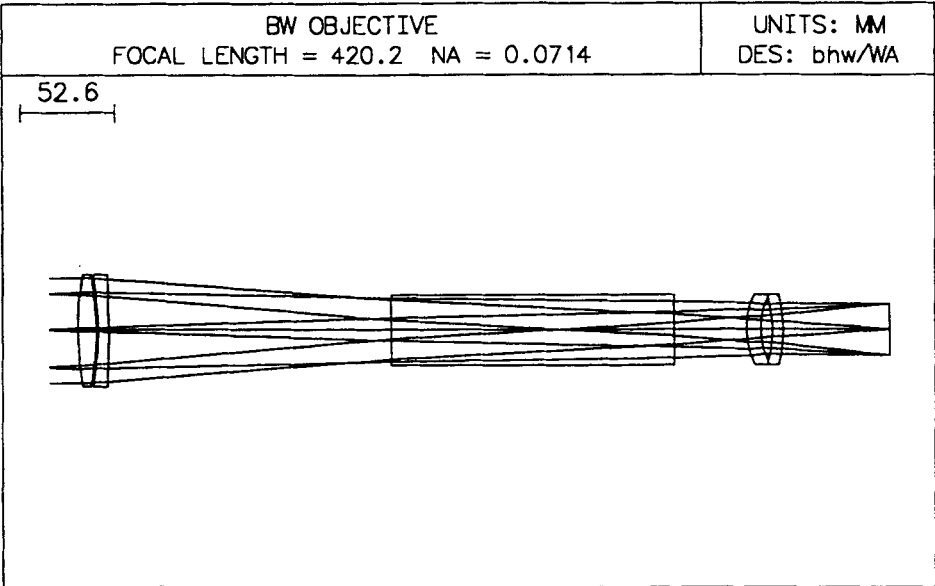
It will be noted that the optical system shown in Fig. 7.10 is similar to one half of a pair of high-quality binoculars. In the design of such a binocular system the optical design for each half would obviously be

nominally identical. The challenge in such a design shifts to the mechanical designer. Generally, a center focus mechanism would be provided to adjust focus in both halves simultaneously. In addition, an individual eyepiece adjustment would be required to accommodate any focus difference between the viewer's right and left eyes. The separation between the two exit pupils would need to be adjustable over a range from 52 to 72 mm. The exiting optical axes of the two telescopes would need to be parallel within less than 5 arc minutes and relative image rotation held to less than 0.5 deg. Any difference in magnification between the two halves would be bothersome, thus a limit of less than 0.5% should be held. Finally, the level of illuminance should not vary by more than 25% and the spectral content of the transmitted light should be the same for both halves. All of these specifications have been culled from general reference material. Any actual design should carefully consider the ultimate application and the nature of the viewers that will be involved.

## 7.6 Review and Summary

This chapter has covered the basic considerations and procedures involved in the design of two quite different telescopes for visual applications. The first is an astronomical telescope, intended for use in serious amateur astronomy applications. The second is a smaller, less powerful telescope, intended for terrestrial viewing in such applications as sports, boating, and bird watching. Both designs required the design of a custom objective lens, tailored for the specific application. Eyepieces were then added to the objective lens designs to make up the complete telescope. In the case of the astronomical telescope it was assumed that a set of commercially available eyepieces would be used. For the terrestrial telescope, an appropriate eyepiece was selected from those designs described in Chapter 5 and its efl was scaled to the established requirement.

In both cases the final image quality was evaluated relative to the maximum resolution capability of the typical eye. The on-axis resolution for both telescopes was found to be eye limited, within a few percent of the theoretical diffraction limit. While both objective lenses maintained this high level of image quality over most of the field, the eyepiece in both cases introduced off-axis aberrations that substantially decreased performance. All of the results presented here take into account the impact of the eye's pupil diameter on final visual performance. As was shown in Fig. 2.3, when the pupil diameter is less than 2 mm or greater than 4 mm, degradation of the eye's image quality must be factored into any related performance predictions.



**\*PARAXIAL CONSTANTS**

Effective focal length:	420.18404	Lateral magnification:	-4.0018e-18
Numerical aperture:	0.07140	Gaussian image height:	14.67315
Working F-number:	7.00307	Petzval radius:	-9350.05342

**\*LENS DATA**

BW OBJECTIVE				GLASS	SPE	NOTE
SRF	RADIUS	THICKNESS	APERTURE RADIUS			
OBJ	--	1.0500e+20	3.6667e+18	AIR		
AST	--	25.00000	30.00000	ASK	AIR	
2	198.16000 V	10.00000	32.00000	BK7	C	
3	-176.28000 V	1.00000	32.00000	AIR		Objective
4	-175.18000 V	6.00000	30.00000	K	F2	C Doublet
5	-1148.40000 V	160.00000	32.00000	AIR		
6	--	160.00000	20.00000	BK7	C	Porro
7	--	40.00000	20.00000	AIR		Prisms
8	46.74000 V	8.00000	20.00000	BK7	C	
9	44.25000 V	6.44000	18.00000	AIR		Field Lens
10	-63.30000 V	6.00000	18.00000	K	F2	C
11	-80.31000 V	60.02000	20.00000	AIR		
IMS	--	--	14.70000			* Image

Figure 7.8 Lens layout and lens data on a 420-mm f/7 objective lens designed for use in a 12× terrestrial telescope application.

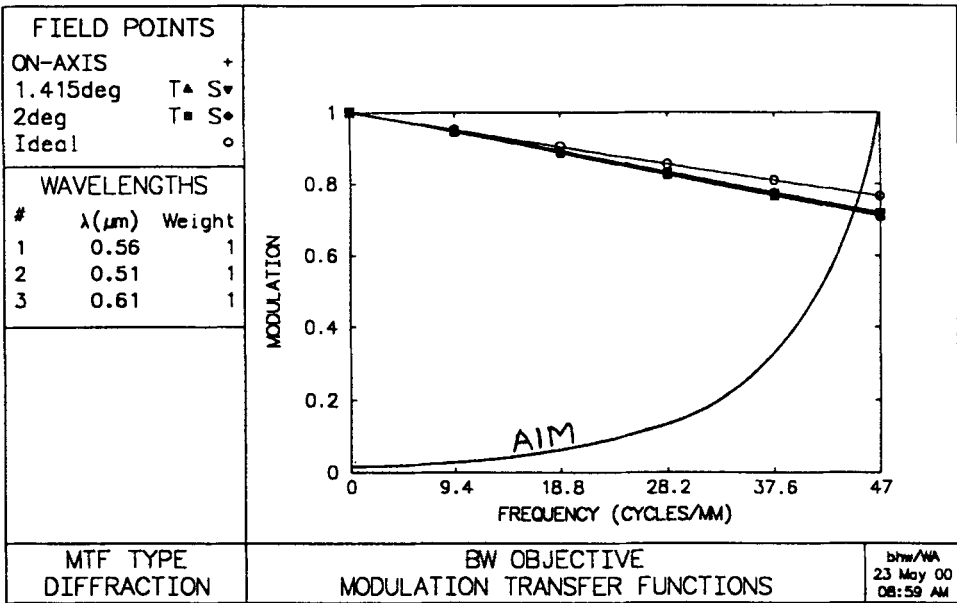
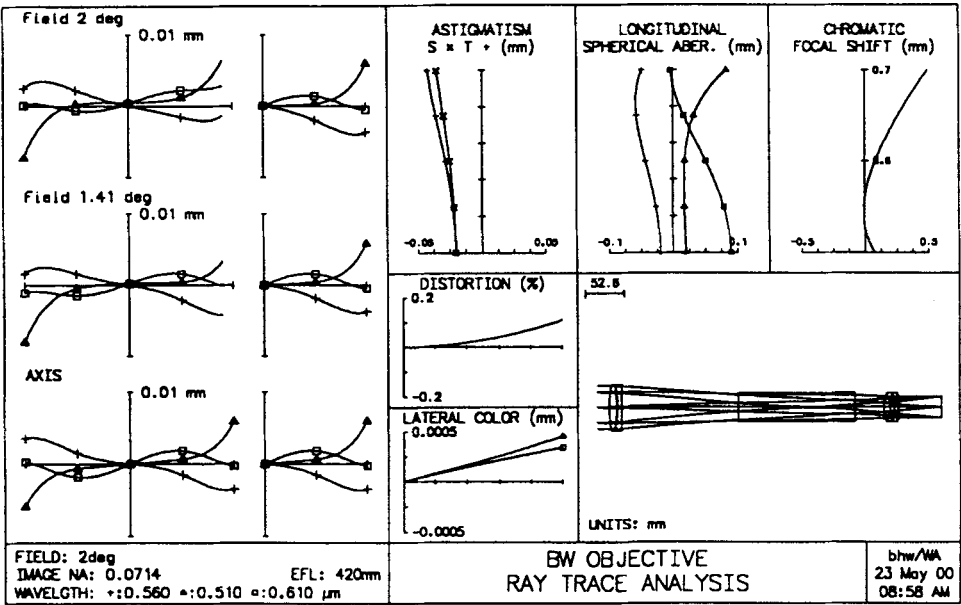
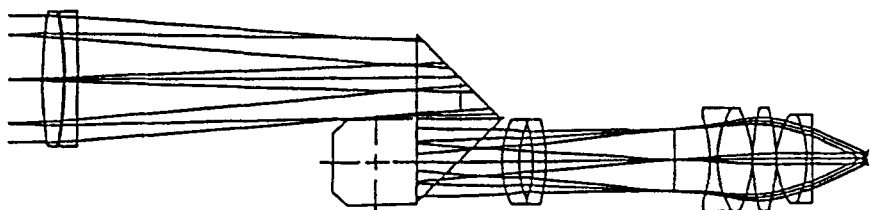


Figure 7.9 Ray trace analysis (aberration curves) and diffraction MTF data for the 420-mm f/7 objective lens designed for use in a 12× terrestrial telescope application.



**\*PARAXIAL CONSTANTS**  
Angular magnification:      -11.98412      Lagrange invariant:      -1.04762  
Eye relief:                    28.0000      Petzval radius:           -60.34795

**\*LENS DATA**  
**BW TELESCOPE**

SRF	RADIUS	THICKNESS	APERTURE RADIUS	GLASS	SPE	NOTE
OBJ	--	1.0500e+20	3.6667e+18	AIR		
AST	198.16000	10.00000	32.00000 A	BK7 C		Objective
2	-176.28000	1.00000	32.00000	AIR		-Lens-
3	-175.18000	6.00000	30.00000 K	F2 C		
4	-1148.40000	160.00000	32.00000	AIR		
5	--	160.00000	20.00000	BK7 C		Porro
6	--	40.00000	20.00000	AIR		Prisms
7	46.74000	8.00000	20.00000	BK7 C		Field
8	44.25000	6.44000	18.00000	AIR		-Lens-
9	-63.30000	6.00000	18.00000 K	F2 C		
10	-80.30000	60.00000	20.00000	AIR		
11	--	16.70000	14.67280 S	AIR	*	Image
12	-64.40000	3.50000	18.00000	SF2 C		
13	47.40000	16.00000	21.00000	SK4 C		Erfl
14	-54.43000	0.63000	21.00000	AIR		Eye
15	94.25000	10.50000	21.00000	SK10 C		
16	-94.25000	0.63000	21.00000	AIR		
17	39.60000	14.00000	21.00000	BK7 C		
18	-47.40000	2.80000	21.00000	F2 C		
19	--	28.00000	21.00000	AIR		
20	--	--	2.50000	AIR	*	Exit Pupil
IMS	--	--	3.41016 S			

Figure 7.10 Lens layout and lens data for the complete 12x terrestrial telescope design. Layout includes the erecting porro prism assembly and the 35-mm focal length Erfl eyepiece.

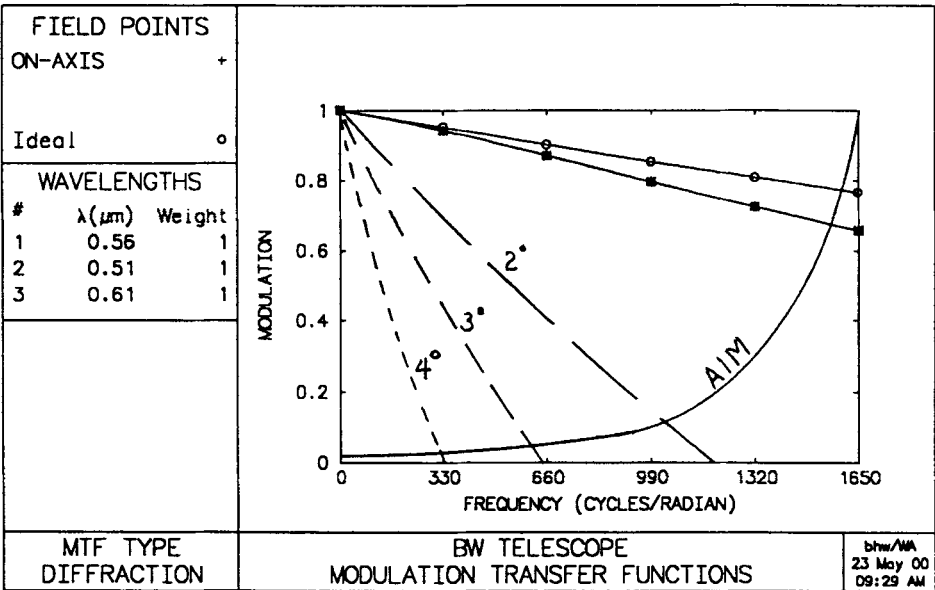
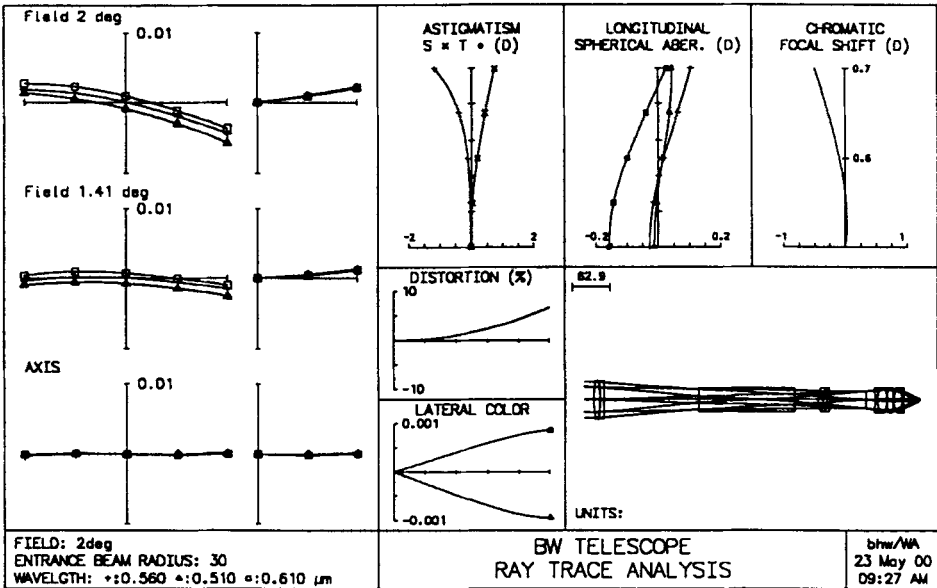


Figure 7.11 Ray trace analysis (aberration curves) and diffraction MTF data for the complete 12× terrestrial telescope. Decreased off-axis performance is due to residual astigmatism of the Erfle eyepiece.

## 8

## The Borescope—Design

---

### 8.1 Introduction

The term *borescope* is frequently applied to a family of optical instruments, designed for a variety of applications. The term no doubt originates from those instruments that were intended for the inspection of the bore of a firearm. Today that family of instruments is used for inspection of many otherwise inaccessible cavities within a variety of mechanical assemblies. A separate branch of the borescope industry has evolved relating to various fields of medicine. In these cases, the medical instrument is used to visually observe and diagnose certain conditions, permitting observation inside the human body by the medical team so that these conditions can be repaired.

In a most general sense, the borescope is a low-magnification optical instrument, typically quite small in diameter ( $<20$  mm), and relatively large in terms of its overall length, often 50 to 100 times its diameter. The optical design of a borescope will be driven by these dimensional limitations, by the precision requirements of the optical components, and by the high level of image quality that is usually required.

### 8.2 General Optical Configuration

The borescope will traditionally consist of three major optical components. These are: the objective lens, the relay optics, and the eyepiece. The objective lens configuration will be dictated by final instrument specifications such as: field of view, lens speed ( $f/\text{number}$ ), distortion, and image quality. The relay optics configuration will be driven by allowable lens diameter, required instrument length, allowable vignetting, and image quality. The eyepiece selection will usually be based on required overall magnification, apparent field of view, and eye relief. Figure 8.1 shows a thin lens layout of a typical borescope optical system. The remaining sections of this chapter will deal with details of the design procedures involved in generating a final optical system that is consistent with the parameters shown in this thin lens layout.



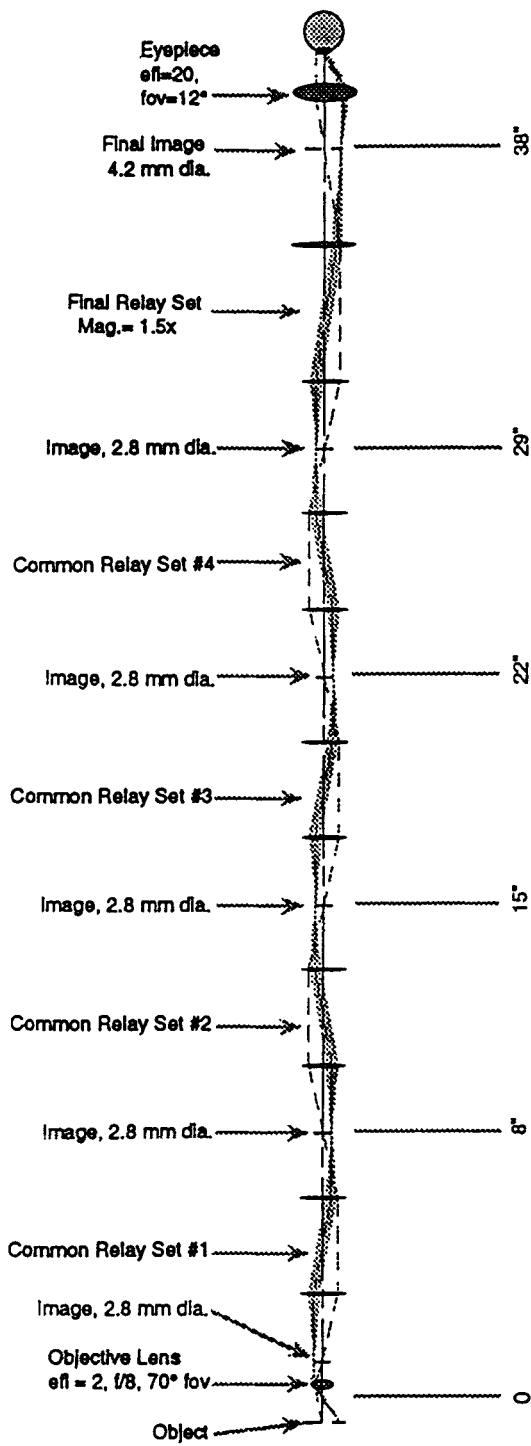


Figure 8.1 Thin lens layout of the borescope to be designed. Maximum lens diameter is 6 mm, total length is 965 mm (38 inches), field of view is 70 deg, on-axis image quality to be eye limited.

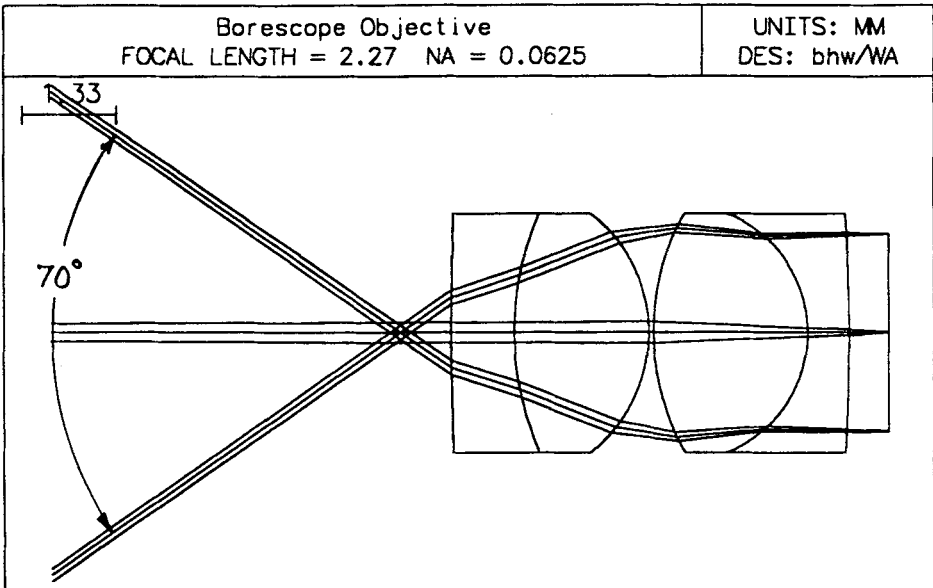
### 8.3 Objective Lens Design

From Fig. 8.1 it will be seen that the objective lens is required to image a 70-deg field of view, forming an image that is 2.8 mm in diameter. The lens is to have an aperture of  $f/8$  and up to 60% vignetting will be allowed. The design of a borescope system will be greatly simplified if it is possible to make all of the optics telecentric in their image space. This means that, for the off-axis image light bundles, the central (chief) ray will be parallel to the optical centerline. If this telecentric condition is maintained, it will not be necessary to insert field lenses at or near the intermediate images. Field lenses introduce two major problems to a design of this type. First, their basic positive lens power will add significantly to the field curvature of the final design. Second, when optical elements are located in close proximity to an image plane, their cleanliness becomes a very serious issue. This not only impacts the initial cost of the optics (very tight scratch-dig specs), but also creates some major maintenance issues. For these reasons the objective lens will be designed to produce this telecentric condition. By nature of their typical function, borescope systems will generally be used to view near objects. In this case we will assume a potential range of object distances from 20 to 150 mm. If the design is generated assuming an object distance of 50 mm, the final design should work well over this range.

The telecentric requirement leads to the entrance pupil of the objective lens being located in object space. This characteristic is similar to that of an eyepiece. For that reason a starting lens form was selected that is similar to the Symmetrical eyepiece described in Chapter 5, Fig. 5.7. This lens was scaled to a focal length of 2.3 mm, the object distance was set to 50 mm, the field of view to 70 deg, and the lens aperture to  $f/8$ . The design was optimized using the default error function in OSLO, modified to make the final design fit established specifications. The resulting objective lens design is shown in Fig. 8.2, which also contains paraxial constants and lens data information. Figure 8.3 contains ray trace analysis and MTF data for the new objective lens.

From the thin lens system data in Fig. 8.1, it is possible to derive the efl of the optics that will be used to view the image formed by the objective lens. That efl is the eyepiece efl (20 mm) divided by the relay magnification ( $1.5\times$ ), or 13.33 mm. The exit pupil diameter for these optics (relays plus eyepiece) will be

$$\text{Exit Pupil Dia.} = \text{efl} / f/\# = 13.33 / 8 = 1.67 \text{ mm.}$$



**\*PARAXIAL CONSTANTS**

Effective focal length:	2.27021	Lateral magnification:	-0.04538
Numerical aperture:	0.06250	Gaussian image height:	1.55947
Working F-number:	8.00000	Petzval radius:	-3.60303

**\*LENS DATA**

**70 Degree Borescope Objective**

SRF	RADIUS	THICKNESS	APERTURE RADIUS	GLASS	SPE	NOTE
OBJ	--	50.00000	34.36405	AIR		
AST	--	0.72000	0.14182 ASK	AIR		
2	54.68000	0.90000	1.70000	SFL6 C		
3	4.26000	1.92000	1.70000 P	LAKN6 C		
4	-2.15000	0.07000	1.70000 PK	AIR		
5	3.49000	2.20000	1.70000 PK	LAKN6 C		
6	-1.83000	0.60000	1.70000 P	SFL6 C		
7	-24.30000	0.56000	1.70000 P	AIR		
IMS	--	--	1.40312		*	

**Figure 8.2** Lens layout and data on the optimized 70-deg f/8 borescope objective lens.

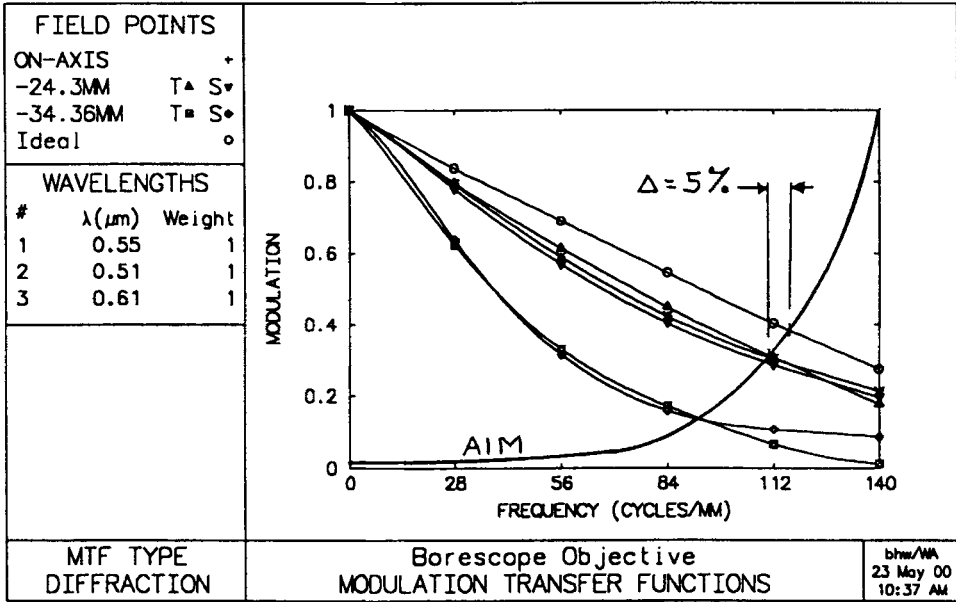
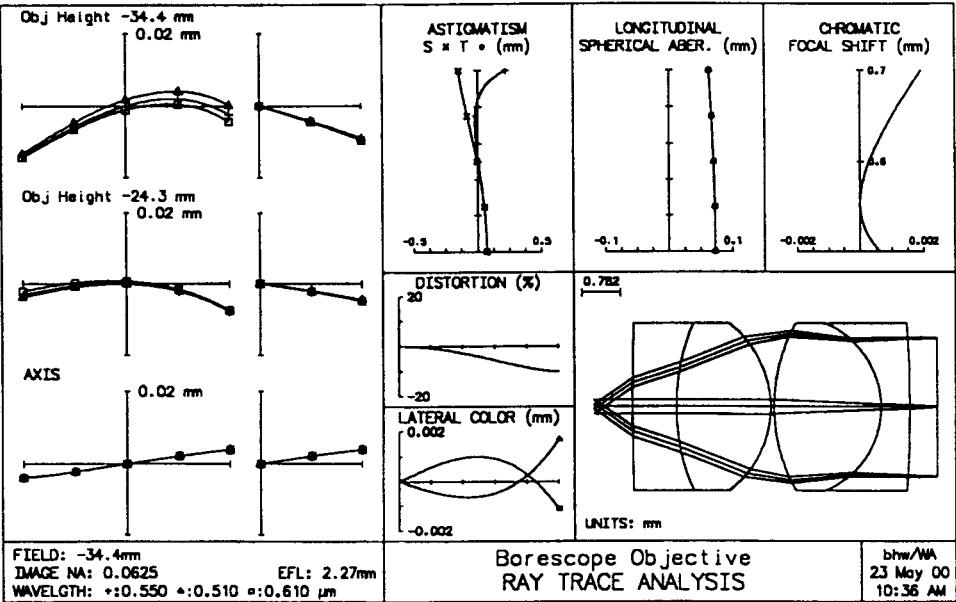


Figure 8.3 Ray trace analysis (aberration curves) and MTF data on the optimized 70-deg f/8 borescope objective lens. AIM curve shown is for the model eye with perfect viewing optics including relay optics and eyepiece.

It is now possible to calculate the approximate limit of visual resolution at the objective lens image. Data shown in Fig. 2.3 indicates that the resolution limit of the typical eye with a pupil diameter of 1.67 mm will be about 7.5 cycles/mm. The magnification of the viewing optics will be

$$\text{Magnification} = 254 / \text{efl} = 254 / 13.33 = 19\times.$$

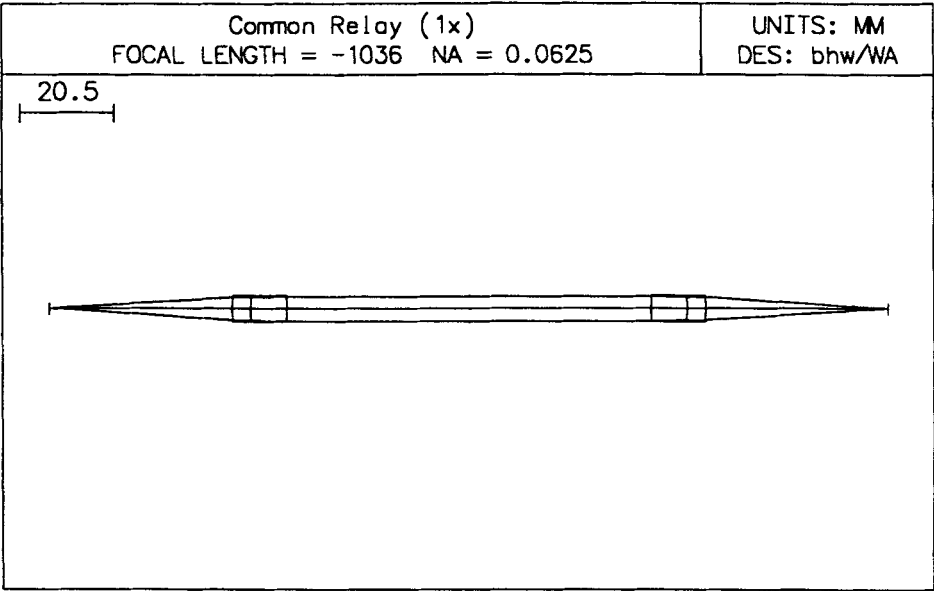
Thus, the resolution limit of the eye plus optics, viewing the image formed by the objective lens, will be  $7.5 \times 19 = 142$  cycles/mm. This is the upper limit of the AIM curve that has been added to the MTF curves in Fig. 8.3. The result indicates that the resolution over the central 70% of the field will be within 5% of the diffraction limit. Review of the data shown in Fig. 8.3 confirms that this new objective lens design represents a very well-balanced solution that will deliver a high level of overall image quality.

## 8.4 Common Relay Lens Design

The common relay set will consist of two identical, cemented,  $f/8$  achromatic doublets. The clear aperture diameter of these lenses will be 5.5 mm (6-mm lens diameter), the object and image diameters will be 2.8 mm, the design will be afocal, and 60% vignetting will be allowed. The design will be precisely symmetrical about a central aperture stop. Based on the clear aperture and  $f$ /number, the starting efl of the doublets was set to 44 mm. The doublet thickness was made equal to about  $2\times$  its diameter. This unusual ratio is helpful in the manufacture and assembly of these relatively small lenses. The object and image distance was set to 40 mm, while the space between lenses was set to 80 mm.

This starting relay lens form was then manipulated and optimized to produce the final design shown in Fig. 8.4. The three lens curvatures were used as variables, with the second lens kept identical to the first through the use of surface curvature pickups. During optimization, spherical aberration and axial color were the aberrations most closely controlled. The symmetry of the relay lens results in coma, lateral color, and distortion being zero by default. Astigmatism in the final design was balanced about a flat image plane, as is seen in the ray trace analysis in Fig. 8.5. From the MTF data presented there it can be seen that the on-axis image quality is diffraction limited, while residual astigmatism drops the resolution by an average of 8% at the 0.7- and full-field points.

A key factor in this design is that the common relay set will be used four times in the final design. Thus, it must be remembered that any residual aberrations permitted to exist in this relay design will be



**\*PARAXIAL CONSTANTS**

Effective focal length:	-1035.67513	Lateral magnification:	-1.00000
Numerical aperture:	0.06250	Gaussian image height:	1.40000
Working F-number:	8.00000	Petzval radius:	-29.45579

**\*LENS DATA**

Common Relay (1x)							
SRF	RADIUS	THICKNESS	APERTURE	RADIUS	GLASS	SPE	NOTE
OBJ	--	40.07000 V	1.40000		AIR	•	Object
1	33.83000 V	4.00000	2.75000 K		SF5 C		
2	13.96000 V	8.00000	3.00000		BAK2 C		Relay
3	-40.00000	40.00000	2.75000 K		AIR		
AST	--	40.00000	2.72855 AS		AIR		ASTOP
5	40.00000 P	8.00000 P	2.75000 K		BAK2 C		
6	-13.96000 P	4.00000 P	3.00000		SF5 C		Relay
7	-33.83000 P	40.07000 P	2.75000 K		AIR		
IMS	-- P	--	1.40028 S			*	Image

Figure 8.4 Lens layout and data on the optimized unity magnification *common* borescope relay lens.

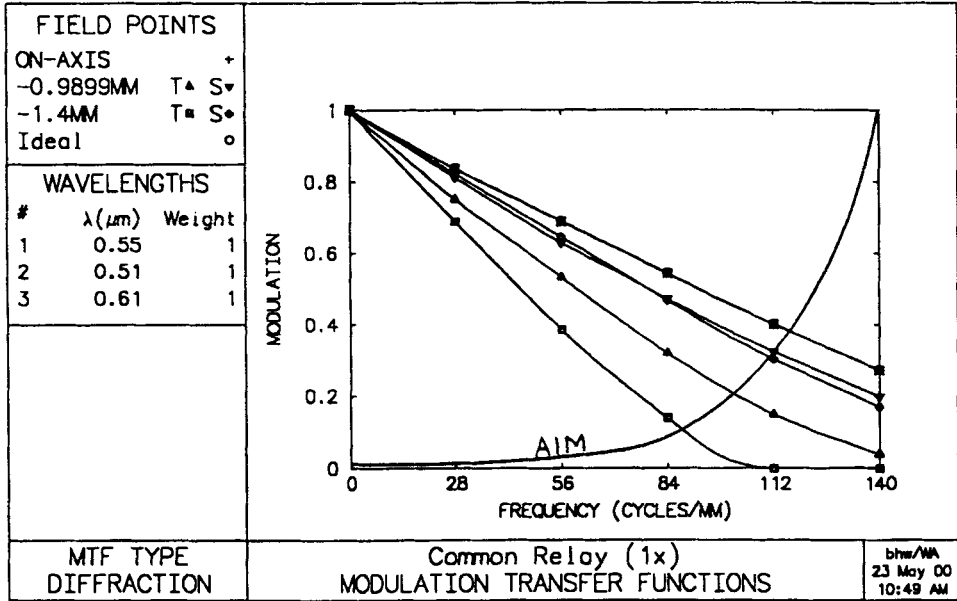
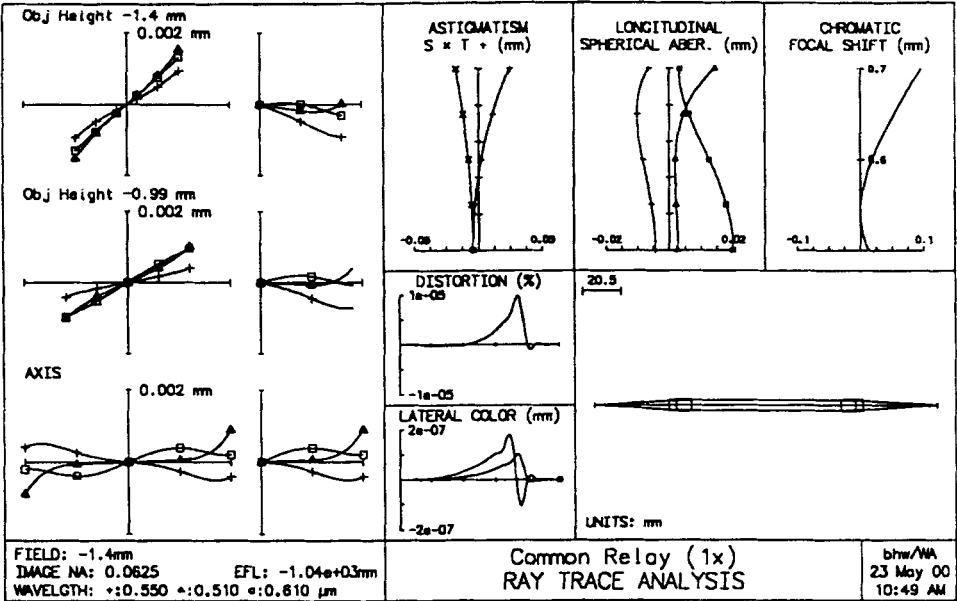


Figure 8.5 Ray trace analysis (aberration curves) and MTF data on the optimized unity magnification *common relay* lens. AIM curve shown is for the model eye with *perfect* viewing optics.

multiplied by a factor of  $4\times$  in the final instrument. The resulting effect is demonstrated in the ray trace analysis and MTF data presented in Fig. 8.6. Here, the objective lens design has been mated to four of the common relay lens sets. Note from the aberration curves that spherical aberration and on-axis color are still well corrected. This is confirmed by the on-axis MTF curve, which clearly indicates diffraction-limited performance, while the residual off-axis aberrations of the objective and relays (primarily astigmatism) cause the resolution to fall to 87% and 69% of the diffraction limit for the 0.7 and 1.0 field points, respectively.

## 8.5 Final Relay Lens Design

The next step in the design process involves adding the final relay set, which introduces a magnification factor of  $1.5\times$ . This was accomplished by taking the  $1\times$  relay set just designed and scaling the second half of the design by a factor of  $1.5\times$ . This configuration was then fine-tuned and optimized for best image quality. Figure 8.7 describes the objective lens, the  $1\times$  relays, and the final  $1.5\times$  relay set. Figure 8.8 contains ray trace analysis and MTF data for this combination of optics. Again, the on-axis MTF is diffraction limited, with the off-axis values falling to 87% and 69% of the diffraction limit at the 0.7 and 1.0 field points, respectively. Note that the maximum frequency for these MTF and AIM curves has been reduced to 95 cycles/mm due to the increased ( $1.5\times$ ) magnification of the final relay lens set.

## 8.6 Eyepiece Selection

In the final step of the borescope design an eyepiece is selected and added for final analysis. From Fig. 8.1 it is seen that a 20-mm efl eyepiece with a 12-deg apparent field of view will be required. An Orthoscopic eyepiece was selected from Chapter 5, and scaled to the desired efl. It was then added to the system in Fig. 8.7, which contains the objective lens, four common ( $1\times$ ) relay sets, and the final magnifying ( $1.5\times$ ) relay set. Eyepiece focus was set such that the final image is formed at infinity. This dictates that the analysis of this system be performed in the *afocal* mode. In the afocal mode the final aberrations are presented as angular rather than linear values. The astigmatism curves are presented in diopters, and the MTF frequency data are presented in angular terms of cycles/radian, rather than cycles/mm (Fig. 8.9). The 1900 cycles/radian maximum value for the MTF and AIM curves is derived from the angular resolution limit of the typical eye. From Fig. 2.3 it is found that such an eye, with a pupil diameter of 1.67 mm, will resolve 7.5 cycles/mm when the target is at the



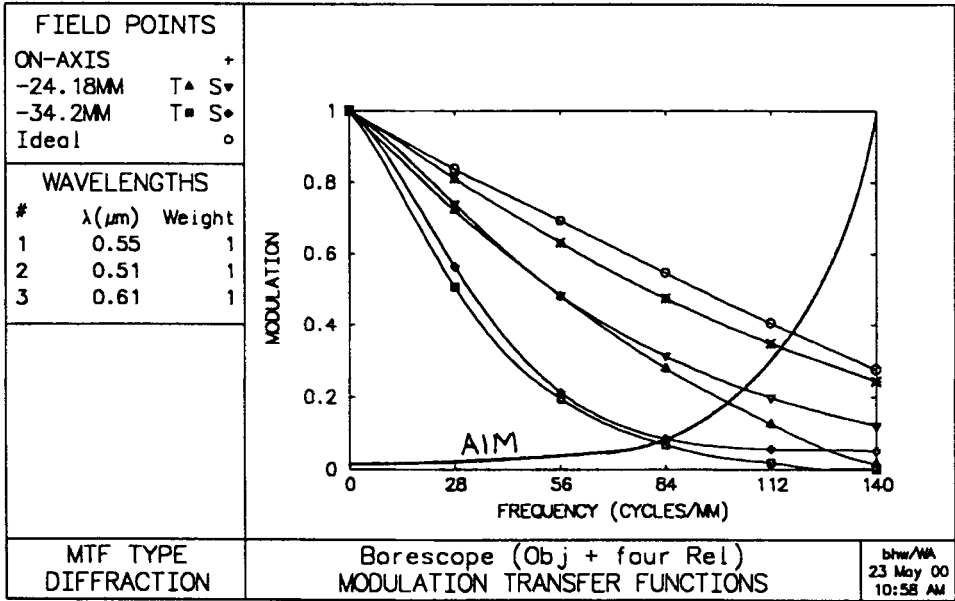
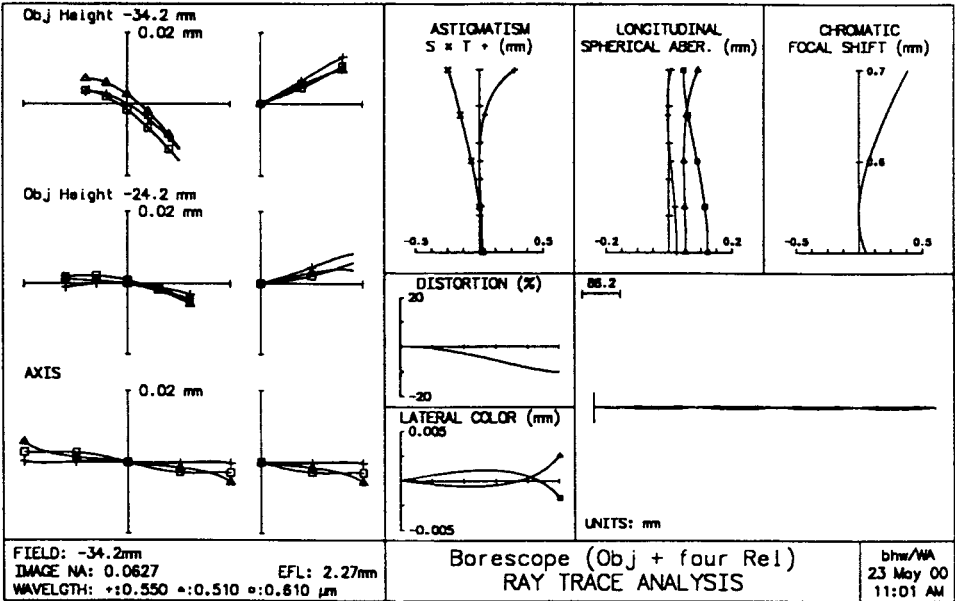
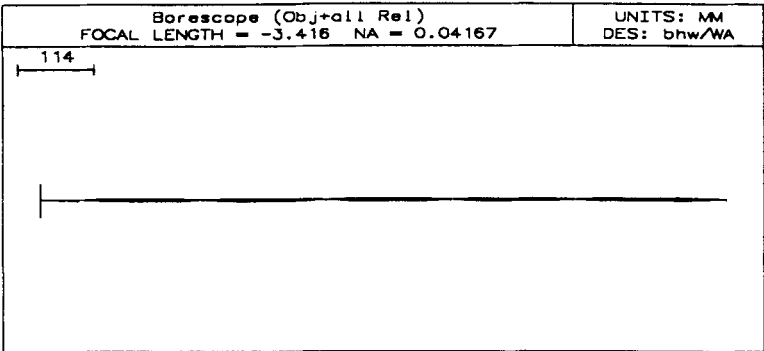


Figure 8.6 Ray trace analysis (aberration curves) and MTF data on the 70-deg f/8 borescope objective lens combined with four unity magnification relay lenses. AIM curve shown is for the model eye with *perfect* viewing optics.



**\*PARAXIAL CONSTANTS**  
Effective focal length: 3.41563 Lateral magnification: -0.06827  
Numerical aperture: 0.04166 Gaussian image height: 2.33484  
Working F-number: 12.00105 Petzval radius: -2.94371

**\*LENS DATA**  
**Borescope (Obj+all Rel)**

SRF	RADIUS	THICKNESS	APERTURE RADIUS	GLASS	SPE	NOTE
OBJ	--	50.00000	34.20000	AIR	*	Object
1	--	0.72000	0.16147 SK	AIR		
2	54.68000	0.90000	1.70000	SFL6	C	
3	4.26000	1.92000	1.70000 P	LAKN6	C	Objective
4	-2.15000	0.07000	1.70000 PK	AIR		
5	3.49000	2.20000	1.70000 PK	LAKN6	C	
6	-1.83000	0.60000	1.70000 P	SFL6	C	
7	-24.30000	0.59000	1.70000 P	AIR		
8	--	40.07000	1.40000	AIR	*	Image
9	33.83000	4.00000	2.80000 K	SF5	C	
10	13.96000	8.00000	3.00000	BAK2	C	
11	-40.00000	40.00000	2.80000 K	AIR		Common
AST	--	40.00000	2.74058 AS	AIR		Relay
13	40.00000 P	8.00000 P	2.80000 K	BAK2	C	
14	-13.96000 P	4.00000 P	3.00000	SF5	C	
15	-33.83000 P	40.07000 P	2.80000 K	AIR		
(Repeat 8 - 15 three more times)						
16	--	40.00000	1.40000	AIR	*	Image
17	33.83000	4.00000	2.80000 K	SF5	C	
18	13.96000	8.00000	3.00000	BAK2	C	
19	-40.00000	40.00000	2.80000 K	AIR		1.5x Mag.
20	--	60.00000	2.79863 S	AIR		Relay
21	50.43000	10.00000	4.00000 K	BAK2	C	
22	-22.55000	6.00000	4.00000	SF5	C	
23	-61.27000	60.00000	4.00000 K	AIR		
IMS	--	--	2.10000			* Image

Figure 8.7 Lens layout and data for the borescope objective, four unity magnification relays, and one final 1.5× magnification relay lens.

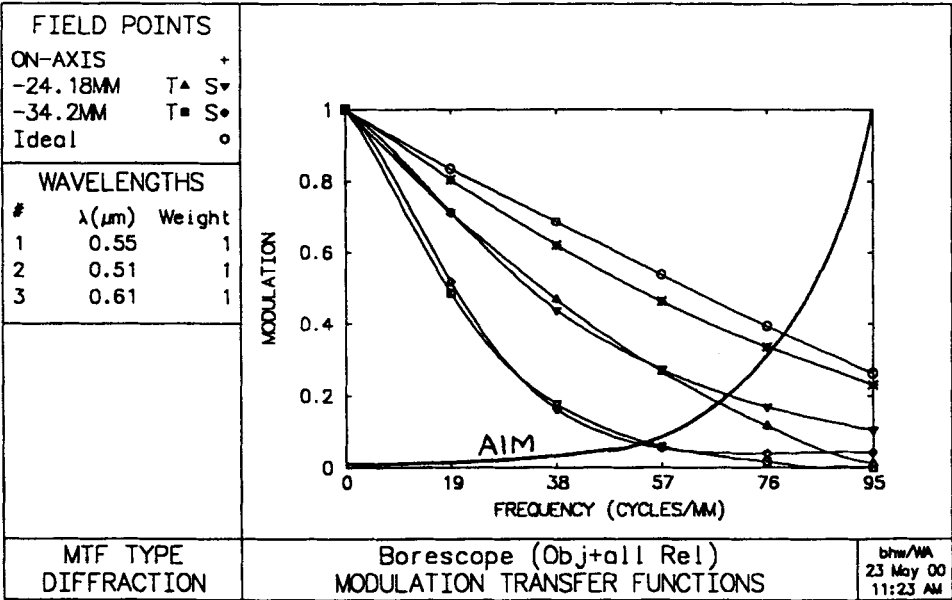
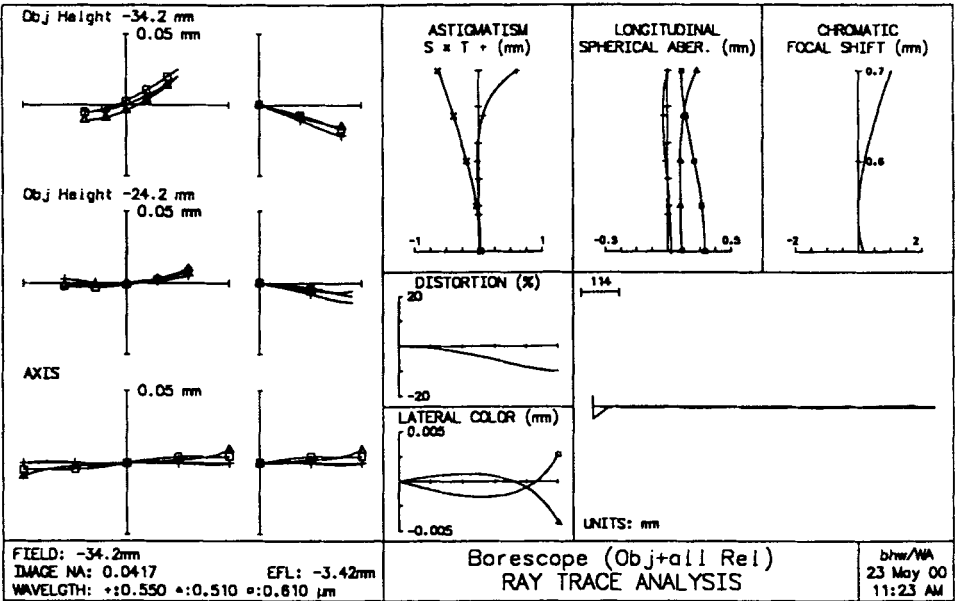


Figure 8.8 Ray trace analysis (aberration curves) and MTF data for the borescope objective, four unity magnification relays, and one final 1.5× magnification relay lens. AIM curve shown is for the model eye with a 1.7-mm pupil diameter and a 20-mm eyepiece.

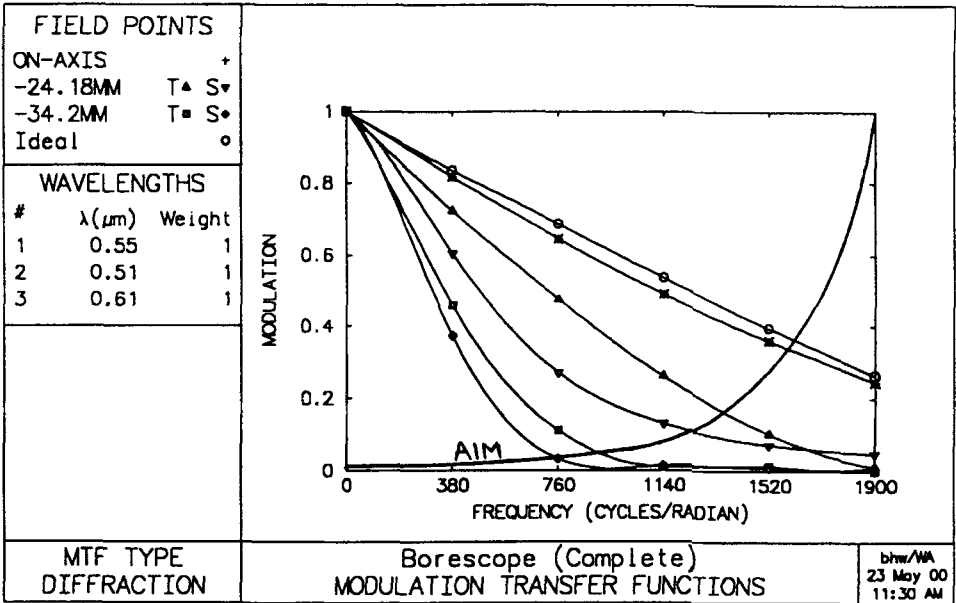
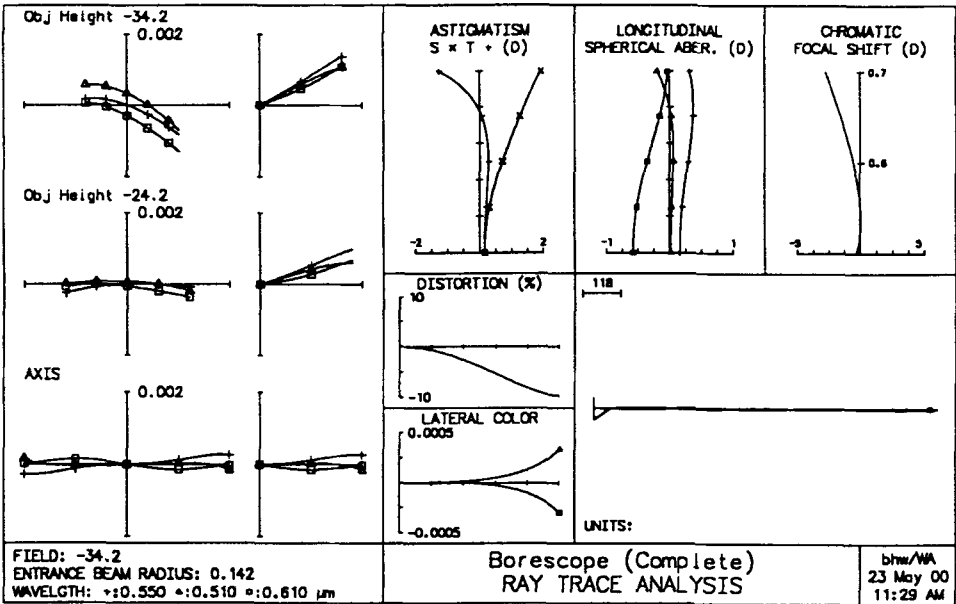


Figure 8.9 Ray trace analysis (aberration curves) and MTF data for the complete borescope assembly including eyepiece. Evaluation is done in afocal mode, which results in angular outputs. AIM curve shown is for the model eye with a 1.7-mm pupil diameter.

near point 254 mm from the eye. Under these conditions, each cycle on the target is  $1/7.5 = 0.1333$  mm in height. The angle subtended by this cycle will be  $0.1333/254 = .000525$  radians. Thus, the angular frequency for this target will be  $1/.000525 = 1905$  cycles/radian.

For the entire visual instrument, then, the MTF curves in Fig. 8.9 indicate that on-axis performance will be diffraction limited, while resolution will drop to 82% and 53% of the diffraction limit for 0.7 and 1.0 off-axis points, respectively. While difficult to quantify, it can be expected that the off-axis resolution will be somewhat better than predicted due to the eye's ability to accommodate for focus differences.

8.7 Magnification Evaluation

Unlike instruments presented in earlier chapters, the definition for magnification of the borescope is a bit more complicated and will often depend on the definition of magnification established by the designer and/or user. In this case, it has been assumed that the borescope is to be inserted into a piece of complex machinery, such as a jet engine, to allow inspection of internal components. Generally, there will be an access port through which the borescope is inserted for viewing. If we assume that the eye is placed at that port without the borescope, and that adequate illumination is available, the viewer will see the object to be viewed as indicated by the dashed lines in Fig. 8.10.

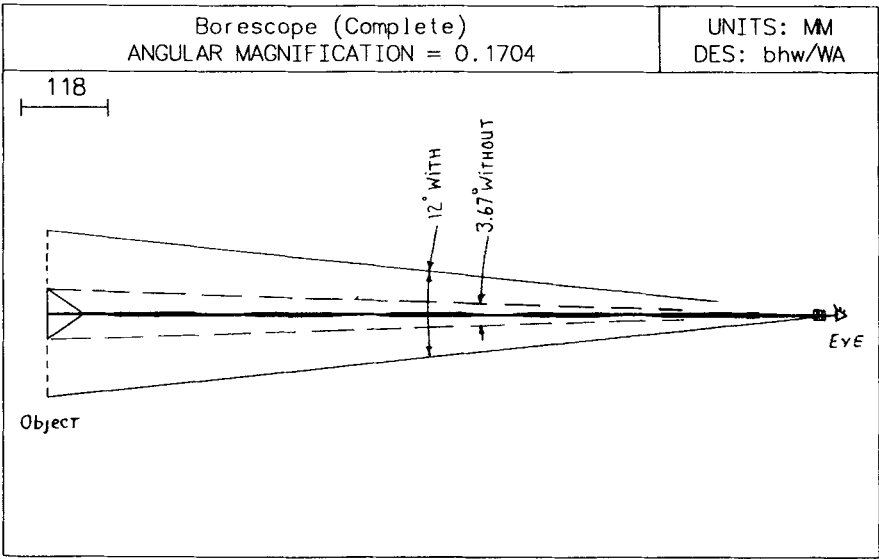


Figure 8.10 Layout of complete borescope assembly set such that the object and final image location coincide. This permits an evaluation of final magnification. In this case,  $\text{Mag.} = 12.0 / 3.67 = 3.3\times$ .

The object has a diameter of 68.4 mm and will be at a distance of 1065 mm from the eye, thus subtending an angle of 3.67 deg to the eye. Now, when the borescope is inserted into the viewing port, such that the entrance pupil of the objective lens is 50 mm from the object, and the viewer's eye is placed at the exit pupil of the borescope, then a 224-mm-diameter image of the 68.4-mm-diameter object will be seen, once again at a distance of 1065 mm from the eye. This image will subtend an angle of 12 deg (Fig. 8.10), representing a magnification factor of  $12 / 3.67 = 3.3\times$ . This magnification factor may be attributed to the borescope just designed.

## 8.8 Review and Summary

This chapter has covered the basic considerations and procedures involved in the design of an optical system to be used in a borescope application. Unique to this family of optical instruments is the small diameter of the optics involved and the relatively great overall length of the borescope. In this case, an instrument was designed for visual observation of a 70-deg field of view. The optics used had a maximum diameter of 6 mm, while the overall length of the system was greater than 1000 mm (40 inches).

The design procedure utilized a modular approach, with an objective lens, a unity magnification common relay, a magnifying relay, and an eyepiece. The objective lens design was optimized to produce a well-corrected image at the first image plane. The common relay was then used (4 times) to transfer this well-corrected image along the length of the system. Correction of this common relay was concentrated on elimination of spherical aberration and primary axial color. Both the objective lens and the common relay lens were designed to be telecentric, which eliminated the need for any field/collector lenses at the intermediate images.

Next, a magnifying relay lens ( $\text{mag.} = 1.5\times$ ) was introduced to produce the final image to be viewed by the eyepiece. This final relay lens form was basically a scaled version of the common relay. Finally, a standard Orthoscopic eyepiece, with a focal length of 20 mm, was added to complete the system.

Throughout the design process, the level of image quality was calculated based on the anticipated performance (from Chapter 2) of the typical visual system that would be accepting the output of the borescope. Final evaluation indicates essentially diffraction-limited performance over the central 50% of the field of view. This diffraction-limited image quality is consistent with performance of the typical eye. As a result, it has been concluded that introduction of this borescope

optical system between the eye and the object to be viewed will produce an effective magnification of  $3.3\times$ , with essentially no negative impact on the image quality observed by the viewer. Thus, in addition to making visual access to the object possible, the borescope has increased the viewer's ability to resolve detail at that object by a factor of  $3.3\times$ . These results are consistent with the basic intent of the borescope's introduction.

## 9

## The Submarine Periscope—Design

---

### 9.1 Introduction

The optical system used in the typical contemporary submarine periscope is unique in that, like the borescope, the length-to-diameter ratio of the optical system may approach a value of 100:1. Figure 9.1 illustrates a modern submarine, and shows the relationship of the periscope to the rest of the boat. Note that the periscope length is chosen such that when in the *down* position the periscope is completely housed within the boat. When in the *up* position, the periscope penetrates the surface, allowing the viewer to observe items on and above the surface, while the boat hovers at a keel depth of some 60 feet. Structural design considerations dictate a maximum periscope diameter of 7.5 inches. This in turn leads to a limitation on the diameter of the internal optics of about 100 mm (4 inches).

### 9.2 General Optical Configuration

The submarine periscope is typically made up of three distinct optical modules: the head, the mast, and the eyepiece box. The head module contains the head window, the head prism, the objective lens, and the telemeter. The mast module contains six relay lenses and two collector/field lenses. The eyepiece box module contains a folding mirror or prism, a stanching window, and the eyepiece.

The head window will generally be racetrack shaped, with a clear aperture of about  $50 \times 150$  mm. The window will have tapered sides and will be installed such that the undersea pressure that will be encountered will assist in forming a reliable seal. The head prism is a right-angle prism which deflects the incoming line of sight, directing it downward into the boat. The head prism will be designed to rotate about a horizontal axis to provide elevation scan capability (Fig. 9.1). Horizontal, or azimuth, scanning of the line of sight is accomplished when the viewer rotates the entire periscope, and himself, about the vertical axis through an unlimited ( $n \times 360$ -deg) scan angle.



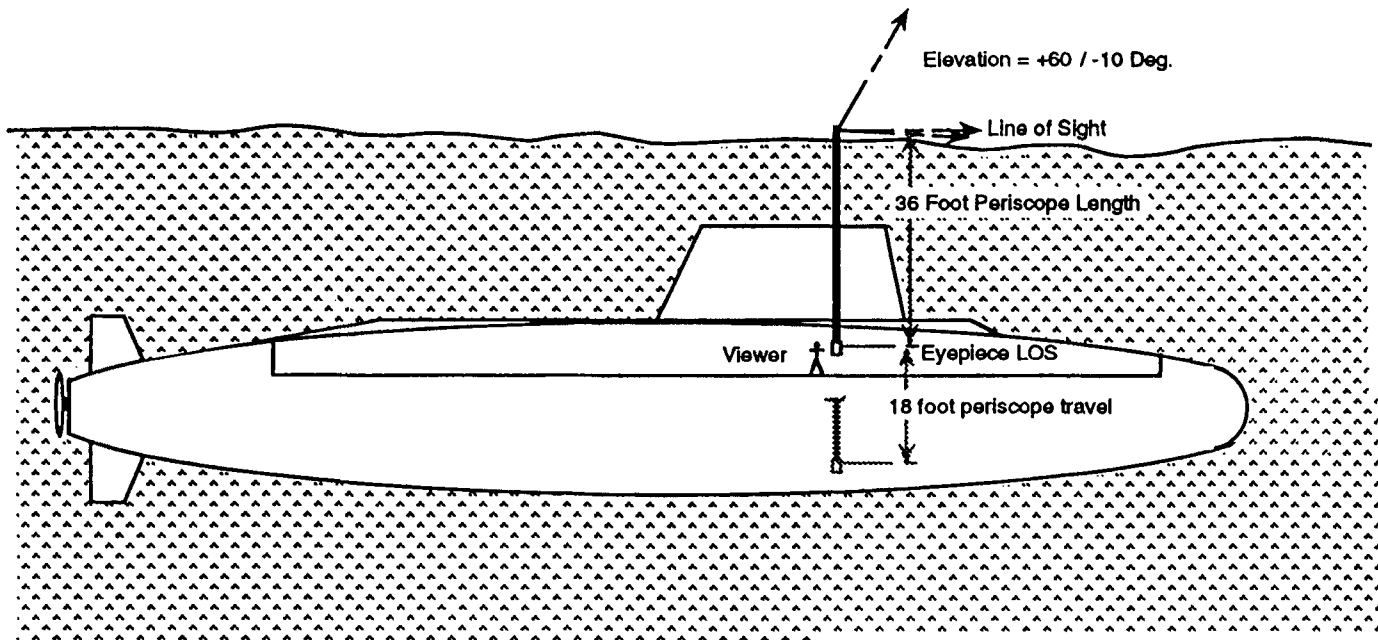


Figure 9.1 The submarine periscope is used to view activities above the water's surface while the submarine remains submerged. Dimensions shown here are approximate, but typical of a contemporary system.

The periscope's objective lens will generally be made up of a compound lens assembly that allows the system to be switched between low and high power modes. The final head module component is the *telemeter*, which is located at the image plane of the objective lens. Essentially a reticle, the *telemeter* designation has evolved because the engraved reticle pattern allows the viewer to estimate range to a target, assuming that the size of that target is known.

### 9.3 Objective Lens Design

This periscope optics design exercise will incorporate traditional dimensions that occur in many of the submarine periscopes in use today, both by the U.S. Navy as well as navies in other countries. The basic form to be described here evolved in the 1940s, in response to a need for a system with photographic as well as visual capability. Many of the basic design characteristics have been in use, in both the United States and in Europe, since the early 1900s.

The submarine periscope usually falls into one of two categories, the *attack* or the *search* periscope. The attack design incorporates smaller optics, making the periscope head smaller and less likely to be seen by the enemy. The search periscope uses larger diameter optics, thus enhancing all aspects of overall optical performance. This design will be for a *search* periscope, with a 42-mm aperture and a field of view of 8 deg in the high-power-mode. The traditional high-power (HP) objective will have a focal length of 429 mm and will be designed assuming a 60% vignetting factor. The basic lens configuration will consist of a cemented achromatic doublet with a focal length close to 429 mm, followed by a *zero-power* air-spaced doublet field corrector lens, located about 70% of the distance to the final image plane. The general design procedure typically followed is to correct on-axis aberrations with the cemented doublet and off-axis aberrations with the zero-power air-spaced doublet. The final image will be flat, with a diameter of 60 mm.

The objective lens was set up for optimization with identical angle solves on the last surface of both doublets to assure the zero-power aspect of the second doublet. After a preliminary design was generated, and all axial distances were frozen, the angle solve constraints were removed to allow some fine-tuning of the design. The resulting high-power objective lens design is shown in Fig. 9.2, along with paraxial constants and lens data. Note from the lens layout that the entrance pupil is located in front of the lens such that, for the maximum field angle, the light bundle utilizes the upper half of the cemented doublet. While the lens as shown will accept light rays into its lower half, we will see as the design progresses that those rays will subsequently be vignetted by relay lens

apertures. Figure 9.3 contains ray trace analysis (aberration curves) and MTF data for the HP objective lens.

As in previous chapters, the acceptability of the design can be judged by evaluating its effect on nominal visual performance. The traditional high-power visual magnification of the periscope is 6 $\times$ . Ignoring the relay lenses for now, it can be assumed that the image of the objective lens will be viewed using an eyepiece with a focal length of

$$\text{Eyepiece efl} = \text{Objective efl} / \text{Mag.} = 429 / 6 = 71.5 \text{ mm.}$$

The exit pupil for the system will be dictated by the f-number of the objective ( $f/10.2$ ) and the eyepiece focal length

$$\text{Exit Pupil Dia.} = \text{efl} / \text{f-number} = 71.5 / 10.2 = 7.0 \text{ mm.}$$

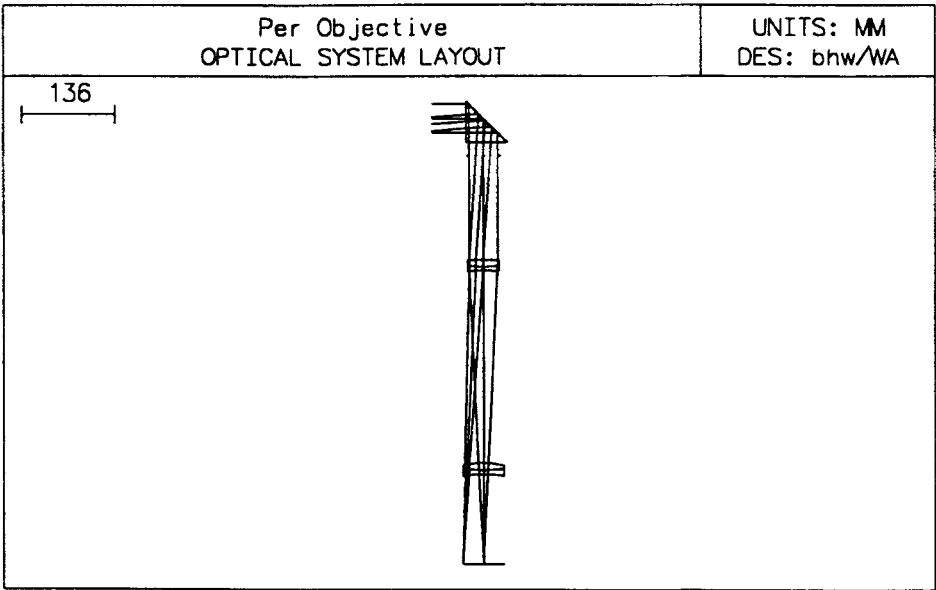
While this large exit pupil will assist in low-light-level viewing, under normal daylight conditions it can be assumed that scene brightness will lead to a viewer's eye pupil of about 4.5-mm diameter. From Fig. 2.3 it can be concluded that the eye's resolution, at the near point, will be about 7 cycles/mm for a pupil diameter of 4.5 mm. The magnification of the eyepiece will give the following

$$\begin{aligned} \text{Max. Resolution} &= \text{Eye Res.} \times \text{Eyepiece Mag.} \\ &= 7.0 \times (254 / 71.5) = 25 \text{ cycles/mm.} \end{aligned}$$

This is the value used for the upper limit of the MTF and AIM curves in Fig. 9.3. From this figure it can be estimated that resolution of the high-power objective lens, over the central 70% of the field, will be within 2% of the diffraction limit, falling to within 5% for the remainder of the field.

Drawing again on traditional periscope design concepts, a 0.25 $\times$  Galilean telescope is placed between the head prism and the high-power objective to form the low-power (LP) objective. The resulting lens will have a focal length of 106 mm, a speed of  $f/10.2$ , and will cover a field of view of about 32 deg. Holding the HP objective constant, a LP design was generated, with the resulting design data shown in Fig. 9.4. Ray trace analysis and MTF data for this design are shown in Fig. 9.5. It can be seen that the resulting design is well corrected for on-axis aberrations, while off-axis performance is degraded by residual astigmatism.

The function and intent of the periscope tells us that the low-power (1.5 $\times$ ), wide-angle (32-deg) mode will be used to scan the scene and detect any potential objects of interest. That object will then be brought to the center of the field of view (by scanning the periscope) and then the



**\*PARAXIAL CONSTANTS**

Effective focal length:	-429.00000	Lateral magnification:	-1.4299e-28
Numerical aperture:	0.04895	Gaussian image height:	29.99687
Working F-number:	10.21370	Petzval radius:	768.68498

**\*LENS DATA**

**High Power Per Objective**

SRF	RADIUS	THICKNESS	APERTURE RADIUS	GLASS	SPE	NOTE
OBJ	--	3.0000e+30	2.0978e+29	AIR		
1	--	30.00000	30.00000	BK7	C *	Head
2	--	-30.00000	42.00000	REFLECT	*	Prism
3	--	-20.00000	30.00000 K	AIR		
AST	--	-150.00000	21.00000 AS	AIR	*	
5	-198.90000 V	-10.00000	21.00000 K	BAK1	C	Objective
6	170.94000 V	-6.00000	23.00000	F2	C	
7	-1718.72000 V	-278.00000	23.00000	AIR		
8	-120.60000 V	-10.00000	30.00000	BK7	C	
9	447.10000 V	-1.05000	30.00000	AIR		Field Lens
10	204.70000 V	-6.00000	28.00000 K	BK7	C	
11	-160.68000 V	-130.00000	30.00000	AIR		
IMS	--	0.00000	30.00000		*	Image

Figure 9.2 Lens layout and data on a 429-mm f/10.2 high-power objective lens. The 60-mm-diameter image represents an 8-deg field of view.

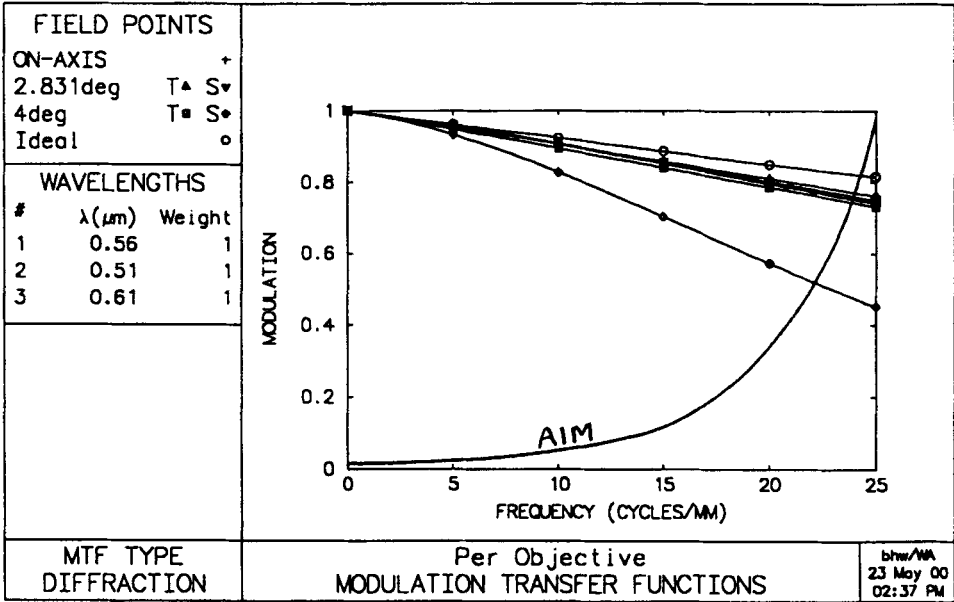
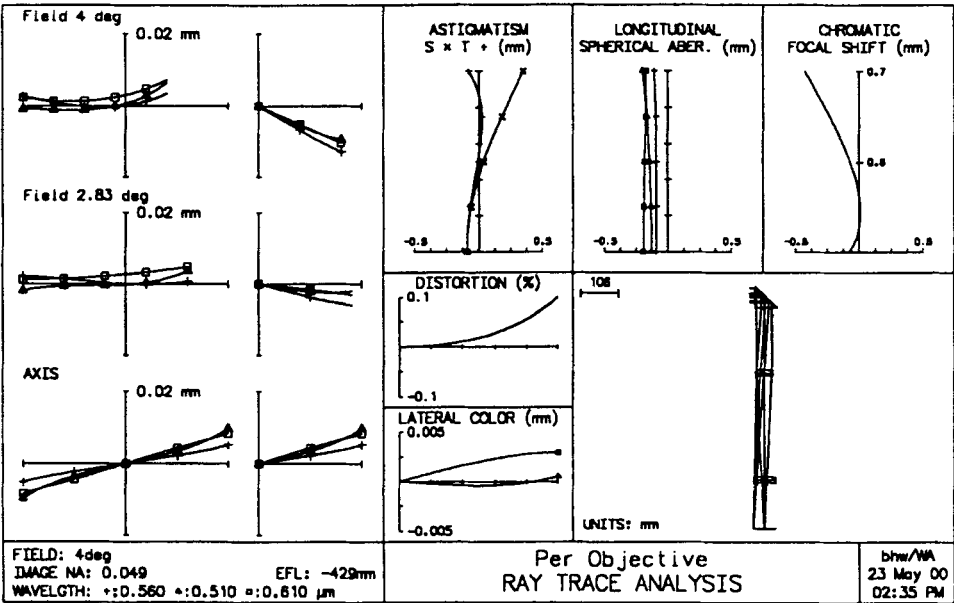
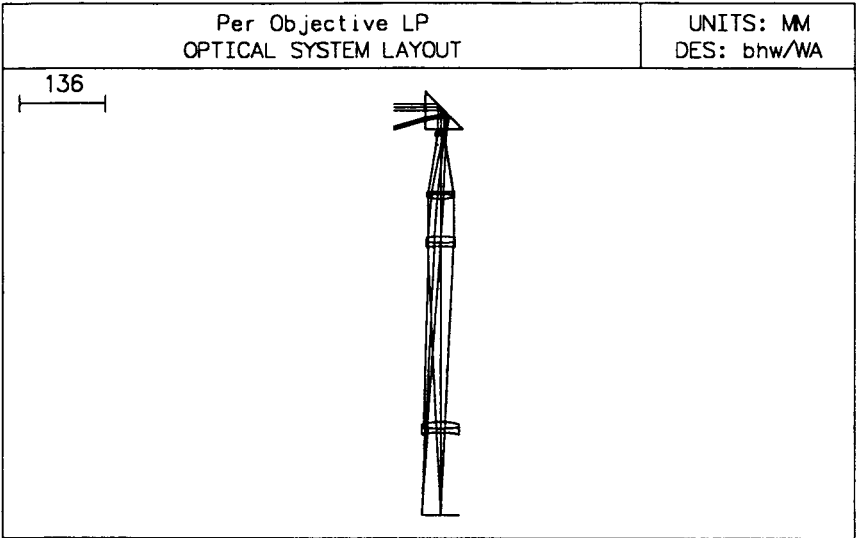


Figure 9.3 Ray trace analysis (aberration curves) and MTF data on the high-power objective lens.



\*PARAXIAL CONSTANTS

Effective focal length: -105.74547      Lateral magnification: -3.5248e-29  
Numerical aperture: 0.04870      Gaussian image height: 30.85292  
Working F-number: 10.26655      Petzval radius: -66.29569

\*LENS DATA

Low Power Per Objective

SRF	RADIUS	THICKNESS	APERTURE RADIUS	GLASS	SPE	NOTE
OBJ	--	3.0000e+30	8.7530e+29	AIR		
1	--	30.00000	30.00000	BK7	C	*
2	--	-30.00000	42.00000	REFLECT		*
3	--	-25.00000	30.00000	AIR		
AST	--	20.00000	5.15000 AS	AIR		*
5	40.31000	-3.70000	9.00000 K	SF1	C	
6	17.88000	-1.00000	9.00000	BK7	C	
7	-21.54000	-88.34000	9.00000	AIR		
8	-1115.00000	-3.20000	22.00000	SF8	C	
9	-89.10000	-8.65000	22.00000	BK7	C	
10	57.84000	-60.00000	22.00000	AIR		
11	-198.90954 V	-10.00000	21.00000	BAK1	C	
12	170.94318 V	-6.00000	23.00000	F2	C	
13	-1718.72019 V	-278.00000	23.00000	AIR		
14	-120.59674 V	-10.00000	30.00000	BK7	C	
15	447.09971 V	-1.04635	30.00000	AIR		
16	204.70741 V	-6.00000	28.00000 K	BK7	C	
17	-160.67553 V	-130.00000	30.00000	AIR		
IMS	--	--	30.00000			*

Figure 9.4 Lens layout and data on a 106-mm f/10.2 low-power objective lens. The 60-mm-diameter image represents a 32-deg field of view. Power change is accomplished by switching in a one-quarter power Galilean telescope between the head prism and the high-power objective.

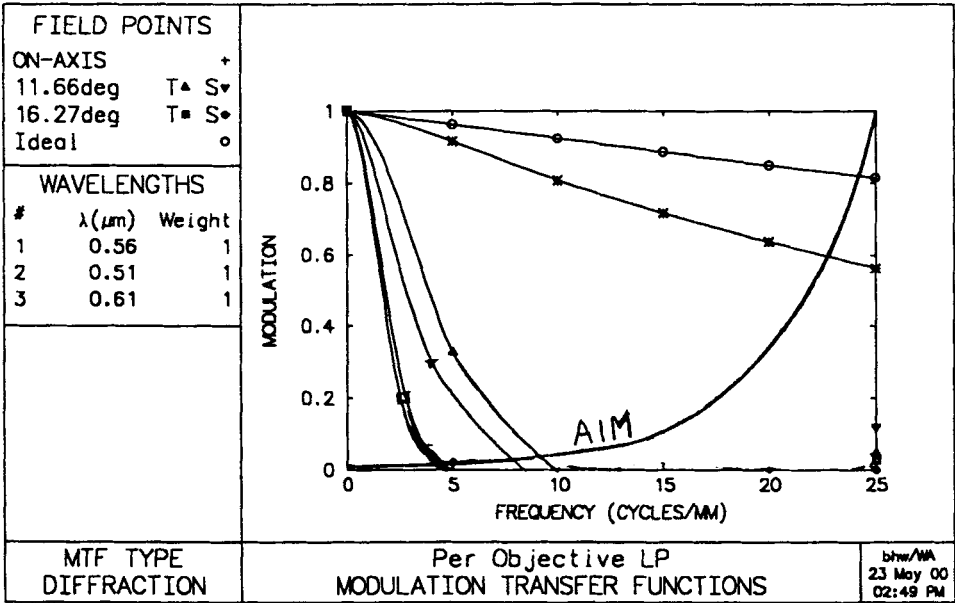
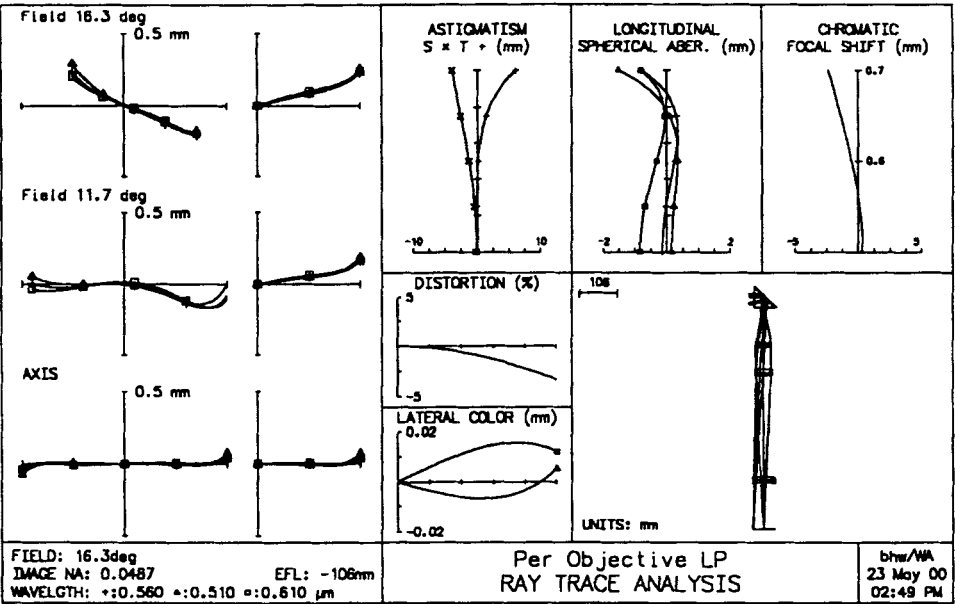


Figure 9.5 Ray trace analysis (aberration curves) and MTF data on the low-power objective lens.

magnification will be switched to the high-power (6×) mode for final observation of that object. The apparent visual field, as seen through the periscope in both high and low powers, is illustrated in Fig. 9.6.

From the HP view shown, it is possible to describe a typical range estimation using the telemeter pattern. Assume that the viewer knows that the height above the water line for the highest point on the ship being viewed is 11 meters. In the high power mode, the telemeter marks are spaced at 1-deg major intervals, which allows the viewer to estimate the vertical angle subtended by the ship at 1.5 deg (.026 radian). From these two pieces of data the range can be estimated

$$\begin{aligned} \text{Range} &= \text{Target Height} / \text{vertical angle} \\ &= 11 \text{ Meters} / .026 \text{ radian} = 420 \text{ Meters.} \end{aligned}$$

This range information may then be used for purposes of target evasion or for weapons delivery.

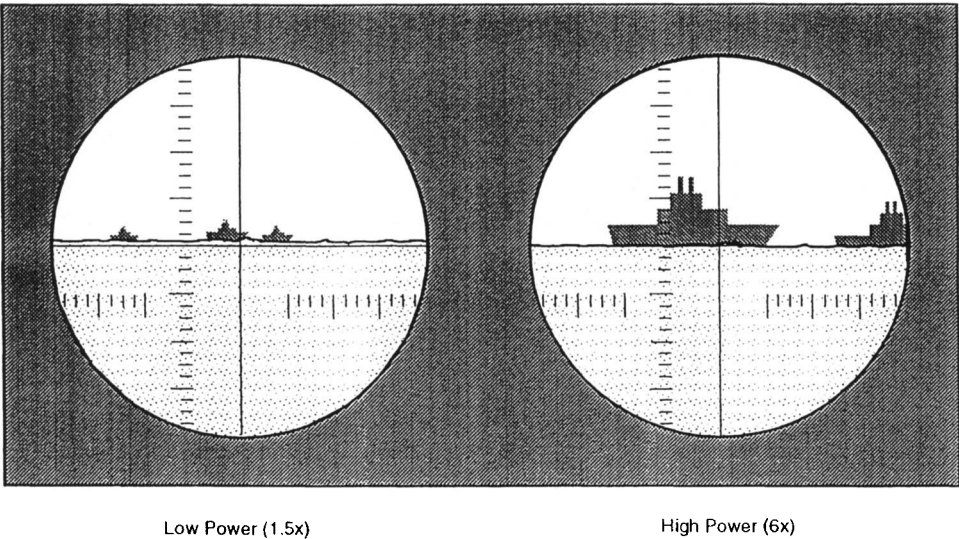


**Figure 9.6** The field of view as seen through a traditional submarine periscope in the low-power (1.5×) mode (left) and the high-power (6×) mode (right). Major reticle marks indicate 4 deg in low power, 1 deg in high power. Both cases represent a 48-deg apparent field of view to the eye.



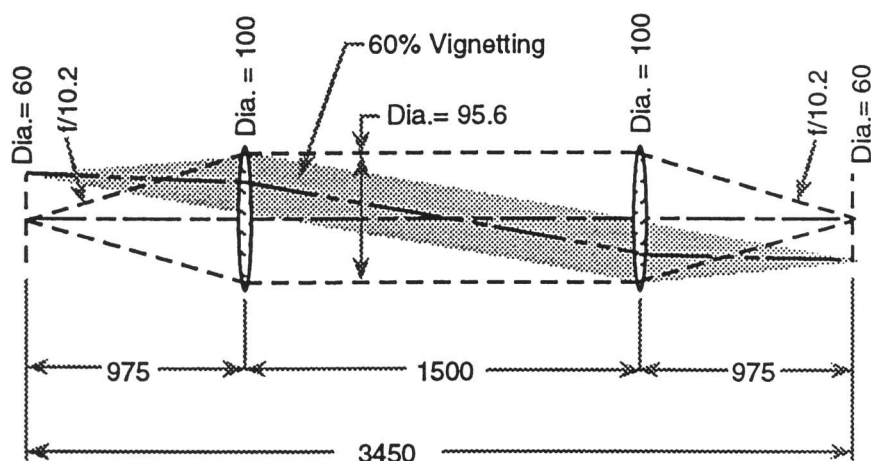
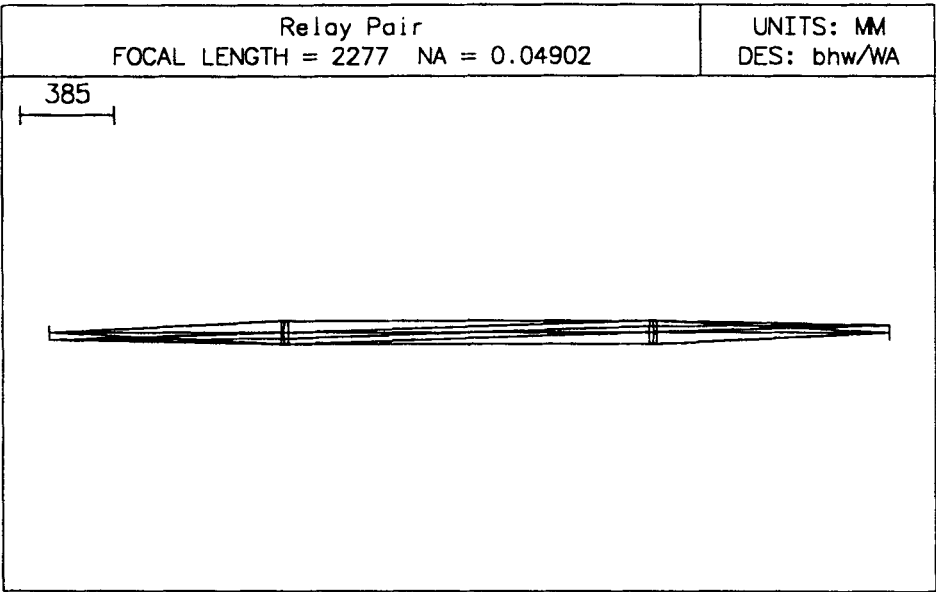


**Figure 9.7** Thin lens layout used to determine basic parameters of the unity magnification relay lens to be used three times in the final periscope optical system.

## 9.4 Relay Lens Pair Design

It will be recalled that this design exercise calls for an optical length (input line of sight to eyepiece line of sight) of 36 feet, or 11 meters for the periscope. From Fig. 9.2 we see that the objective lens assembly is 646-mm long, which leaves a remaining length of 10,354 mm for the relay lenses. Assuming that the final image will be close to the eyepiece centerline, and that we will be incorporating three unity magnification relay pairs, the overall length of one relay pair can be found by dividing the remaining length by three. This leads to an approximate length of 3451-mm-per-relay pair. The thin lens layout shown in Fig. 9.7 indicates that a relay lens focal length of 975 mm, with a space between relays of about 1500 mm, will result in the required overall length with a maximum vignetting factor of 60%. A cemented achromat design was generated, with an efl of 975 and a speed of  $f/10.2$ . Two of these lenses were then set up in the form of a unity magnification relay set. Maintaining perfect symmetry, the three lens curvatures were used as variables and the design was optimized. Following several iterations, the design shown in Fig. 9.8 resulted. Ray trace analysis and MTF data were then generated with the results shown in Fig. 9.9. As with the objective lens, a frequency of 25 cycles/mm was used as a maximum value for the MTF and AIM curves. Results indicate that the resolution over the central 70% of the image will be within 3% of the diffraction limit, falling to a worst case of 7% for the maximum field point.



*PARAXIAL CONSTANTS			
Effective focal length:	2276.98879	Lateral magnification:	-0.99994
Numerical aperture:	0.04902	Gaussian image height:	29.99831
Working F-number:	10.20000	Petzval radius:	-716.73351

*LENS DATA						
Relay Pair						
SRF	RADIUS	THICKNESS	APERTURE RADIUS	GLASS	SPE	NOTE
OBJ	--	951.95000	30.00000	AIR	*	
1	1042.90000 V	12.00000	50.00000	F2	C	
2	260.97000 V	18.00000	50.00000	BAK1	C	
3	-905.83000 V	750.00000	50.00000 K	AIR		
AST	--	750.00000 P	47.21161 AS	AIR		
5	905.83000 P	18.00000 P	50.00000 K	BAK1	C	
6	-260.97000 P	12.00000 P	50.00000	F2	C	
7	-1042.90000 P	951.95000 P	50.00000	AIR		
IMS	--	--	30.00000		*	

Figure 9.8    Lens layout and data on the optimized final design of the unity magnification relay lens to be used three times in the final periscope optical system.

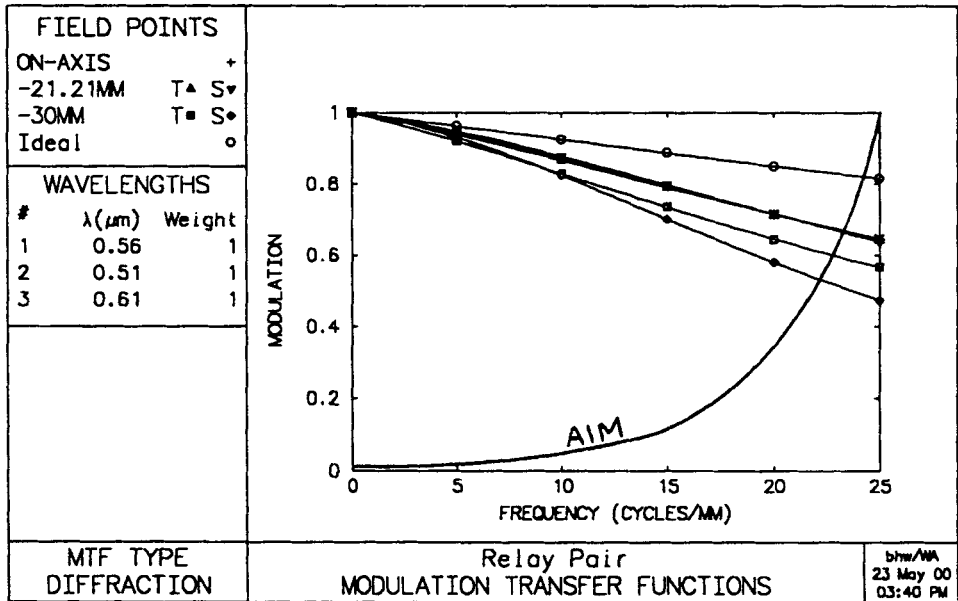
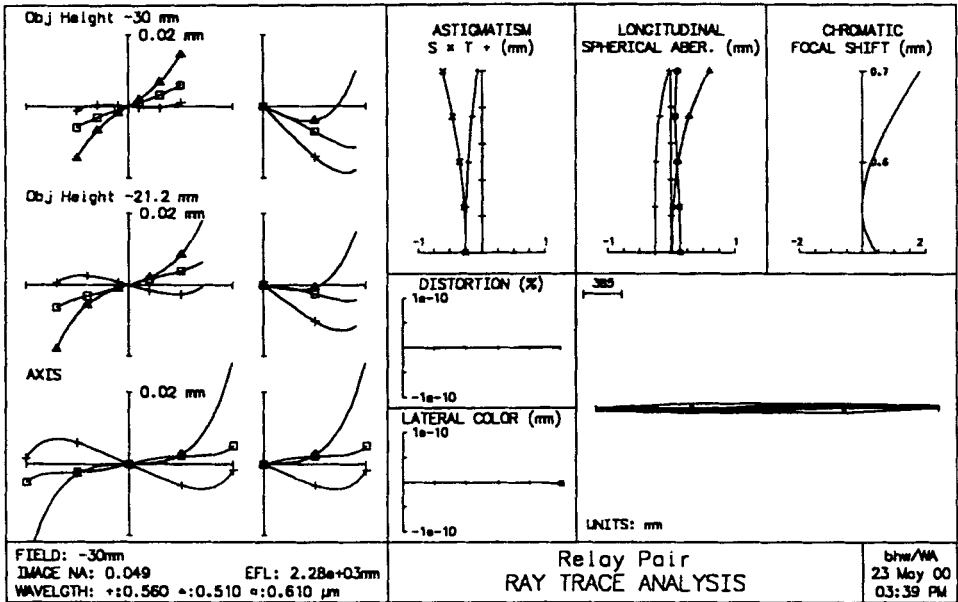


Figure 9.9 Ray trace analysis (aberration curves) and MTF data on the final design of the unity magnification relay lens to be used three times in the final periscope optical system. AIM curve shown is for the model eye with a 4.5-mm pupil diameter and the 3.5× periscope eyepiece.

The achromatic doublet generated at this step is the lens that will be used for all six relay lenses (R1 through R6). In the case of R3 and R4, identical double convex collector/field lenses are placed 50 mm from the input and output images. These lenses will function to refract the incident off-axis light bundles and redirect them into the relay lens aperture that follows. Likewise, when the telemeter is added to the objective lens design, its second surface (the nonreticle surface) is given positive lens power to direct the off-axis light bundles into the aperture of the first relay lens (R1).

The high-power objective lens was combined with a telemeter lens, six relay lenses, and two collector/field lenses to produce the mast optics system shown and described in Fig. 9.10. Ray trace analysis and MTF data for this combination is presented in Fig. 9.11. The final 60-mm-diameter image produced by these optics, which is the subject of the analysis shown in Fig. 9.11, is the actual image that will be viewed using the periscope's 71.5-mm efl eyepiece. The MTF calculation shown was done assuming a reduced entrance pupil diameter of 27 mm, which corresponds to the aperture utilized when the eye's pupil is at 4.5-mm diameter. From the combination of MTF and AIM curves in Fig. 9.11, it can be concluded that the on-axis resolution will be within 9% of the diffraction limit, falling to 15% and 22% at the 0.7 and 1.0 field points, respectively. This degradation in image quality for the complete mast optics is primarily a result of accumulated secondary chromatic aberration present at each cemented achromat, and astigmatism for the off-axis points. This secondary color cannot be corrected without shifting the design into the area of apochromatic (corrected for three wavelengths) optics. This move would be too complex and too expensive to be considered for this design.

## 9.5 Visual Performance Analysis

The next step in the design process involves adding the eyepiece box, containing a folding optic, a stanching window, and an eyepiece, to the mast optics to complete the optics of the periscope. The folding optic can be either a mirror or a prism; the window is included to seal the interior of the periscope in the event of damage to the head and subsequent periscope flooding. The eyepiece described here is a traditional periscope eyepiece form, dating back to very early periscope designs. The final relay lens and subsequent optics from the resulting 6× visual system are shown in Fig. 9.12, along with paraxial constants and lens data. Figure 9.13 contains ray trace analysis and MTF data for the 6× visual system. Once again, the MTF calculations assume a 4.5-mm exit pupil, which

PARAXIAL CONSTANTS					
Effective focal length:		-434.31642	Lateral magnification:		1.4477e-28
Numerical aperture:		0.04835	Gaussian image height:		-30.37036
Working F-number:		10.34087	Petzval radius:		-137.05238
*LENS DATA					
HIGH POWER MAST OPTICS					
SRF	RADIUS	THICKNESS	APERTURE RADIUS	GLASS	SPE NOTE
OBJ	--	3.0000e+30	2.0978e+29	AIR	
1	--	60.00000	30.00000	BK7 C	* Head
2	--	20.00000	30.00000 K	AIR	Prism
3	--	150.00000	21.08283 S	AIR	*
4	198.90000	10.00000	21.00000 K	BAK1 C	
5	-170.94000	6.00000	23.00000	F2 C	
6	1718.72000	278.00000	23.00000	AIR	Objective
7	120.60000	10.00000	30.00000	BK7 C	
8	-447.10000	1.05000	30.00000	AIR	
9	-204.70000	6.00000	28.00000 K	BK7 C	
10	160.68000	130.00000	30.00000	AIR	
11	--	10.00000	32.00000	BK7 C	Telemeter
12	-270.00000	945.35000	32.00000	AIR	
13	1042.90000 V	12.00000	50.00000	F2 C	
14	260.97000 V	18.00000	50.00000	BAK1 C	R1
15	-905.83000 V	750.00000	48.00000 K	AIR	
AST	--	750.00000 P	46.55144 AS	AIR	
17	905.83000 P	18.00000 P	48.00000 K	BAK1 C	
18	-260.97000 P	12.00000 P	50.00000	F2 C	R2
19	-1042.90000 P	951.95000	50.00000	AIR	
20	--	50.00000	30.38994 S	AIR	* Image
21	2500.00000	10.00000	35.00000	BK7 C	
22	-2500.00000 P	894.23000	35.00000	AIR	Collector
23	1042.90000	12.00000	50.00000	F2 C	
24	260.97000	18.00000	50.00000	BAK1 C	R3
25	-905.83000	750.00000	50.00000 K	AIR	
26	--	750.00000 P	46.21363 S	AIR	
27	905.83000 P	18.00000 P	50.00000 K	BAK1 C	
28	-260.97000 P	12.00000 P	50.00000	F2 C	R4
29	-1042.90000 P	894.23000 P	50.00000	AIR	
30	2500.00000 P	10.00000	35.00000	BK7 C	
31	-2500.00000 P	50.00000 P	35.00000	AIR	
32	--	951.95000	30.40902 S	AIR	* Image
33	1042.90000	12.00000	50.00000	F2 C	
34	260.97000	18.00000	50.00000	BAK1 C	R5
35	-905.83000	750.00000	48.00000 K	AIR	
36	--	750.00000 P	48.00757 S	AIR	
37	905.83000 P	18.00000 P	48.00000 K	BAK1 C	
38	-260.97000 P	12.00000 P	50.00000	F2 C	R6
39	-1042.90000 P	951.95000	50.00000	AIR	
IMS	--	--	30.30000		* Image

Figure 9.10 Paraxial constants and lens data for the complete high-power periscope mast optics system (except eyepiece), forming the final 60-mm-diameter image within the eyepiece box.

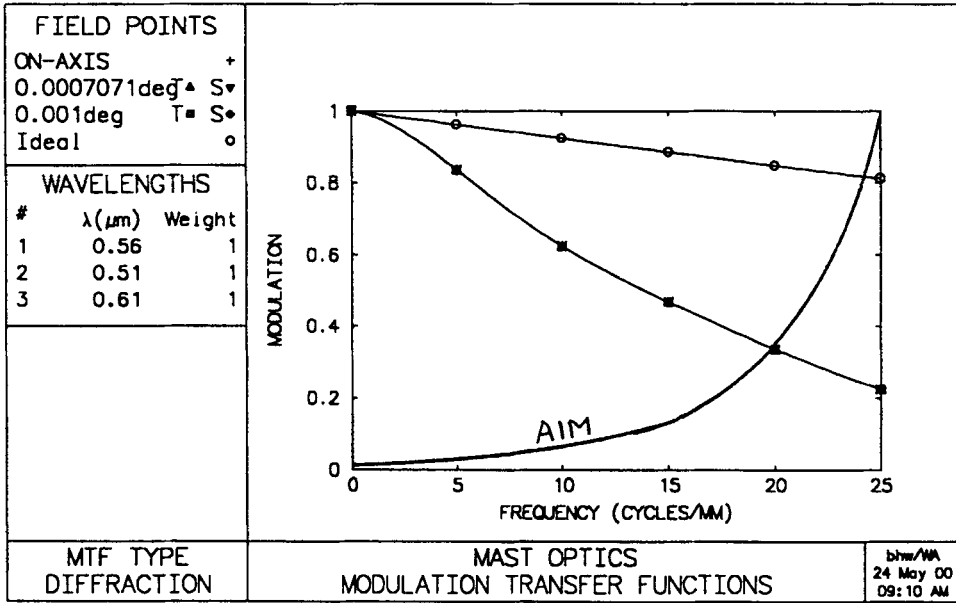
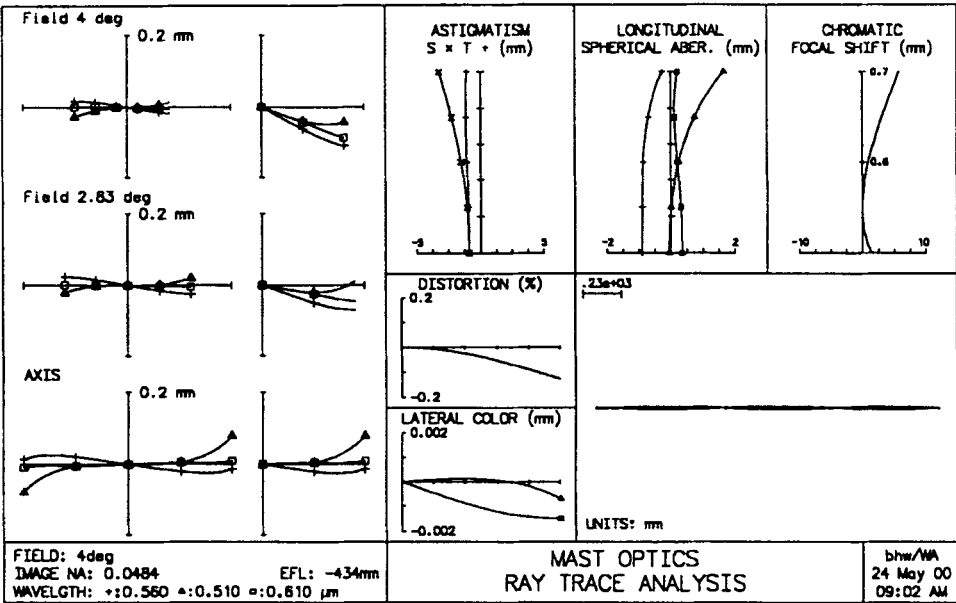
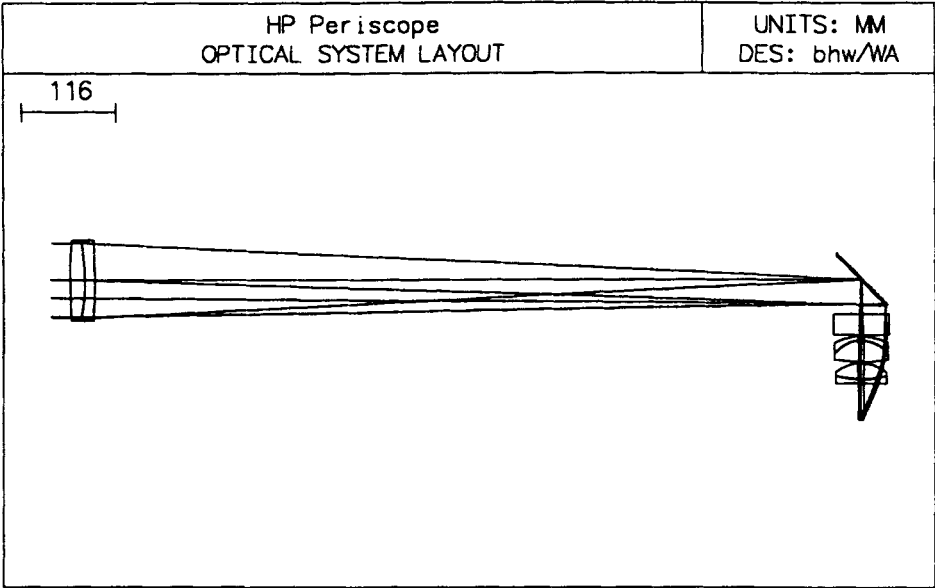


Figure 9.11 Ray trace analysis (aberration curves) and on-axis MTF data on the complete high-power periscope optical system (except eyepiece) forming the final 60-mm-diameter image. AIM curve shown is for the model eye with a 4.5-mm pupil diameter and the 3.5 $\times$  periscope eyepiece.



**\*PARAXIAL CONSTANTS**  
Angular magnification: -6.00000      Lagrange invariant: -1.46846  
Eye relief: -45.00000      Petzval radius: 57.07857

**\*LENS DATA**  
**HP (6x) Periscope**

SRF	RADIUS	THICKNESS	APERTURE RADIUS	GLASS	SPE	NOTE
37	905.83000 P	18.00000 P	48.00000 K	BAK1	C	
38	-260.97000 P	12.00000 P	50.00000	F2	C	R6
39	-1042.90000 P	951.95000	50.00000	AIR		
40	--	-42.25000	45.00000	REFL_HATCH		* Image
41	--	-25.00000	35.00000	BK7	C	Stanching
42	--	-2.00000	35.00000	AIR		-Window-
43	-76.22000	-5.00000	34.00000	SF8	C	
44	-43.93000	-26.00000	34.00000	BK7	C	
45	224.67000	-2.00000	34.00000	AIR		
46	-51.24000	-19.00000	32.00000	BK7	C	Eyepiece
47	153.66000	-1.00000	32.00000	AIR		
48	119.12000	-5.00000	30.00000	SF8	C	
49	-723.50000	-45.00000	32.00000	AIR		
IMS	--	--	3.50715 S			* Exit Pupil

Figure 9.12 Lens layout and data for the final relay lens and eyepiece box optics (using high-power objective lens).

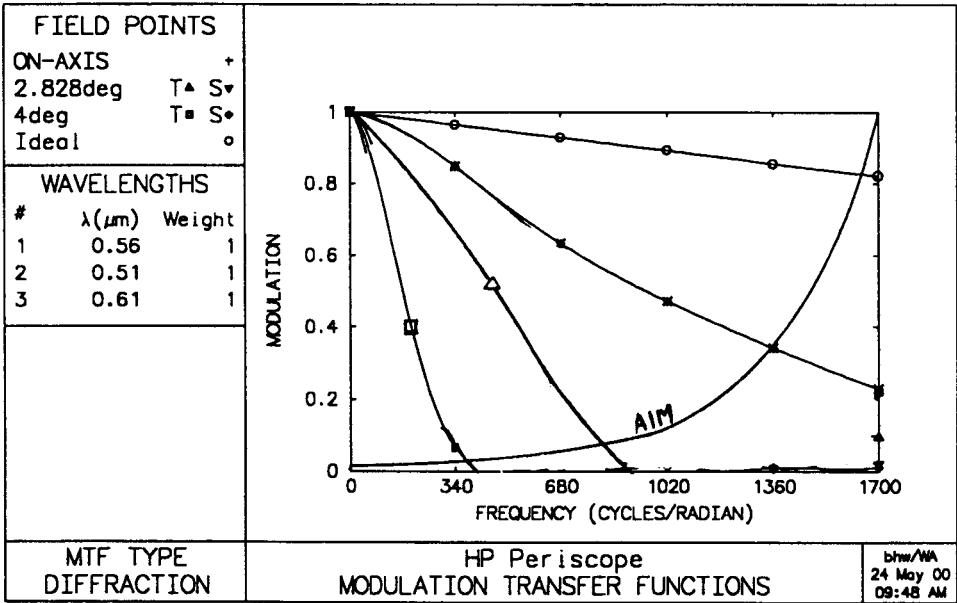
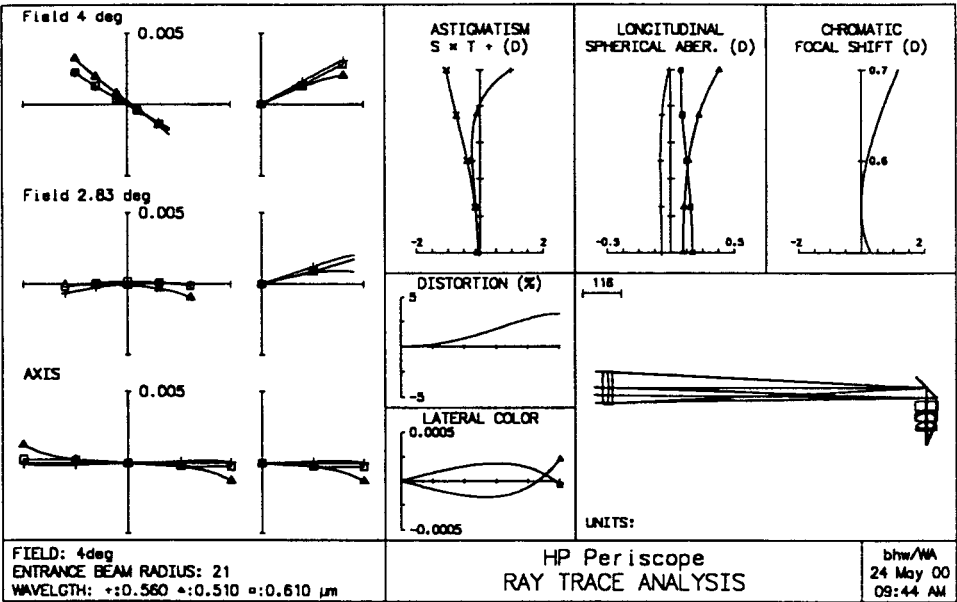


Figure 9.13 Ray trace analysis (aberration curves) and MTF data on the complete periscope optical system in the high-power mode. AIM curve shown is for the model eye with a 4.5-mm-diameter pupil.



leads to the maximum frequency of 1700 cycles/radian. From Fig. 9.13 it can be concluded that the on-axis visual resolution, through the periscope, will be 1450 cycles/radian.

Addition of the 0.25× Galilean telescope to the objective lens leads to the low power (1.5×) system shown and described in Fig. 9.14. Ray trace analysis and MTF data for the low-power (1.5×) visual system are shown in Fig. 9.15. It is interesting to note that, for the low-power system, the eyepiece cancels out much of the astigmatism that was found in the low-power objective lens (Fig. 9.5). This results in quite uniform image quality over the full 32-deg field, as demonstrated by the MTF data in Fig. 9.15.

## 9.6 True Resolution Gain

This section will deal with the actual advantage that will be realized by viewing a target through the high-power (6×) periscope optics. Looking back at Fig. 9.6, we will assume that the periscope is being used to view a ship with a height above water of 11 meters, at a range of 420 meters. This ship subtends a vertical angle of

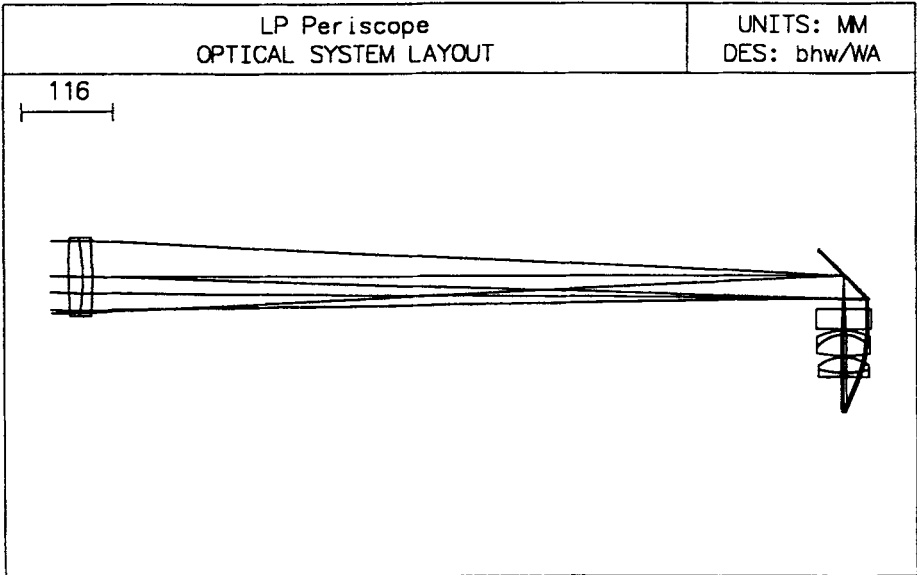
$$\text{Angle} = \text{Height} / \text{Range} = 11 / 420 = .026 \text{ radian.}$$

It has been assumed earlier that the naked eye will resolve about 1700 cycles/radian. For this target it can be concluded that the naked eye will resolve  $1700 \times .026 = 44$  cycles, or 88 elements, over the height of the target. This means that the eye will resolve elements at the target that are  $11 \times 1000 / 88 = 125$  mm (5 inches) in size.

Let's now calculate the advantage that will be realized when the same target is viewed using the 6× periscope optics. From Fig. 9.13 it was concluded that the viewer will resolve 1450 cycles/radian for an on-axis object, when using the high power (6×) optics of the periscope. The magnification of the optics will result in the target subtending an angle of  $.026 \times 6 = .156$  radians to the eye. The total number of cycles over the target height will now be  $1450 \text{ cycles/radian} \times .156 \text{ radian} = 226$  cycles, or 452 resolved elements. The size of each resolved element at the target will be

$$11 \times 1000 / 452 = 24.3 \text{ mm (about 1 inch).}$$

The actual gain then, resulting from use of the 6× periscope optics, will be  $125 / 24.3 = 5.1\times$ . A perfect optical system with a magnification of 6× would result in a 6× gain in resolved detail. This means that the optics of the periscope will introduce a 15% degradation in image quality



**\*PARAXIAL CONSTANTS**  
Angular magnification: -1.50000 Lagrange invariant: -1.46240  
Eye relief: -45.00000 Petzval radius: 881.16849

*LENS DATA							
LP (1.5x) Periscope							
SRF	RADIUS	THICKNESS	APERTURE	RADIUS	GLASS	SPE	NOTE
43	905.83000 P	18.00000 P	48.00000 K		BAK1 C		
44	-260.97000 P	12.00000 P	50.00000		F2 C	R6	
45	-1042.90000 P	951.95000	50.00000		AIR		
46	--	-42.25000	45.00000		REFL_HATCH	*	Image
47	--	-25.00000	35.00000		BK7 C		Stanching
48	--	-2.00000	35.00000		AIR		-Window-
49	-76.22000	-5.00000	34.00000		SF8 C		
50	-43.93000	-26.00000	34.00000		BK7 C		
51	224.67000	-2.00000	34.00000		AIR		
52	-51.24000	-19.00000	32.00000		BK7 C		Eyepiece
53	153.66000	-1.00000	32.00000		AIR		
54	119.12000	-5.00000	30.00000		SF8 C		
55	-723.50000	-45.00000	32.00000		AIR		
IMS	--	--	3.46262 S				* Exit Pupil

Figure 9.14 Lens layout and data for the final relay lens and eyepiece box optics (using low-power objective lens).

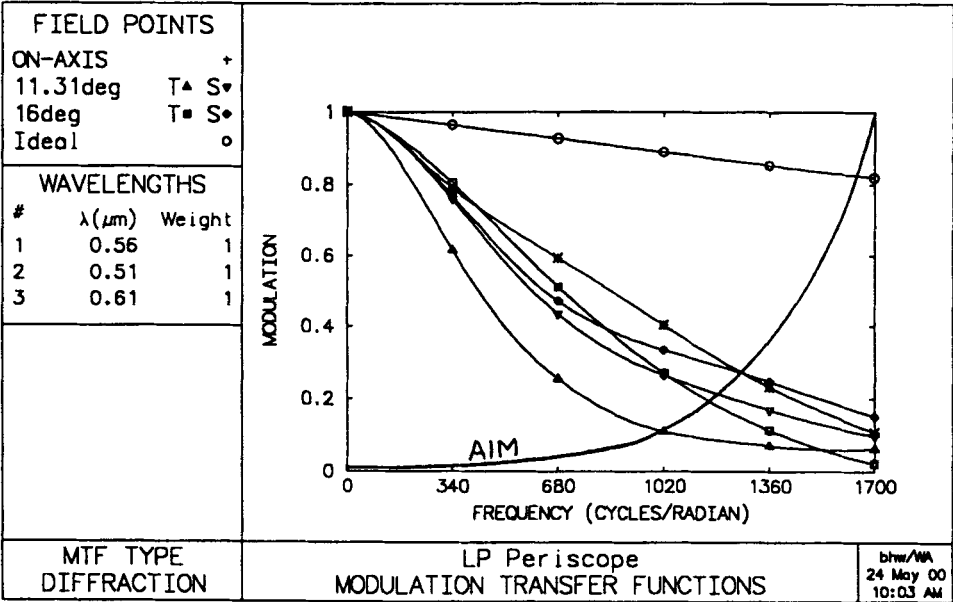
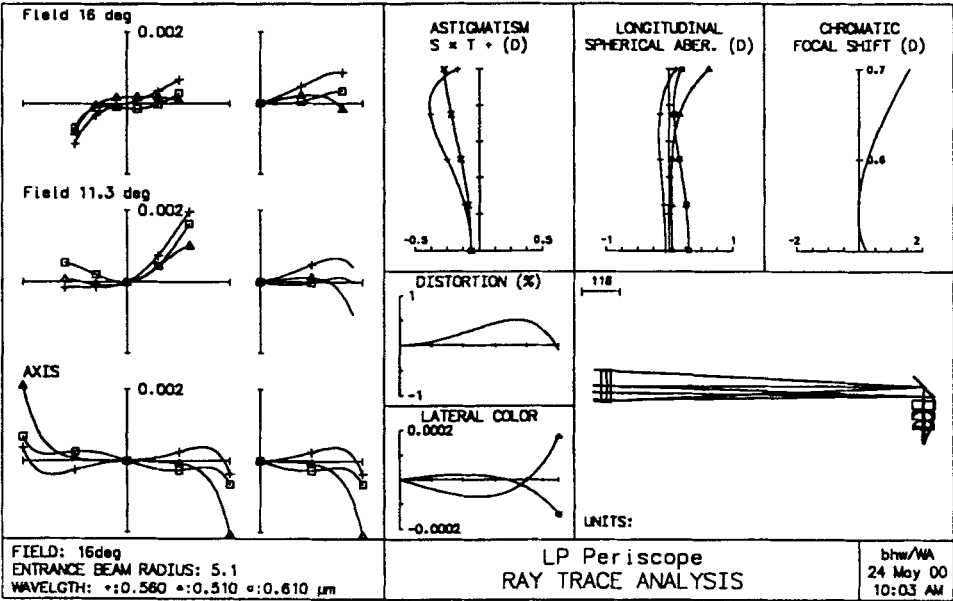


Figure 9.15 Ray trace analysis (aberration curves) and MTF data on the complete periscope optical system in the low-power (1.5 $\times$ ) mode. AIM curve shown is for the model eye with a 4.5-mm-diameter pupil.

relative to the performance of that *perfect* 6× optical system. As was touched upon earlier, this loss is due primarily to the residual chromatic aberration of the relay lenses. This loss is unavoidable in the design of a system with the physical characteristics of a submarine periscope, unless we were to resort to the cost and complexity of an apochromatic design. The 15% performance degradation appears to be a reasonable trade off in order to avoid those complications.

## 9.7 Review and Summary

This chapter has covered the basic considerations and procedures involved in the design of a traditional submarine periscope optical system. Basic overall system parameters that lead to the periscope configuration have been presented. The design of an optical system for a traditional *search* periscope has been covered. A design has been generated that incorporates established design approaches of the low-power Galilean and the eyepiece, combined with more comprehensive and original methods for the design of the dual-power objective and relay optics. All image quality evaluation has been based on the performance limit of the *typical* eye, when it is used with the periscope optics. A brief example of range estimation using the telemeter is included. Finally, calculations have been presented that demonstrate the gain in resolution that will be realized when using the periscope to view a distant target. While a 6× gain in resolved detail would represent the theoretical limit, assuming a perfect optical system, it was found that the system presented here would yield a gain of 5.1× in resolved detail relative to what would be observed with the naked eye.

# 10

## Biocular Design

---

### 10.1 Introduction

The term biocular refers to an optical system in which the optical components are shared by both of the viewer's eyes. The unusual aspect of a biocular design is that, while it must have a large exit pupil in order to accommodate both eyes, the instantaneous image quality will be determined by the relatively small pupil of the eye.

Critical to good performance in a biocular design is the condition that both eyes perceive the common point being viewed as originating at the same object point in space. Equally important is the correction of aberrations—such as spherical and coma—over the entire lens pupil which, if present, would result in apparent motion of the object (*swimming*) as the head moves about the exit pupil. This chapter will deal with the basic optical design considerations involved in generating and evaluating optical designs for two biocular devices.

### 10.2 Biocular Eyepiece

Figure 10.1 is an illustration of a periscopic night vision sight. This system is made up of two separate and distinct optical components. They are the objective lens and the biocular eyepiece. Because there is an image intensifier tube between these components, their optical designs are completely independent of each other. Information on design of the objective lens has been included for completeness. While its parameters do enter into certain final system specifications, the objective lens design has no impact on the basic design of the biocular eyepiece.

Figure 10.2 contains a lens layout, ray trace analysis, and MTF data for the objective lens. The upper frequency limit for the MTF and AIM curve is derived from the maximum resolution of the image intensifier tube. Combined resolution (lens plus tube) will be approximately 35 cycles/mm. Spectral wavelengths and weights are derived from a combination of typical night sky radiation and the spectral sensitivity of

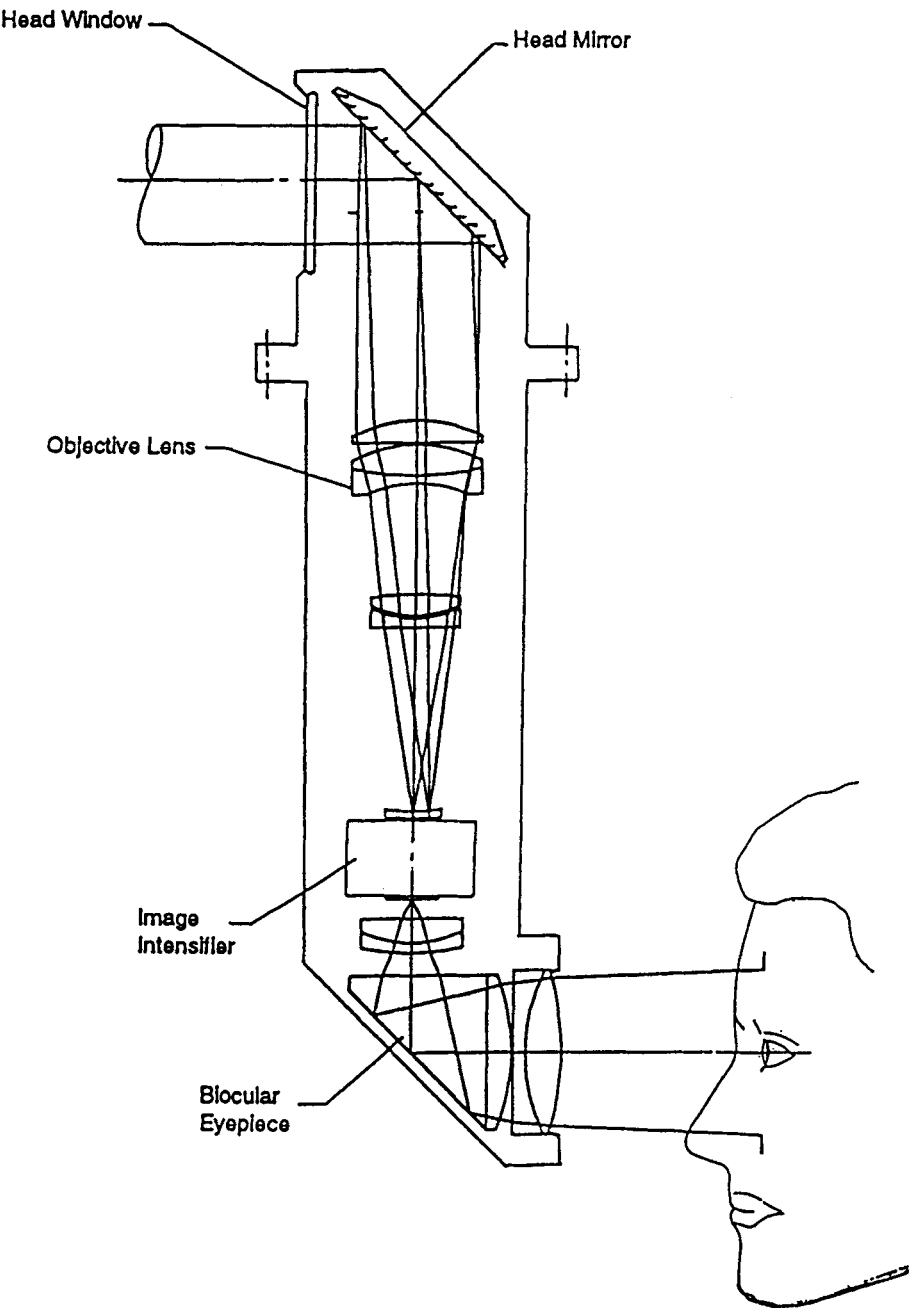


**Figure 10.1** Outline drawing of a periscopic night vision sight equipped with a biocular eyepiece to provide enhanced viewer comfort and flexibility.

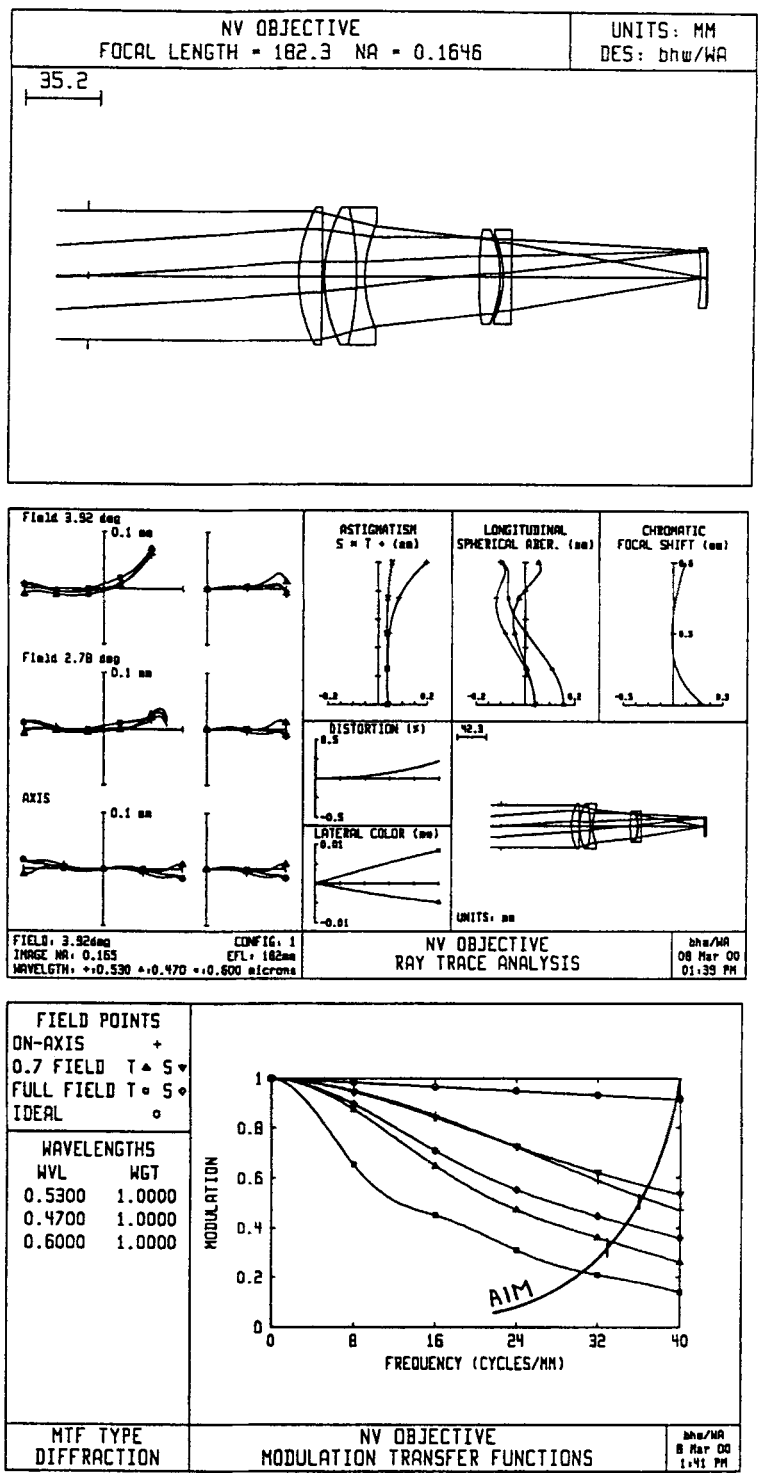


Figure 10.2 Lens layout, ray trace analysis (aberration curves), and MTF data on the periscopic night vision sight objective lens.

the tube. Following electronic amplification, the output from the tube will be essentially monochromatic (green).

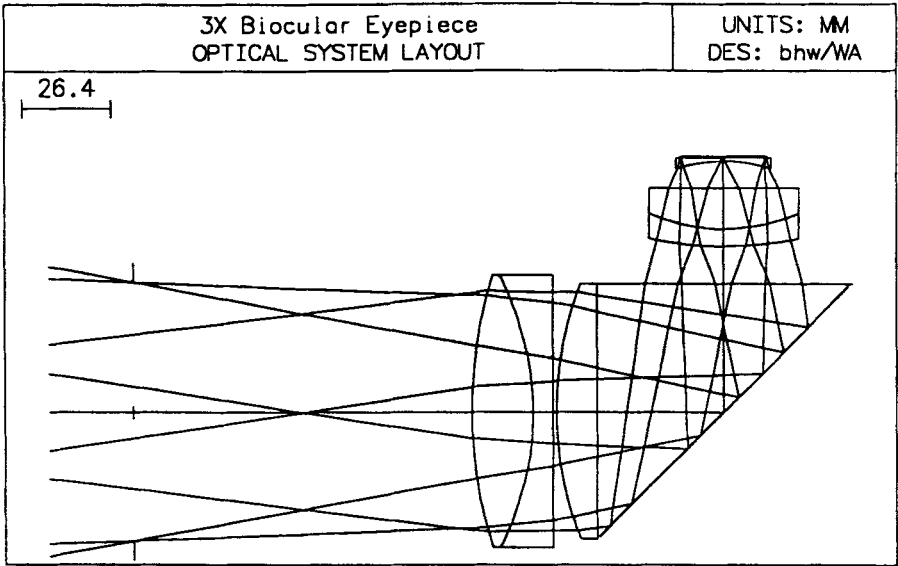
Figure 10.3 contains a lens layout, paraxial constants and lens data for a completed biocular eyepiece design. In this case, optical performance and mechanical packaging, including a folding prism, have been given equal importance. This design has an exit pupil that is 76 mm in diameter, with an eye relief of 100 mm. The output from the 25-mm-diameter intensifier tube is projected to the viewer's eyes, covering a field angle of 16.4 deg, with the final image formed at a distance of 1 meter in front of the eyes.

Image quality for the biocular eyepiece has been evaluated with two separate aspects of performance in mind. First, ray trace analysis was performed over the full 76-mm aperture to determine the general state of aberration correction. The resulting aberration curves are shown in Fig. 10.4 (top). From these curves it can be seen that distortion and astigmatism are well corrected. Aberration curves indicate the presence of residual spherical aberration and coma. The significance of these aberrations will be manifested by the resulting angle of projected rays at the exit pupil of the lens. In particular, we must be concerned with angular differences between rays originating at a common object point, entering the left and right eyes. In general it can be stated that if these differences are less than one-half deg, then the eyes will adjust to compensate and fuse the two images. In the aberration curves in Fig. 10.4, the vertical scale is  $\pm 0.2$  mm. Knowing the efl of the lens to be 87 mm, this 0.2-mm dimension can be converted to an angle of 0.13 deg, about one-quarter of the acceptable limit.

We can assume that each eye will collect a light bundle that is about 5 mm in diameter, and that the distance between eyes is 65 mm. In Fig. 10.5, a layout of these typical eye pupils has been superimposed on the spherical aberration curve for the biocular eyepiece. Note that for the worst case shown, the angular difference between the bundles entering the eyes is 0.021 deg.

Next, MTF calculations were used to evaluate the image quality that will result based on the 5-mm-diameter light bundle that enters the eye. First, based on the analysis of the objective lens, it will be assumed that the maximum resolution at the output of the intensifier is 35 cycles/mm. The 87-mm efl of the eyepiece would make its nominal visual magnification  $254/87 = 3\times$ . Referring once again to Chapter 2, Fig. 2.3, it will be seen that the typical eye with a 5-mm pupil will resolve 6.7





*PARAXIAL CONSTANTS			
Effective focal length:	-87.20000	Lateral magnification:	0.08655
Numerical aperture:	0.43872	Gaussian image height:	12.46367
Working F-number:	1.14000	Petzval radius:	311.15311

*LENS DATA							
3X Biocular Eyepiece							
SRF	RADIUS	THICKNESS	APERTURE RADIUS	GLASS	SPE	NOTE	
OBJ	--	-1000.00000	144.00000	AIR			
AST	--	100.00000	38.00000 AS	AIR			
2	--	--	38.00000 K	AIR			
3	134.76000 V	18.00000	40.00000	LAKN12	C		
4	-86.15000 V	6.00000	40.00000	SF56A	C		
5	--	1.00000	40.00000	AIR			
6	101.50000 V	12.00000	37.50000 K	LAKN12	C		
7	--	37.50000	37.50000	SF56A	C		
8	--	-37.50000	52.00000	REFLECT	*		
9	--	-10.90000 V	38.00000 K	AIR			
10	-107.89000 V	-5.00000	22.00000	LAKN12	C		
11	-55.90000 V	-12.00000	22.00000	SF56A	C		
12	--	-8.00000 V	22.00000 K	AIR			
13	44.00000	-1.00000	13.00000	BK7	C		
14	--	-0.63000	14.00000	AIR			
IMS	--	V	--	12.50000		*	

Figure 10.3 Lens layout and data on the 87-mm (3×) f/1.0 biocular eyepiece final design.

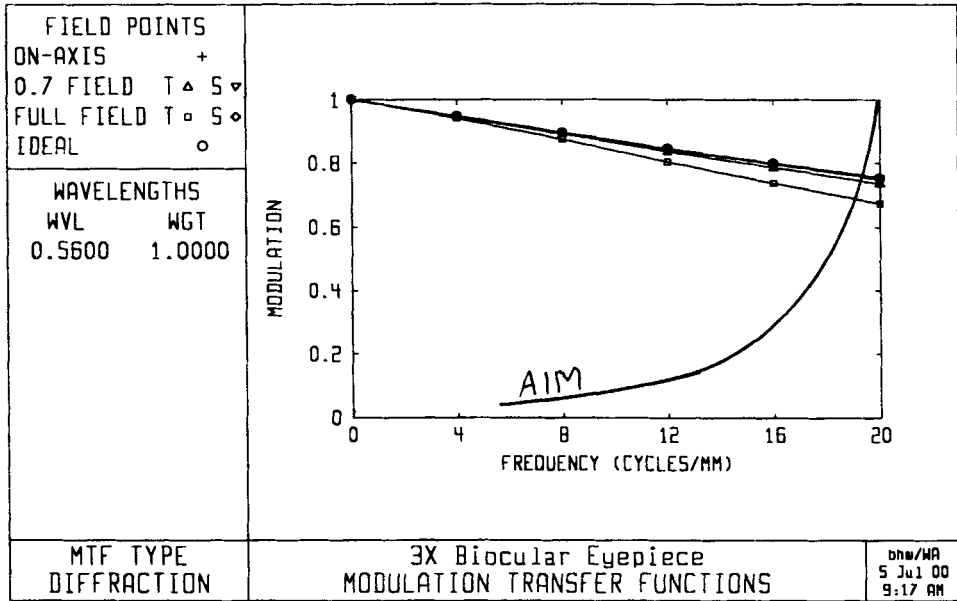
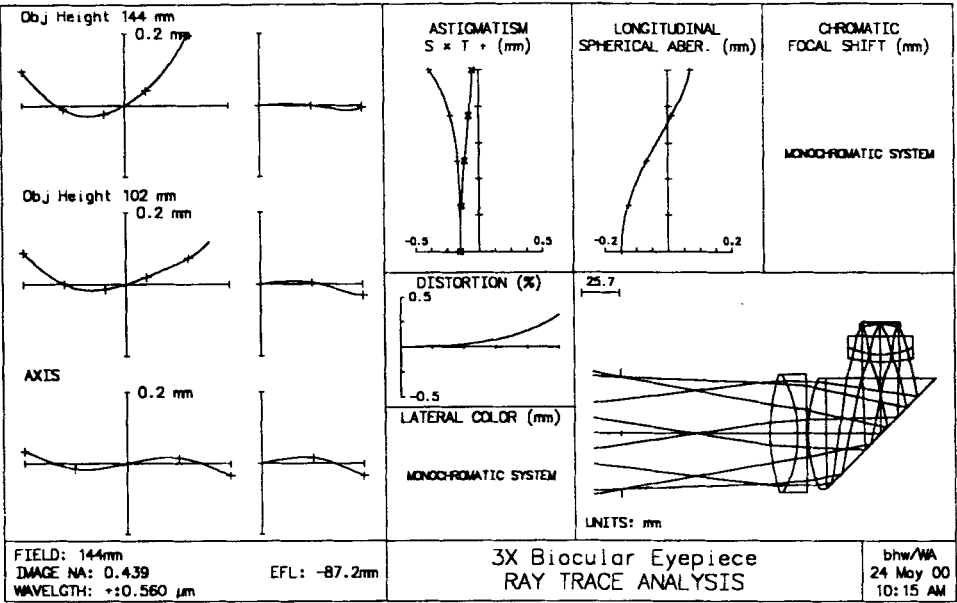


Figure 10.4 Ray trace analysis (aberration curves) and MTF data on the 87-mm (3×) f/1.0 biocular eyepiece final design. MTF and AIM data shown assume the model eye with a 5.0-mm-diameter pupil.

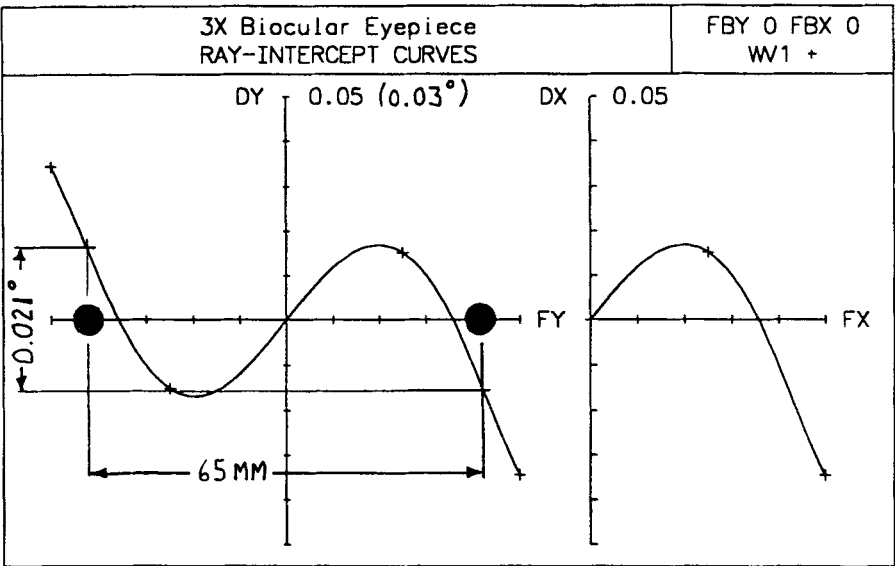


Figure 10.5 Spherical aberration curve over the full 78-mm aperture of the biocular eyepiece. A pair of 5-mm-diameter eye pupils are superimposed to permit an estimate of the angular error that will exist at each eye.

cycles/mm at its near point. The 3× eyepiece magnification will increase this theoretical visual resolution limit to 20 cycles/mm. Thus, the upper limit for the AIM curve of the eye plus the 3× biocular eyepiece will be 20 cycles/mm [Fig. 10.4 (bottom)]. From the MTF and AIM data shown, it can be concluded that the visual resolution will be 19 cycles/mm over 70% of the field and about 18 cycles/mm over the remainder. These two methods of image quality evaluation for the biocular eyepiece indicate that performance will be at the theoretical upper limit of what is achievable and quite acceptable for this application.

Finally, an overall evaluation of the complete night vision sight optical performance is now possible. As in previous examples, it will be most meaningful to compare the resolution capability of the naked eye with that of the eye used in conjunction with the sight. Obviously, a major advantage of the sight is its ability to display low-light-level night targets that would otherwise not be visible. This aspect of sight performance is a given, and will not be discussed further. Objective lens analysis indicates that the sight will cover a true field of 7.84 deg. Biocular eyepiece analysis indicates that this field will be presented to the eye covering an apparent field of 16.4 deg. From these data points the angular magnification of the complete sight can be calculated:

$$\text{Magnification} = \text{Apparent Field} / \text{True Field} = 16.4 / 7.84 = 2.1\times.$$

The sight's true field of view is 7.84 deg, or 0.137 radian. It has been shown earlier that the typical naked eye, with a 5-mm pupil, will resolve 1700 cycles/radian. Therefore, it can be concluded that the naked eye will resolve

$$\begin{aligned}\text{Resolution over Field} &= \text{Angular Eye Resolution} \times \text{Angle of Field} \\ &= 1700 \text{ cycles/radian} \times .137 \text{ radians} = 233 \text{ cycles} \\ &= 466 \text{ resolved elements over the field.}\end{aligned}$$

Using the biocular eyepiece, it can be concluded from Fig. 10.4 that the eye would resolve 19 cycles/mm at the 25-mm-diameter output surface of the intensifier. This means that a total of  $19 \times 25 = 475$  cycles will be resolved over the image of the 7.84 field of view, seen at the output of the intensifier. The total number of resolved elements will be

$$475 \text{ cycles} \times 2 = 950 \text{ elements.}$$

It has been found useful to compare the performance of an instrument such as this with a theoretically perfect instrument with identical parameters. A perfect  $2.1\times$  sight would have increased the eye's resolution to

$$\text{Max possible res.} = \text{Eye Res.} \times \text{Mag.} = 466 \times 2.1 = 979 \text{ elements.}$$

Thus, with the periscopic night sight, the visual resolution achieved is within 3% of the maximum possible. This is indicative of a system with performance that is consistent with the capabilities of the typical eye.

The advantages of using this periscopic night vision sight can now be reviewed. Assume the viewer is inside an armored vehicle and is responsible for locating and identifying potential targets in an unfriendly environment. First, the periscopic configuration will allow the viewer to remain securely *buttoned up* within the vehicle while making observations. Next, the image intensifier will amplify the apparent light level at the target by up to 40,000 times, making viewing possible under low-light conditions, such as nighttime with quarter-moon illumination. Next, the  $2.1\times$  magnification, combined with the quality of the optics, will allow the viewer to resolve detail at the target that is twice as fine as what could be resolved with the naked eye. Finally, the biocular configuration of the viewing eyepiece will result in comfortable viewing, with generous eye relief and relaxed positioning of the eyes with respect to the sight. All

of these features are indicative of a successful design of a sophisticated visual instrument.

### 10.3 Head-Up Display (HUD)

Another application of the biocular design is the head-up display (HUD), found in nearly all modern fighter aircraft. In a typical HUD system, critical data dealing with flight characteristics and/or weapons delivery is displayed on a CRT or flat-screen device. In order to minimize distraction of the pilot from his forward field of vision, this data is projected via a HUD to the pilot's eyes. The projected information is collimated by a large HUD projection lens and reflected from a combining glass to the pilot's eyes. The combining glass is a precision dichroic filter, which reflects a very narrow bandwidth (usually green or red) and very efficiently transmits the remainder of the visual spectrum. The result is that the pilot sees objects in the outside world with the data projected by the HUD superimposed on those objects. As with the biocular eyepiece discussed earlier, the HUD projection lens will have a relatively large aperture, while actual image quality will be determined by the limited size of the eye's pupils. The design will require correction of aberrations such that the angular difference between the two light bundles seen by the eyes will be reduced to less than one-half deg. Correction of distortion in the HUD projection lens is critical, in that the system is usually involved in the aiming and delivery of weapons.

The example to be presented here is derived from an early design generated for use in the A-10 *Warthog* close support fighter aircraft. The basic projection lens has a focal length of 176 mm (7 inches) and a speed of  $f/1.0$ . The data source assumed for this design is a 44-mm square flat display. This will correspond to a 14.25-deg square field of view being presented to the pilot.

Figure 10.6 contains a layout of this HUD, along with paraxial constants and tabulated lens data. The lens type is basically a Petzval lens with field flattener. The  $f/1$  lens speed leads to the need for a split positive element in the first group. As noted in the lens data, there is a cemented spectral filter behind the rear lens group. Because this is basically a monochromatic design, the emphasis on aberration correction was on spherical aberration, coma, astigmatism, and field curvature. In addition, because this is a fighter aircraft application, it is essential that residual distortion be held to less than 1 percent.

Figure 10.7 contains ray trace analysis (aberration curves) and spot diagram analysis. From the ray trace analysis it can be estimated that the maximum ray error, tracing from infinity, through the exit pupil and onto the CRT image surface, is about 0.1 mm. For the 176-mm focal length, this

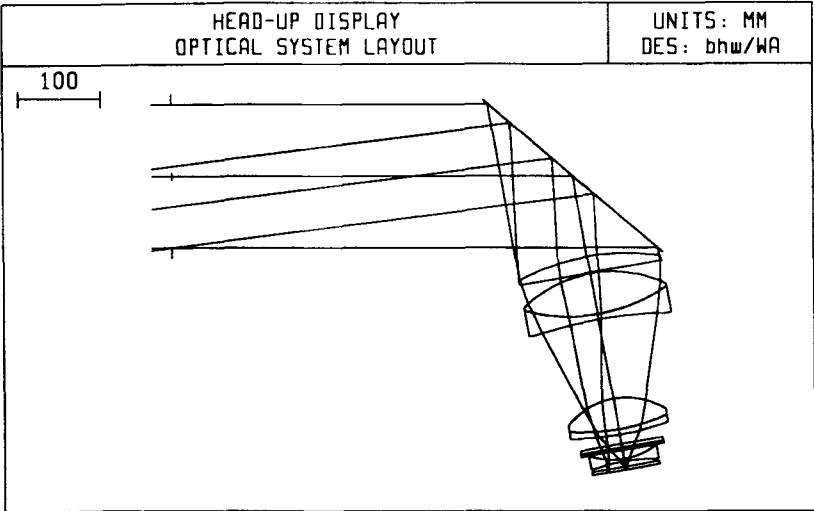
maximum ray error, tracing from infinity, through the exit pupil and onto the CRT image surface, is about 0.1 mm. For the 176-mm focal length, this error would correspond to an angle of about .033 deg. This is well within the one-half deg acceptable limit of the eye for angular difference between eyes. Considering the ability of the pilot to aim a weapon system using the HUD system, this 0.1-mm ray error at the CRT corresponds to a pointing error of 0.6 milliradian (mr). A common, acceptable pointing error tolerance in systems such as this is 1.0 mr.

The spot diagrams shown in Fig. 10.7 can also be used to estimate angular errors at the exit pupil of the HUD system. The average spot radius from the analysis shown is about 0.05 mm, which corresponds to an angular error of about 0.25 mr. These spot diagrams have been generated by tracing rays over the full 7-inch-diameter pupil of the HUD lens. All of these results are indicative of very good optical performance for this HUD optical system. This fact was confirmed by early reports of A-10 pilots when the prototype system was introduced.

## 10.4 Review and Summary

Design and analysis of biocular optical systems requires special considerations because performance of a relatively large and fast optical system will, in reality, be limited by the restricted pupil of the viewer's eye. Special attention must be paid to the presentation of a common object point to the two eyes of the viewer, which are typically separated by a distance of 65 mm. The bottom line during the design and optimization phase is that a very well-corrected design (in all of the traditional ways) will be required. When the residual aberrations have been adequately reduced, the viewer will be able to place his or her eyes at any point within the system's exit pupil and comfortably view a high-quality image.

As with all optical design assignments, it is essential to the successful design of a biocular system that the designer has a complete and thorough understanding of the ultimate system application. Having this knowledge, combined with an equally complete understanding of the function and limits of the human visual system, the designer will be well equipped to produce a successful final optical system design.



**\*PARAXIAL CONSTANTS**  
Effective focal length: -176.00000      Lateral magnification: -5.8668e-29  
Numerical aperture: 0.50000      Gaussian image height: 22.00000  
Working F-number: 1.00000      Petzval radius: 1784.24310

**\*LENS DATA**  
**HEAD-UP DISPLAY**

SRF	RADIUS	THICKNESS	APERTURE RADIUS	GLASS	SPE	NOTE
OBJ	--	3.0000e+30	3.7499e+29	AIR		
AST	--	500.00000	88.00194 ASK	AIR		Exit Pupil
2	--	-101.00000	145.00000	REFLECT		* Combiner
3	-285.35000	-20.00000	89.00000	BK7 C		
4	--	-1.27000	89.00000 K	AIR		
5	-157.30000	-51.00000	89.00000	BK7 C		Collimating
6	211.45000	-0.40000	89.00000	AIR		-Lens-
7	208.30000	-6.40000	89.00000 K	F2 C		
8	-543.80000	-99.10000	82.00000	AIR		
9	-92.80000	-38.00000	61.00000 K	BK7 C		
10	236.90000	-0.25000	61.00000	AIR		
11	240.00000	-6.40000	58.00000	F2 C		
12	359.00000	-11.40000	61.00000 K	AIR		
13	--	-5.00000	51.00000	BK7 C		Spectral
14	--	-3.00000	51.00000	K5 C		Filter
15	--	-11.00000	51.00000	AIR		
16	88.94000	-3.00000	42.00000	SF2 C		
17	-195.00000	-6.60000	34.00000	AIR		
18	--	-3.80000	42.00000	K4 C		Filter
19	--	--	42.00000	AIR		
IMS	--	--	22.00000			* Source (CRT)

Figure 10.6 Lens layout and data on the 176-mm f/1 head-up display (HUD) lens designed originally for the A-10 Warthog fighter aircraft.

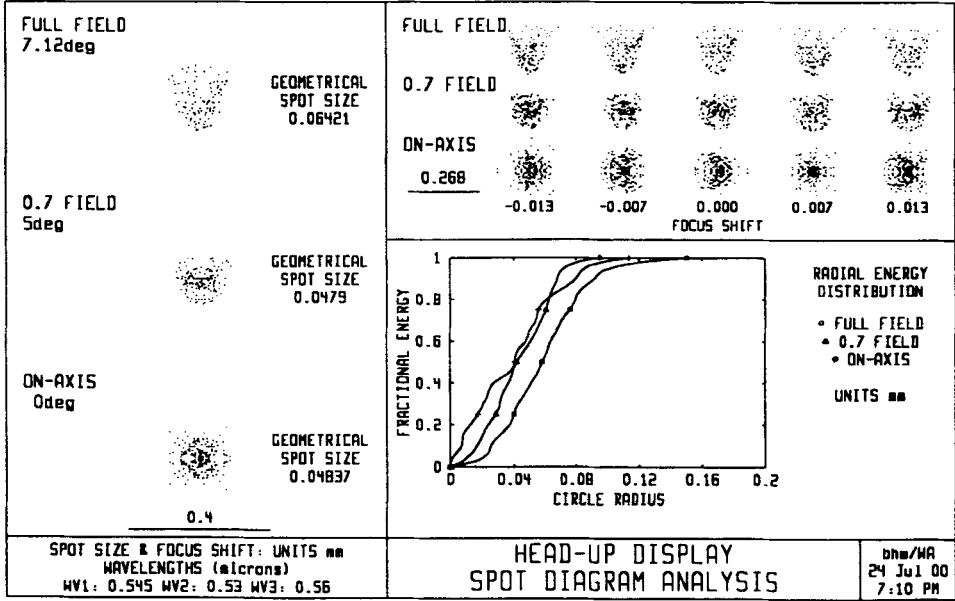
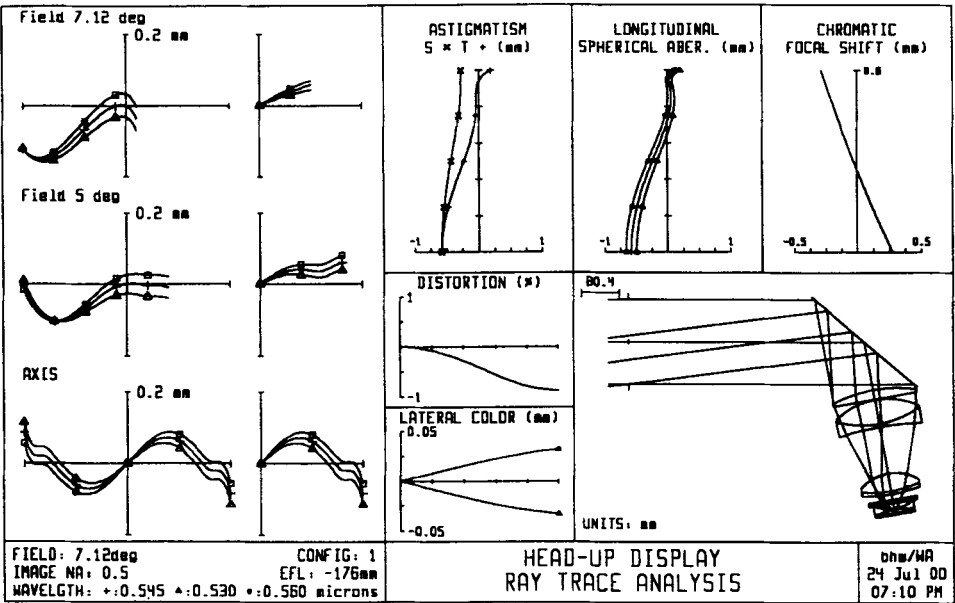


Figure 10.7 Ray trace analysis (aberration curves) and spot diagram analysis on the 176-mm f/1 head-up display (HUD) lens designed originally for the A-10 Warthog fighter aircraft. Spot diagrams are for the entire 176-mm (6.9-inch) lens aperture.



# 11

## Review and Summary of Design Concepts

---

### 11.1 Introduction

In this book we have presented many of the basic concepts and procedures applicable to the design of optical systems for use in visual applications. The goal in presenting this information has been twofold. First, it is intended that reading of this book, and working through some of the design exercises, will result in a better understanding of the basic optical characteristics and the performance limitations of the human eye. Secondly, it is expected that the reader will come away with an improved feel for the important aspects of optical engineering and lens design as they apply to the design of the visual instrument.

### 11.2 The Model Eye

A model of the *typical* human eye has been generated in Chapter 2. This model, while admittedly a simplified version, is quite close to the actual physical configuration and dimensions of the average eye. The lens parameters of the model eye have been adjusted such that the on-axis image quality is very close to values established and commonly accepted. Data for the model eye is presented which represent the relaxed eye, viewing a target at infinity, and for the fully-accommodated eye, viewing a target at the near point of vision, i.e., 10 inches or 254 mm. The pupil of the model eye is assumed to be variable, from 1.0 mm under very bright lighting conditions, to 7.0 mm when the ambient light level is very low. When viewing objects at infinity, the focal length of the model eye is 17.3 mm. When accommodated for viewing objects at the near point, the power of the eyelens is increased, reducing the focal length of the model eye to 16.6 mm.

### 11.3 Model Eye Resolution

The fovea, which is only 0.3 mm in diameter, is the spot near the center of the retina that is capable of maximum resolution. The field of optimum

visual resolution is limited to about 1 deg by the size of the fovea. The fovea contains about 15,000 high-resolution receptors known as cones, which are arranged with an average center-to-center spacing of 2.5 microns. Based on this construction data, it has been estimated that the maximum resolution possible at the fovea, assuming the optics of the eye are perfect, is approximately 140 cycles/mm. When the MTF of the model eye's optics (with a pupil diameter of 2.5 mm) is added to the analysis, the maximum resolution at the fovea is found to be 117 cycles/mm. Assuming that the resolution target being viewed is at a distance of 254 mm, the magnification factor between that object and its image at the fovea will be 0.067 $\times$ . As a result, the resolution at the target, corresponding to the 117 cycles/mm at the fovea, will be 7.82 cycles/mm. In terms of angular resolution, this value can be converted to a corresponding value of 1986 cycles/radian.

These then are the visual resolution limits that have been used throughout this book to evaluate the instrument designs that have been presented. An important new concept has been introduced here, where the effect of the eye's pupil diameter on visual resolution is presented. Figure 2.3 shows that, as the pupil diameter of the eye adjusts from 1.0 to 7.0 mm, the angular resolution will range from 1400 cycles/radian (at 1.0 mm), to a peak of 1986 cycles/radian (at 2.5 mm), and then fall back to 1400 cycles/radian for a maximum pupil diameter of 7.0 mm. The reduction in resolution at minimum pupil diameter is due to diffraction effects, while the reduction at maximum pupil diameter is due to spherical and chromatic aberration in the optics of the eye.

## 11.4 Visual Magnification

In Chapter 3 the subject of visual magnification has been covered. Understanding the limit of resolution at the retina, due to the optics of the eye and the size and spacing of the cones at the fovea, it is found that increasing the size of the image at the retina will increase the ability to resolve detail proportionately. As the object being viewed is brought closer to the eye its image size will increase. For the typical eye, this procedure is limited by the ability of the eye to accommodate (focus) at close distances. The accepted standard limit for close viewing has been established as being 10 inches, or 254 mm. As a point of reference, when viewing an object at this near point, the magnification factor between the object and its image at the retina will be approximately  $1/15^{\text{th}}$ .

When a positive lens is placed in close proximity to the eye, the object may be brought even closer and a magnified image will result. As a general rule of thumb, the magnification factor for the lens may be found by dividing its focal length into the established near point of vision

(10 inches or 254 mm). Typical magnification factors achieved with a simple magnifier will range from  $2\times$  to  $20\times$ .

When greater magnification is required, a microscope system is employed. In the microscope an objective lens is used to produce a magnified image of the object and that image is viewed with a magnifier lens, now referred to as an eyepiece. Total microscope magnification is found by multiplying the magnification factors of the objective and the eyepiece. Common microscope systems will yield magnification factors ranging from  $10\times$  to  $800\times$ .

## 11.5 Other Visual Instruments

While the magnifier and microscope are used to view and magnify close objects, the telescope and its derivatives are used to view objects at great distances. In this case the objective lens of the telescope will form an image of a distant object and the eyepiece will be used to view that image. Telescope magnification is calculated by dividing the focal length of the objective lens by the focal length of the eyepiece. When an optical system contains relay optics between the objective lens and the eyepiece, the magnification factor of those relay optics must be included in the final determination of instrument magnification.

The final design examples presented deal with the rather unique area of biocular optical systems. In this case the optics must be designed and analyzed to account for the simultaneous use of both eyes to view the object. This requirement dictates a very fast system, with a large pupil, where only a small portion of that pupil is being utilized by the viewer's eyes. The advantage of the biocular system is generally found in the increased comfort of the viewer, permitting more relaxed viewing over extended periods of time.

## 11.6 Conclusion

The success of any optical design will be decided when the performance of that optical system is merged with the performance of the system's ultimate detector, be it film, a CCD array, an IR detector or, as this book attempts to demonstrate, the typical human eye and visual system. Obviously, due to its complexity and flexibility, a complete and definitive description of the eye is not possible. To that end, a model of a typical eye, including the retina, has been generated here that some critics may argue is not in agreement with their understanding and knowledge of that system. With all due respect to those critics, it must be recalled that the human eye comes in an infinite range of sizes, shapes, and performance characteristics. The model generated in Chapter 2, and used

throughout the text as a point of reference, is admittedly a simplified version, intended only as a valid representation of the *typical* eye. This model eye is used primarily to introduce the reader to the basic function and performance of the eye, and then to allow meaningful and valid evaluation of the optical designs presented, in terms of their impact on the performance of that typical eye. It is felt that the simplified eye model and concepts used here have allowed these objectives to be met.

## References

---

The following reference material has been used by the author in preparation of this book. This material will be helpful to the reader in achieving a more comprehensive understanding of the topics covered. While all are valuable, the author has listed these references in descending order of usefulness, based on his experience working in the field of optical engineering and lens design.

1. Warren J. Smith, *Modern Optical Engineering (Second Edition)*, McGraw-Hill, 1990.
2. Pantazis Mouroulis, *Visual Instrumentation, Optical Design and Engineering Principles*, McGraw-Hill, 1999.
3. Bruce H. Walker, *Optical Engineering Fundamentals*, SPIE Optical Engineering Press, 1998.
4. Milton Laikin, *Lens Design*, Marcel Dekker, Inc., 1991.
5. Robert E. Hopkins, *MIL-HDBK-141 Section 4, Visual Optics*, Defense Supply Agency, 1962 (out of print).

# INDEX

---

## Index Terms

## Links

### A

Aberration curves	84	94
Accommodation	3	152
Achromatic doublet	52	84
Aerial image modulation (AIM)	xiii	8
Afocal mode	2	94 109
Air spaced achromat	84	
Apochromatic	129	137
Apparent visual field	125	
Aqueous	3	
Astigmatism	94	106
Astronomical telescope	83	

### B

Biconvex magnifier	29	
Binoculars	94	
Biocular optical systems	139	153
Biocular	xiii	139
Borescope	101	

### C

Camera, 35mm	89	
CCD	26	
Center focus	95	
Chief ray	62	103

## **Index Terms**

## **Links**

Chromatic aberration	5	7	11	52
	84	137	152	
Collector lens	129			
Combining glass	147			
Cones	7	152		
Cornea	3			

## **D**

Diffraction effects	152			
Diffraction limited resolution	70	80	84	94
Diopter adjustment	94			
Diopter focus setting	62			
Diopters	60			
Distant object magnification	21			
Distortion	52	62		
Doublet magnifier	31			

## **E**

Erfle eyepiece	56	93	94	
Exit pupil	92	142		
Eye lens	47			
Eye model	xiii	3	151	
Eye relief	47	69	91	142
Eye	3			
Eyelens	3			
Eyepiece box, periscope	117			
Eyepiece focus	60	94		
Eyepiece, generic	47			
Eyepiece, periscope	117	129		
Eyepiece	47	90	101	

<u>Index Terms</u>	<u>Links</u>			
<b>F</b>				
Field curvature	52			
Field lens	47	94	103	129
Field of view (eye)	11	47		
Field of view (HUD)	147			
Film	89			
Focal	1			
Focal length (eye)	151			
Fovea	7	11	151	
<b>G</b>				
Glass type	56	84		
<b>H</b>				
Hastings triplet	39			
Head up display (HUD)	147			
Head, periscope	117			
Head prism	117			
Head window	117			
High power objective, periscope	119			
HUD projection lens	147			
Huygenian eyepiece	49			
<b>I</b>				
Image intensifier	139			
Image quality	8			
Image rotation	95			
Iris	3			



<u>Index Terms</u>	<u>Links</u>			
<b>J</b>				
JML catalog	39			
<b>K</b>				
Kellner eyepiece	52			
<b>L</b>				
Laikin, Milton	71			
Lateral color	52			
Line spread function	81	89		
Lister lens form	71			
Loupe magnification	16			
Loupe	16			
<b>M</b>				
Magnification	15	69	114	
Magnification difference	95			
Magnification factor	152			
Magnification power	18			
Magnification, angular	145			
Magnification, telescope	23	152	153	
Magnification, visual	152			
Magrufier, simple	29	152		
Magnifier	29			
Magnifying glass	16			
Mast optics, periscope	129			
Mast, periscope	117			
Microscope magnification	19			
Microscope	19	69	83	153
Milton Laikin	71			

<u>Index Terms</u>	<u>Links</u>			
Minimum resolved separation	80	89		
Modulation transfer function (MTF)	xiii	8		
Moon	21			
MTF analysis	71			
MTF data	84	94		
<b>N</b>				
Near object	15			
Near point of vision	3	15		
Normal vision	8			
Normal visual acuity	11			
Normal visual resolution (20/20)	8			
Numerical Aperture (NA)	69			
<b>O</b>				
Objective (microscope)	69	71		
Objective lens (telescope)	83	93		
Objective lens (borescope)	101	103		
Objective lens (periscope)	117	119		
Off-axis (lateral) color	52	94		
Optical glass	56	84		
Optical path difference (OPD)	62	71	74	
Optimization	36	74	119	
Orthoscopic eyepiece	52	69	77	109
OSLO	xiv	2	29	39
	43	62	71	103
<b>P</b>				
Peripheral vision	7	11		
Petzval lens	147			
Photographic systems	24			

**Index Terms**

**Links**

Point spread function	84			
Pointing error	148			
Porro prism	93	94		
Primary color	84			
Pupil diameter	4			

**R**

Ramsden eyepiece	49			
Range estimation	125			
Ray trace analysis	71	74		
Rayleigh criteria	80	89		
Refracting design	83			
Relay lens, periscope	126			
Relay optics	101	106	153	
Resolution (eye)	6	8	90	91
Resolution (video)	26			
Resolution gain	134			
Resolution, angular	91	152		
Resolution	8	70		
Retina	7			
RKE eyepiece	52	60	90	
Rods	7			

**S**

Scidmore eyepiece	56			
Scratch-dig	103			
Secondary chromatic aberration	129			
Sinclair Optics	xiv	2		
Spectral sensitivity	4			
Spectral wavelengths	139			

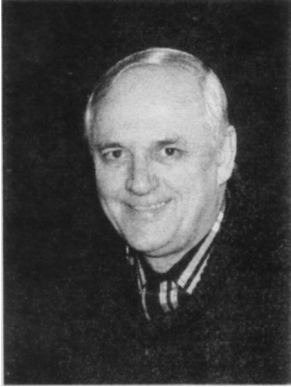
<u><b>Index Terms</b></u>	<u><b>Links</b></u>			
Spherical aberration	4	7	11	84
	152			
Spot diagrams	148			
Spot size, RMS	62			
Spot size	6			
Stanching window	117	129		
Submarine periscope	117			
Symmetrical eyepiece	56	62		
Symmetrical magnifier	43			
<b>T</b>				
Telecentric	103			
Telemeter	117	119	129	
Telescope	83	153		
Television	26			
Terrestrial telescope	93			
Triplet magnifier	39			
<b>U</b>				
USAF resolution target	15	17	43	
<b>V</b>				
Video systems	26			
Vignetting	101	103	106	126
Visual acuity	11			
Vitreous	7			
<b>W</b>				
Wavefront error (OPD)	71	62		

**Index Terms**

**Links**

**Z**

Zero power doublet	119
Zoom eyepiece	90



Bruce H. Walker, founder and president of Walker Associates, has been active in the fields of optical engineering and lens design since 1960. His initial work was with General Electric, where he received four patents for unusual lens designs. He was with the Electro-Optical Division of Kollmorgen Corp. for 20 years, first as a senior optical engineer and later as manager of optical engineering. From 1970 to 1999 Mr. Walker was a member of the Editorial Advisory Board of the Laurin Publishing Company. During that period he had more than 30 articles published and made numerous significant contributions to the *Photonics Handbook and Dictionary*. In 1995, Mr.

Walker authored the textbook *Optical Engineering Fundamentals*, presently available as part of the SPIE Tutorial Texts Series (TT30). Since 1990 he has worked as an independent consultant, specializing in the solution of optical engineering problems and the generation of many specialized lens designs.